

**BIOGEOCHEMICAL FACTORS AFFECTING MERCURY METHYLATION
IN HIGH ARCTIC SOILS ON DEVON ISLAND, CANADA**

A thesis submitted to the College of Graduate Studies and Research
In Partial Fulfillment of the Requirements for the Degree of

Master of Science

In the

Department of Soil Science

University of Saskatchewan

Saskatoon

By

Lindsay Oiffer

© Copyright Lindsay Oiffer, January 2008. All Rights Reserved.

PERMISSION TO USE

In presenting this thesis in partial fulfillment of the requirements for a postgraduate degree from the University of Saskatchewan, I agree that the libraries of this University may make it freely available for inspection. I further agree that permission for copying of this thesis in any manner in whole or in part, for scholarly purposes may be granted by the professor or professors who supervised my thesis work or, in their absence, by the Head of the Department or the Dean of the College in which my thesis work was done. It is understood that any copyright or publication or use of this thesis or parts thereof for financial gain shall not be allowed without my written permission. It is also understood that due recognition shall be given to me and to the University of Saskatchewan in any scholarly use which may be made of any material in my thesis.

Requests for permission to copy or make other use of material in this thesis in whole or in part should be addressed to:

Head of the Department of Soil Science
University of Saskatchewan
Saskatoon, Saskatchewan
S7N 5A8

ABSTRACT

Recent research has shown that the Arctic may be a sink for mercury, however, the fate of this deposited mercury in the environment is not known. The objective of this project was to determine the factors affecting methyl mercury (MeHg) production in Arctic organic soil on the Truelove Lowlands, Devon Island, Canada. In the field we observed a steady decrease in MeHg over time, with MeHg concentration at many sampling locations declining below detection limits. This decrease did not correlate to any chemical or biophysical parameter measured. During the study the Lowlands appeared to be mildly reducing with dissolved Fe(II) being present in the porewater, however, no correlation was observed between MeHg production and the variables measured. The dissolved organic matter concentration of the porewater was quite high, the pH was circumneutral and it would seem that in the absence of more highly reducing conditions that mercury would be unavailable for methylation.

It seems likely under field conditions MeHg was much more bioavailable than inorganic mercury. This would lead to a higher rate of demethylation than methylation and a net decrease in MeHg. Little research has been done on demethylation and the effect of environmental conditions on demethylation, especially in arctic environments. However, it is possible that the rate of demethylation was not affected by changes in temperature or any other parameter measured over the course of the field study.

Laboratory microcosm studies using saturated soil from the organic horizons demonstrated little potential for unspiked organic soil to produce significant amounts of MeHg. The spiked treatment, however, had an eight fold increase in MeHg concentration and the sterile treatment showed no change in MeHg concentration over 40 days of freeze (-5°C) and 59 days of thaw (4°C).

Our data suggests that a combination of atmospheric and in-situ processes maintain a cycle of MeHg production (spring) and loss (summer) in arctic soils. It would seem that Arctic wetland soils are not a significant source of MeHg to the Arctic ecosystem and that snowmelt is the dominant source.

ACKNOWLEDGEMENTS

Firstly I would like to thank Andrea for supporting me during my master's and always being there to listen to me complain when my project was not going well. I would also like to thank my family for their continued support throughout my education and always being there to lend a hand when I needed it.

I would like to thank my supervisor Dr. Steven Siciliano for his help guiding my project and ensuring I never got off track. Thanks also go to my committee members: Dr. Derek Peak for helping answer my numerous environmental chemistry questions; Dr. Rich Farrell for all the advice on field equipment construction and laboratory analysis; and Dr. Dan Pennock for chairing my committee, as well as, offering advice on the field and statistical portions of my project.

I would also like to acknowledge all the staff in the department who helped me get my project off the ground. I would especially like to thank Dr. Renato De Freitas for helping me on numerous occasions in the lab and with analytical equipment. The completion of my project would also have not been possible without the help of everybody in Dr. Hudson's lab, especially Brian Vermillion, who helped introduce me to analytical chemistry, as well as, providing extensive technical support for MeHg analysis over the past two years. As well, thanks go to Jordan Marit and Dr. Susan Ferguson for all the help in the field.

Finally I would like to acknowledge all the graduate students in the department who made my time as a master's student enjoyable and everybody in my lab group: Wai, Brian, Alexis, Jola, Jen and Christian for helping me with my project and who made working in the lab an enjoyable experience. I would also like to thank Lori Phillips and Arlette Seib for help with the use of the Soil Microbiology Laboratory's equipment and offering advice on numerous occasions.

This project was funded by NSERC and the Northern Scientific Training Program. The Polar Continental Shelf Project provided logistical support during the field season.

TABLE OF CONTENTS

PERMISSION TO USE	i
ABSTRACT	ii
ACKNOWLEDGEMENTS	iii
TABLE OF CONTENTS	iv
LIST OF TABLES	vii
LIST OF FIGURES	viii
LIST OF ABBREVIATIONS	x
1.0 INTRODUCTION	1
2.0 LITERATURE REVIEW	2
2.1 Mercury	2
2.1.1 Biogeochemistry	2
2.2 MeHg in the environment	5
2.2.1 MeHg in the arctic	7
2.3 Redox conditions in the soil environment	8
2.3.1 Dissimilatory iron reducing bacteria	9
2.3.2 Iron biogeochemical cycling in terrestrial environments	11
2.4 Methods of MeHg analysis	12
2.4.1 Hg-thiourea complex ion chromatography and Atomic Fluorescence Spectrometric Detection	12
2.4.2 Alternative methods	13
3.0 METHYL MERCURY PRODUCTION TRUELOVE LOWLAND, DEVON ISLAND, CANADA: A FIELD STUDY	14
3.1 Introduction	14
3.1.1 Truelove Lowland	14
3.2 Objective	18
3.3 Methods	18
3.3.1 Sampling protocol	18
3.3.2 Soil sampling	21
3.3.3 Pore water sampling	21

3.3.4 Field measurements	22
3.3.5 Field equipment construction	22
3.3.6 Analysis	25
3.3.7 MeHg extraction	25
3.3.8 MeHg analysis	26
3.3.9 Hg analysis	28
3.3.14 Dissolved (DOC) and total organic carbon (TOC) analysis.....	29
3.3.10 Sulfide analysis.....	30
3.3.11 Iron analysis.....	30
3.3.12 Major cation analysis.....	33
3.3.13 Major anion analysis.....	33
3.3.15 Statistics.....	34
3.4 Results	35
3.4.1 MeHg concentration in Of horizon.....	35
3.4.2 Dissolved mercury	35
3.4.3 Dissolved organic carbon	35
3.4.4 Sulfide data	39
3.4.5 Iron data	39
3.4.6 Dissolved cations and anions.....	39
3.4.7 Field measured parameters	44
3.4.8 Results of modeling in Visual Minteq.....	44
3.5 Discussion.....	47
3.5.1 Geochemical conditions during study	47
3.5.2 Methyl mercury dynamics	48
3.6 Conclusions	50
4.0 USING SOIL MICROCOSMS TO ELUCIDATE THE MECHANISMS OF MeHg PRODUCTION IN ARCTIC SOIL.....	53
4.1 Introduction	53
4.2 Objectives	53
4.3 Methods	54
4.3.1 Microcosm Experiment	54

4.3.2 Sampling Methods	56
4.3.3 Statistical Analysis	58
4.4 Results	58
4.5 Discussion.....	63
4.6 Conclusion.....	69
5.0 GENERAL CONCLUSION.....	71
6.0 BIBLIOGRAPHY	73
APPENDIX A. RESULTS FROM FIELD STUDY	84
APPENDIX B. QUALITY ASSURANCE/QUALITY CONTROL RESULTS FOR SELECTED ANALYSIS	107
APPENDIX C. EQUILIBRIUM CONSTANTS USED IN SPECIATION CALCULATIONS	116
APPENDIX D. RESULTS FROM MICROCOSM EXPERIMENT	117
APPENDIX E. QAQC RESULTS MICROCOSM CHAPTER.....	123

LIST OF TABLES

Table 2.1. General biogeochemistry of mercury in soils (Morel 1998 and Gabriel and Williamson 2004). General sulfide speciation is based on modeling in Visual Minteq (Gustafsson 2006) using thermodynamic data from Goulet et al. (2007) at STP assuming an infinite dilution.	4
Table A.1 Results from field measurements Truelove Lowland, Devon Island.....	84
Table A.2 Summary of results for mercury and organic carbon (DOC/TOC) present in pore water, and methylmercury in soil on Truelove Lowland, Devon Island	92
Table B.1. Field blanks and MDL results for mercury analysis in porewater	107
Table B.2. Recovery and percent deviation of duplicate results for pore water mercury analysis.	108
Table B.3. Quality assurance and control results from MeHg extractions and analyses.....	110
Table B.4. Method detection limit based on a spike into mineral WSM soil.....	111
Table B.5. Precision of dissolved organic carbon analyzer	111
Table B.5. Precision of dissolved organic carbon analyzer	112
Table B.6. Precision of AA cation analysis	113
Table B.7. Precision of capillary electrophoresis for anion analysis.....	114
Table B.8. Detection limit of capillary electrophoresis for detection of anions in water samples.	115
Table D.1 Gas sampling data from microcosm experiment corrected to room temperature	117
Table D.2 MeHg concentration in soil and porewater data from microcosm experiment. Absorbance of filtered porewater is unitless.	119
Table D.3. Soil water extractable mercury and oxalate extractable iron.	122
Table E.1. Summary of QAQC for the microcosm chapter	123

LIST OF FIGURES

Figure 3.1.1. Typical catena on Truelove Lowland. The WSM refers to the wet sedge meadow, LFS refers to the lower foreslope, UFS refers to the upper foreslope and the RBC is representative of the raised beach crest. Information obtained from Walker and Peters (1977). Soil classification based on Walker and Peters (1977).	16
Figure 3.3.1. Map of the Truelove Lowland with locations of Catenas	19
Figure 3.3.2. Diagram of instrumentation installation.....	20
Figure 3.3.3. Diagram of fully constructed redox probe	24
Figure 3.3.4. Overview of HPLC system (flow rate is in mL min ⁻¹).....	27
Figure 3.4.1. Mean MeHg concentrations in wetland soil over time. Error bars represent 95% confidence intervals.	36
Figure 3.4.2. Mean MeHg concentration at each catena. Error bars represent 95% confidence intervals.....	36
Figure 3.4.3. Mean dissolved mercury (DHg) over the course of the summer sampling period. Error bars represent 95% confidence intervals. DHg is mercury which remains after filtration with a 0.45 µm PVDF membrane.....	37
Figure 3.4.4. Mean concentrations of dissolved mercury in pore water at each catena. Error bars represent 95% confidence interval for mean DHg concentrations. DHg is mercury remaining after filtration with a 0.45 µm PVDF membrane.	37
Figure 3.4.5. Mean DOC concentration over sampling period. Error bars represent 95% confidence intervals. DOC defined as organic carbon fraction which can pass through a 0.45 µm filter.	38
Figure 3.4.6. Mean DOC concentration by catena. Error bars represent 95% confidence intervals. DOC defined as fraction of organic carbon which can pass through a 0.45 µm filter.....	38
Figure 3.4.7. Median Iron(II) concentrations over time (data from lysimeters only) ...	40
Figure 3.4.8. Mean Iron(III) concentrations over time (data from lysimeters only). Error bars represent standard error of mean.	40
Figure 3.4.9. Median Fe(II) concentration by catena (data from lysimeters only). Error bars represent 1 st and 3 rd quartiles of distribution.	41
Figure 3.4.10. Mean Fe(III) concentration by catena (data from lysimeters only). Error bars represent standard error of mean.	41
Figure 3.4.11. Mean concentration of calcium (Ca), magnesium (Mg), potassium (K) and sodium (Na) in soil water. Error bars represent standard error for untransformed data (Ca and Mg) and 95% confidence intervals for log transformed data (K and Na).	42

Figure 3.4.12. Mean chloride concentration by catena. Error bars represent standard error of mean.	43
Figure 3.4.13. Mean chloride concentration by calendar day. Error bars represent standard error of the mean.	43
Figure 3.4.14. Eh measurement (mV) over sampling period. Points indicate average redox potential for the calendar day at all four locations. Error bars represent the standard error of the mean.	45
Figure 3.4.15. Mean temperatures over time for the soil profile. Error bars represent standard error of the mean.	45
Figure 3.6.1. Flow chart depicting the effect of available mercury and MeHg on methylation/demethylation.	51
Figure 4.4.1. MeHg concentration as a function of treatment (mercury spiked (4.4 µg mercury), natural or gamma radiation sterilized) over time. Error bars represent standard error of mean concentration (n = 4, except natural treatment (sampling day 99) where n = 5). Dashed line indicates the beginning of the 4 °C incubation.	60
Figure 4.4.2. Average redox potential (corrected to SHE) as measured in surrogate microcosms over time. Error bars represent standard error of sample mean (n = 3 except sampling day 40 where n = 2). Open circles correspond to the average oxalate extractable iron in the natural treatment over time. Error bars represent standard error of sample mean (n = 4 except sampling day 99 where n = 5).	61
Figure 4.4.3. Mean colour (absorbance (unitless) at 420 nm) of porewater as a function of sampling day in the spiked and natural treatments. Error bars represent standard error of absorbance (n=4 except natural treatment (sampling day 99) where n = 5).	62
Figure 4.4.4. Median cumulative N ₂ O release over time standardized to one gram of dry soil. Error bars represent 1 st and 3 rd quartiles of distribution (n = 4). Dashed line indicates beginning of 4°C incubation	64
Figure 4.4.5. Median cumulative CO ₂ release over time standardized to one gram of dry soil. Error bars represent 1 st and 3 rd quartiles of distribution (n = 4). Dashed line indicates beginning of 4°C incubation.	65
Figure 4.4.6. Median cumulative CH ₄ release over time standardized to one gram of dry soil. Error bars represent 1 st and 3 rd quartiles of distribution (n = 4). Dashed line indicates beginning of 4°C incubation.	66

LIST OF ABBREVIATIONS

CFU	colony forming units
CVAFS	cold vapour atomic fluorescence spectroscopy
DHg	dissolved mercury
DOC	dissolved organic carbon
DOM	dissolved organic matter
GC	gas chromatography
HDPE	high density polyethylene
HPLC	high pressure liquid chromatography
ICP-MS	inductively coupled plasma mass spectrometry
Kow	octanol water partition coefficient
LFS	lower foreslope
MeHg	methyl mercury
PCO	photocatalytic oxidation
pHg	particulate mercury
PTFE	polytetrafluoroethylene
PVC	polyvinyl chloride
PVDF	polyvinyl difluoride
RBC	raised beach crest
SHE	standard hydrogen electrode
SRB	sulfate reducing bacteria
STP	standard temperature and pressure
THg	total mercury
TOC	total organic carbon
TU	thiourea
UFS	upper foreslope
UV	ultraviolet
WSM	wet sedge meadow

1.0 INTRODUCTION

Increased industrialization in the past century has led to an increase in the global production and spread of contaminants. Mining and other industrial processes such as coal burning power plants have been major sources of mercury releases into the environment (Evers 2005). It is estimated that the amount of mercury has increased two to three times in the oceans and atmosphere because of anthropogenic activities (Macdonald 2005). Mercury (Hg) has begun to appear in ecosystems in significant quantities and because it can reside in the atmosphere for periods up to one year, mercury is a candidate for long-range transport (Evers 2005; Morel et al. 1998).

In a recent article published by the Biodiversity Research Institute (Evers 2005) the distribution of mercury in northern ecosystems was highlighted. The authors found mercury in significantly high levels in areas that were distant from any mercury point sources. The authors also found that mercury was not only accumulating in aquatic systems but also in terrestrial ecosystems where they discovered high concentrations of mercury in avian species. With the increase in industrialization, anthropogenic pollution and climate change, a greater focus on the fate and transport of contaminants is required. All ecosystems are at risk including sensitive ecosystems such as the arctic (Macdonald 2005). Recently it has been shown that the arctic may be acting as a global sink for atmospheric mercury (Schroeder et al. 1998). Primarily Arctic mercury research has focused on atmospheric fluxes of mercury, however, recent work has shown that Arctic wetlands may be a source of methyl mercury (MeHg), but the means by which this occurs are not yet known (Loseto et al. 2004a).

The objectives of this thesis were to examine the biogeochemical factors affecting MeHg production in arctic wetland soil. To accomplish this objective a field experiment (Chapter 3) to determine the relationship between redox potential and MeHg production and a laboratory experiment (Chapter 4) to determine the effects of thaw and mercury availability on MeHg production were undertaken.

2.0 LITERATURE REVIEW

2.1 Mercury

Mercury is a toxic and hazardous metal that can occur naturally in the earth's crust (Tchounwou et al. 2003). Elemental mercury is unique in that it can occur as a gas or a liquid at room temperature (Morel et al. 1998). Natural or anthropogenic events can introduce mercury into the environment, with mining and fossil fuel use being major conduits of mercury release into ecosystems (Evers 2005).

The presence of mercury in environmental media is concerning because of the ability of mercury to appear in the environment and ascend trophic levels, bioaccumulating in organisms that are consumed by the human population (Tchounwou et al. 2003; Morel et al. 1998). Mercury can cause significant effects on the central, peripheral nervous and respiratory systems as well as the immune system (Tchounwou et al. 2003; ATSDR 1999). Methyl mercury (MeHg) is a species of concern because it can bioaccumulate in the food chain (ATSDR 1999). Recent studies have identified the arctic as a sink for long-range organic and inorganic pollutants (Schroeder et al. 1998).

2.1.1 Biogeochemistry

Mercury can occur in a multitude of different forms. Elemental mercury (Hg^0) and ionic mercury (Hg^{2+} , Hg_2^{2+}) are uncomplexed species found in the environment (Ravichandran 2004; Gabriel and Williamson 2004). Other common forms of mercury are methyl, dimethyl and ethyl mercury as well mercury can form numerous minerals or precipitates such as low solubility cinnabar (HgS) (Ravichandran 2004; Morel et al. 1998; ATSDR 1999; Schuster 1991).

Mercury can partition between the aqueous, particulate and colloidal phases in water (Morel et al. 1998) as well as being adsorbed (non-specific or specific) to the surface of clays or other particles in soils (Gabriel and Williamson 2004). Adsorption to soil particles binds a majority of the mercury in soils, because mercury is present in

trace amounts and because of the availability of adsorption sites in most soils (Schuster 1991). Non-sorbed mercury is more bioavailable to microbes (Gabriel and Williamson 2004). An increase in ligand concentration, e.g. chloride, leads to a decrease in mercury adsorption, because the ligands can form stable complexes with mercury. In acidic conditions the potential negative charge of oxyhydroxides in the soil decreases (increase in protonation) as hydrogen ions out compete Hg^{2+} (mercuric mercury) for exchange sites on soil particles (Gabriel and Williamson 2004) and thus, organic matter is the principal adsorbent at low pH. At neutral pH, mercury adsorbs to iron oxides or clay particles in soils (Schuster 1991; Jackson 1998). Under basic conditions mercury adsorption may decrease relative to adsorption under neutral conditions because of the formation of large mercury hydroxide complexes which do not adsorb as readily to exchange sites (Collins et al. 1999)

Divalent mercury (Hg^{2+}) is a dominant form of mercury in the soil; it reacts readily with dissolved ligands and is highly soluble (Gabriel and Williamson 2004). The other charged form of inorganic mercury, mercurous mercury (Hg_2^{2+}), is only stable in the aqueous phase (Morel et al. 1998). Divalent mercury has an affinity for large, non-polar ligands that exhibit Lewis base characteristics (Jackson 1998). Mercury is able to complex with Cl^- , OH^- , S^- and NH_3 (present in trace amounts) because of their abundance and the stability of the complexes that they form (Schuster 1991). Thus, under oxidizing conditions mercury forms complexes with Cl^- , OH^- and dissolved organic matter (DOM). In contrast, under anaerobic conditions the dominant species are sulfide and polysulfide mercury complexes (especially at low pH) (Gabriel and Williamson 2004; Morel et al. 1998; Ravichandran 2004). A summary of mercury speciation in the environment can be found in Table 1. Similar to organic matter, sulfide complexation of mercury can lead to a reduction in its bioavailability, and typically mercury bioavailability declines as sulfide concentrations increase (Goulet et al. 2007). This is thought to be related to the formation of charged sulfide complexes at elevated sulfide concentrations, whereas neutral HgS complexes, formed at low sulfide concentrations, are thought to be more bioavailable (Benoit et al. 1999). Dimethyl, ethyl and methyl mercury are the known organo metallic forms of mercury.

Table 2.1. General biogeochemistry of mercury in soils (Morel 1998 and Gabriel and Williamson 2004). General sulfide speciation is based on modeling in Visual Minteq (Gustafsson 2006) using thermodynamic data from Goulet et al. (2007) at STP assuming an infinite dilution.

	Aerobic	Sulfate reducing conditions
Low pH	Mercury Adsorbs primarily to organic matter particles. Chloride complexes dominate (HgCl_2) and to a lesser extent Hg-SO_4 , as well as, Hg-DOM complexes.	HgS , $\text{Hg}(\text{SH})_2$, HgSH^+
Neutral pH	Mercury adsorbs to iron oxides and clay particles. Mercury in solution complexes with chloride and hydroxide to form HgCl_2 , HgClOH and HgOH_2 , as well as DOM-mercury complexes	HgS , $\text{Hg}(\text{SH})_2$, HgS_2^{-2} , HgS_2H^- , HgSH^+ , $(\text{Hg}(\text{S}_n)_2)^{-2}$, HgS_nOH^-
High pH	Mercury hydroxide complexes are dominant $\text{Hg}(\text{OH})_2$, HgOH^+ , as well mercury will complex with DOM	HgS_2^{-2} , HgS_2H^- , $(\text{Hg}(\text{S}_n)_2)^{-2}$, HgS_nOH^-

Dimethyl mercury is considered stable in soil because Hg^{+2} bonds covalently with two methyl groups to form this molecule (Morel et al. 1998).

The high affinity of mercury for organic matter is largely a result of the reduced sulfur functional groups present in organic matter (Ravichandran 2004). Mercury (including elemental Hg) is attracted to and forms strong ionic bonds with reduced sulfur sites on DOM. The DOM in solution limits the bioavailability of mercury to microorganisms because the size of organic matter particles is too large to penetrate microbial membranes. Despite this decrease in bioavailability, the mobility of mercury in an ecosystem is increased by binding to dissolved organic matter (Schuster 1991).

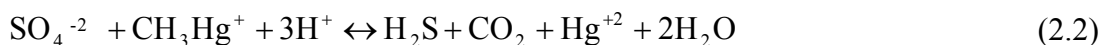
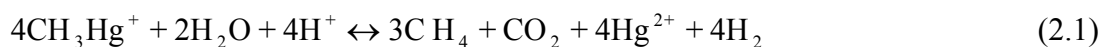
2.2 MeHg in the environment

Methyl mercury (MeHg) can be produced both biotically and abiotically in the environment. Methylation is typically an anaerobic process; aerobic methylation is less common (Gilmour et al. 1998; Goulet et al. 2007). Methylation requires the transfer of an alkyl anion group, however, this anion is unstable in water and the reaction requires photochemical or microbial catalysts (Morel et al. 1998). Numerous studies have established sulfate-reducing bacteria (SRBs) as the primary methylators of mercury in the environment (Warner et al. 2003; Gilmour et al. 1992; Compeau and Bartha 1985; Goulet et al. 2007). Microbial methylation can occur spontaneously outside the cell through the reaction of methylcobalamin with Hg^{2+} , but it is thought to be primarily an enzymatically catalyzed process (Choi et al. 1994).

Microbial mercury methylation occurs through uptake of mercury into bacterial cells (Choi et al. 1994; Morel et al. 1998). When mercury concentrations are high, microbial uptake proceeds via transmembrane cation transporters (Morel et al. 1998). At low concentrations mercury enters the cell through diffusion, this is regulated by the octanol-water partition coefficient (K_{ow}) for the mercury species, e.g. high K_{ow} is correlated with a higher rate of diffusion (Morel et al. 1998). Methylation is thought to occur through the acetyl-CoA pathway in sulfate reducing bacteria (SRBs) (Choi et al. 1994). Methylation via the acetyl-CoA pathway occurs when a protein transfers a methyl group to mercury. This reaction is thought to occur in two steps with methyl transferase enzymes facilitating the reaction (Choi et al. 1994). However recently it has

been established that there could be an alternative pathway involving methionine synthase (Ekstrom et al. 2003; Siciliano and Lean 2002). This pathway involves the transfer of a methyl group from methyltetrahydrofolate to homocysteine which can then methylate mercury (Siciliano and Lean 2002).

Some bacteria are also capable of demethylating mercury (Pak and Bartha 1998a). Demethylation is thought to occur through two main pathways under reducing conditions (Dipasquale and Oremland 1998):



Equation 2.1 and 2.2 illustrate oxidative demethylation pathways which are mediated by methanogens and sulfidogens respectively. It is also possible for mercury to be demethylated, under more oxidizing conditions, via a reductive biochemical pathway, which, is mediated by the organo mercury lyase enzyme (Barkay and Poulain 2007).

Iron reducing conditions can inhibit or stimulate MeHg production (Warner et al. 2003; Fleming et al. 2006). Iron reducing conditions can be a barrier to methylation either through inhibition of bacterial pathways or adsorption of mercury onto iron oxide surfaces which reduces the availability of mercury (Goulet et al. 2007). However, Fleming et al. (2006) found that iron reducing sediments were able to produce MeHg even when sulfate reducers were completely inhibited through the addition of molybdate. The authors isolated the bacterium responsible for iron reduction and found that it was capable of methylating mercury at rates comparable to SRBs. Fleming et al. (2006) hypothesized that iron reduction increased methylation through dissolution of iron colloids, thus increasing the bioavailable pool of mercury or that methylation occurred during the reduction of iron by the iron reducing bacterium.

Warner et al. (2003) found that methanogenic sediments had similar methylation rates to sulfate reducing sediment and hypothesized that SRBs and methanogens were functioning symbiotically to methylate mercury. However, other studies have shown that methanogenic conditions only contribute to demethylation (Pak and Bartha 1998b; Goulet et al. 2007; Oremland et al. 1991). There are also abiotic methylation pathways (Weber 1993; Falter 1999). Some general pathways for abiotic MeHg formation involve reactions with methylcobalamin, methyltin compounds and humic matter (Weber

1993). Humic matter is thought to be the most likely source of abiotic methylation in the environment (Weber 1993).

Soils have the ability to sequester MeHg and act as long term sinks and sources for wetlands and other water bodies (Gabriel and Williamson 2004). MeHg tends to be stored in the upper portion of the soil profile, which makes it possible for MeHg to be released into runoff either by erosion or dissolution (Gabriel and Williamson 2004). The methylation of mercury increases its mobility in soils and wetlands (Regnell and Hammar 2004), because of MeHg's high affinity for organic matter and the subsequent mobility of organic matter (Hintelmann et al. 1995). However, the association of increased MeHg concentration with increased DOM may not be related to increased mobility but may be related to increased methylation occurring due to stimulation by DOM, which acts as a carbon source (Gilmour et al. 1998).

2.2.1 MeHg in the arctic

Mercury in the form of mercury vapour (Hg^0) is being transported from industrialized countries to the Arctic (in the atmosphere) where it is converted at polar sunrise to particulate or reactive gaseous mercury and deposited onto the landscape (Schroeder et al. 1998). The exact method of conversion is photo-induced oxidation; bromine and chlorine molecules convert gaseous elemental Hg^0 into Hg^{2+} (reactive gaseous or particulate mercuric mercury) (Lindberg et al. 2002). The mercuric products of this reaction are then deposited onto the snowpack (St. Louis et al. 2005). Most of the Hg^{2+} deposited onto the snowpack is thought to be re-volatilized into the atmosphere through photo-induced reduction (Lahoutifard et al. 2005). St. Louis et al. (2005) found that atmospheric depletion events resulted in a 100 fold increase in mercury concentrations in snow. However this was quickly photoreduced and the net result was that only a small amount of mercury is deposited from the atmosphere. Once deposited the remaining Hg^{2+} could be converted into MeHg either in the soil or groundwater.

Recently St. Louis et al. (2005) and Lahoutifard et al. (2005) hypothesized that MeHg is deposited onto the arctic landscape as photodegraded dimethyl mercury. St. Louis et al. (2005) found MeHg levels up to 0.28 ng L^{-1} in the snow which represented a significant portion of the total mercury. However, they disagreed about the source of dimethyl mercury; St. Louis et al. (2005) hypothesized that it comes directly from the

ocean where it escapes through openings in the ice, because of a correlation between chloride and MeHg concentrations in the snowpack. In contrast, Lahoutifard et al. (2005) found no correlation between chloride and methyl mercury concentration. Barkay and Poulain (2007) have also suggested that mercury deposited onto the snowpack at polar sunrise may be highly bioavailable and methylation may occur in the snowpack.

Loseto et al. (2004b) found that the contribution of wetlands to methyl mercury loading in lakes was site specific. Wetlands on Cornwallis Island did not contribute to MeHg input into lakes, but wetlands did affect MeHg input into a lake on Ellesmere Island (Loseto et al. 2004b). MeHg in snowmelt was found to be the dominant source of MeHg to arctic lakes (Loseto et al. 2004b). Wetlands were also thought to be sources of MeHg in a previous study on Cornwallis island because wetland surface water increased from $\sim 0.02 \text{ ng L}^{-1}$ at the inflow to $\sim 1.2 \text{ ng L}^{-1}$ at the wetlands outflow (Loseto 2004a).

Arctic organic soil in laboratory incubations has been shown to methylate mercury at low temperatures (4°C) (Loseto et al. 2004a). Methyl mercury increased 100 fold from initial concentrations 0.065 ng g^{-1} . However, SRBs do not appear to be the dominant methylators in the arctic environment, due to low numbers of SRBs in arctic wetland soil (Loseto 2004a). Loseto et al. (2004a) found that the amount of SRB, determined using most probable number techniques, were several orders of magnitude lower than SRB found in other harsh environments. The gene specific for sulfate reduction was also only amplifiable at one sampling site, which did not correspond to elevated MeHg levels. Loseto et al. (2004a) postulated that other bacteria or abiotic factors may be causing mercury methylation in the arctic. A 60 day incubation of the same soils found that methyl mercury decreased to sub parts per billion levels in some sites, however, soil from three sites continued to produce methylmercury after 30 days (Loseto et al. 2004a). The authors postulated that bioavailability may be affecting the net production of methylmercury.

2.3 Redox conditions in the soil environment

Redox reactions in the environment involve the transfer of electrons from one atom to another (Stumm and Morgan 1996). Microbes are the primary catalyst for redox

reactions in the environment, which they use to obtain energy from the metabolism of organic matter. Electron accepting molecules are reduced by the electrons generated from the decomposition of organic matter and in turn generate energy for the bacteria. The more easily reduced the electron acceptor the more energy is gained from the reaction. In aerobic conditions oxygen is the dominant electron acceptor and is reduced through several steps into water. In the absence of oxygen other compounds will be reduced; the energy gained from the reduction of electron acceptors other than oxygen is dependent on how thermodynamically favorable the reaction is. In anaerobic systems generally the reaction order is: nitrate, iron oxides, sulfate and then the reduction of organic matter (methanogenesis). These shifts in redox conditions from aerobic to increasingly reducing conditions lead to functional changes in the microbial communities with denitrifying bacteria giving way to iron reducers until finally methanogens are dominant (Kirk 2004). The reduction/oxidation of iron may be of particular concern to MeHg production in the Arctic, because sulfate reduction may be limited in Arctic wetlands (Loseto 2004a) and iron reduction has recently been tied to methylation in lake sediments (Fleming et al. 2006)

2.3.1 Dissimilatory iron reducing bacteria

Ferric iron [Fe(III)] is an abundant terminal electron acceptor in the environment, representing a significant portion of the sediment by weight (Lovley 1991). Dissimilatory iron reduction is an important pathway for the oxidation of organic matter and organic contaminants, and refers to those bacteria that do not accumulate ferrous iron [Fe(II)] inside their cells (Lovley 1991). Iron reduction can also occur abiotically (Fleming et al. 2006).

Lovley and Phillips (1988) identified the first dissimilatory iron and manganese reducer in environmental matrices (G-15). This bacterium was fermentative and a facultative iron reducer (Luu and Ramsay 2003). However, recently fermentative reducers have been found to be an insignificant portion of iron reducers with less than 5% of their energy being derived from fermentation (Luu and Ramsay 2003; Lovley 1991). Instead most iron reducers use the end products of fermentation as electron donors (Lovley 1993). There are five general groups of iron reducers described by Lovley (1991): i. Fermentative iron reducers ii. Sulfur oxidizing iron reducers iii.

Hydrogen-oxidizing iron reducers iv. Organic acid oxidizing iron reducers v. Aromatic compound oxidizing iron reducers. This is a diverse group of organisms with many considered to be facultative iron reducers (Nealson and Saffarini 1994). Most iron reducers belong to the δ subdivision of Proteobacteria, however other bacteria outside this subdivision can also reduce iron (Luu and Ramsay 2003).

Recently several authors have identified bacteria which are capable of reducing iron in cold environments (Kostka et al. 1999; Vandieken et al. 2006). However, most research appears to be focused on ocean sediment processes where sulfate is most likely not limited and therefore may not apply to arctic soil where the chemical composition of the soil solution would be quite different. Recent research in acidic pit lakes also indicates that iron reduction may be temperature dependent and the relative activity of iron and sulfate reducers may vary with temperature (Meier et al. 2005).

Iron is unique when compared to other electron acceptors in that most of it is present as insoluble iron oxides (Luu and Ramsay 2003). The structure of iron oxides affects the ability of iron reducing bacteria to reduce iron (Nealson and Saffarini 1994). Oxides with a higher degree of crystallinity are much more resistant to reduction (Luu and Ramsay 2003). Poorly crystalline oxides coating soil surfaces (clay primarily) seem to be the primary source of reducible iron (Luu and Ramsay 2003). The availability of surface sites for enzymatic contact also affects the reducibility of iron complexes (Roden and Zachara 1996). Fe(II) saturation of the iron oxide surface can limit reduction and limit electron transport to the surface of the iron oxides (Roden and Zachara 1996; Luu and Ramsay 2003).

Oxidized Fe(III) is fairly insoluble in the soil environment with solubilities approaching 10^{-9} M at neutral pH (Chipperfield and Ratledge 2000). This complicates the means of microbial electron transport, which is poorly understood, for iron reducing bacteria (Luu and Ramsay 2003). Fe reduction is hypothesized to occur by a variety of methods including cellular contact, chelating agents which solubilize iron and electron shuttling compounds (Luu and Ramsay 2003). The enzyme that is responsible for the reduction of Fe(III) is thought to be a dissimilatory iron reductase enzyme that is produced in anaerobic environments; ferric reductase enzymes are common to most organisms (Nealson and Saffarini 1994). This enzyme is typically active in the

membranes of dissimilatory iron reducing bacteria (Nealson and Saffarini 1994). Numerous studies have shown that bacterial reduction relates to the amount of bacterial cells attached to the oxide surface (Das and Caccavo 2000; Lovley and Phillips 1988). Enzymes, with cytochromes centers, could occur on the outside of the cell membrane and transfer the electrons from the cell to Fe(III) during cellular contact (Magnuson et al. 2001). Another model of reduction, by cellular contact, hypothesizes that nicotinamide adenine dinucleotide (NADH) hydrogenase, can transfer electrons through a series of cytochromes to Fe(III) (Lovley 2000).

Microorganisms that assimilate Fe(III) into their cells use siderophores (high affinity Fe(III) chelators) (Luu and Ramsay 2003). Siderophores could also have a role in extracellular solubilization of Fe(III) (Luu and Ramsay 2003). Electron shuttling compounds such as humin, cytochromes or quinones could carry electrons between dissimilatory iron reducing bacteria and Fe(III) (Luu and Ramsay 2003; Nevin and Lovley 2002; Newman and Kolter 2000). Humic substances act as electron shuttles between the bacterial cells and Fe(III) (Lovley et al. 1996). Shuttling refers to the reduction of humic compounds by iron reducers, the re-oxidation of humic compounds through electron transfer to Fe(III) and its subsequent reduction to Fe(II). Humic substances may also facilitate Fe(III) reduction by complexing Fe(II) which prevents Fe(II) absorption to cell or oxide surfaces (Royer et al. 2002). Bacteria that do not possess extracellular means of Fe(III) reduction, (e.g. chelating agents or electron shuttling compounds) develop flagella and pilli in the presence of insoluble Fe(III) (chemotaxis) (Childers et al. 2002).

2.3.2 Iron biogeochemical cycling in terrestrial environments

Iron is different than many redox species because it can be readily reoxidized to Fe(III) and re-accumulate in the sediment or soil (Luu and Ramsay 2003). Reduction of iron was discussed in detail in the previous section. The other aspects of iron cycling in terrestrial environments are the re-oxidation, precipitation and sorption of iron species. Iron is present primarily as iron oxides in soils in a variety of climatic regions globally (Schwertmann and Taylor 1989). These oxides are then dissolved primarily through the microbiological processes mentioned above. Oxidation of ferrous minerals can occur anaerobically at low or neutral pH (Senko et al. 2005; Fortin and Langley 2005) or

aerobically (Temple and Colmer 1951). Iron Oxidation can also occur chemically at neutral pHs in the presence of oxygen in a kinetically fast reaction (Fortin and Langley 2005). The cycling and distribution of Fe(III) is dependent on organic matter input, most Fe(III) accumulates in sediment, in the absence of organic matter (Luu and Ramsay 2003). Reduced Fe(II) can form insoluble precipitates such as pyrite (FeS_2) (Luu and Ramsay 2003). Bacteria may also assimilate iron and use it for growth (Luu and Ramsay 2003).

2.4 Methods of MeHg analysis

Analytical methods for MeHg typically involve four steps (Shade and Hudson 2005): **i.** the separation of mercury from the samples matrix; **ii.** concentration of the extract onto a solid phase; **iii.** separation of MeHg from Hg^{2+} and Hg^0 during analysis; **iv.** quantification. Commonly used separation steps can be time consuming and can lead to artifactual MeHg formation (e.g. distillation) (Shade and Hudson 2005). Also current and accepted techniques like distillation/ethylation, e.g. EPA method 1630, are difficult to automate and require highly skilled technicians (Shade and Hudson 2005). These problems have lead to research into new techniques of MeHg analysis.

2.4.1 Hg-thiourea complex ion chromatography and Atomic Fluorescence Spectrometric Detection

Shade and Hudson (2005) developed a new method of MeHg analysis that allows for simple, rapid and accurate analysis of MeHg in environmental samples. This method uses high-pressure liquid-ion chromatography (HPLC), photocatalytic oxidation (PCO) and cold vapour atomic fluorescence (CVAFS) to detect MeHg in tissue and sediments to picogram levels.

MeHg is separated from the sample matrix using solvent-extracted digests. MeHg in soil samples are extracted using $\text{HNO}_3/\text{CuSO}_4$, separated using toluene, then back extracted in acidic thiourea (TU) and filtered (Shade and Hudson 2005). Thiourea complexes with the organic and inorganic mercury species in the back extract. The extract is preconcentrated on a thiol trap at a pH of 3.5 or 4 and then eluted with an acidic (pH \sim 1) TU solution, which outcompetes the resin's thiol sites for mercury at low pH. The advantage of using thiourea (TU) over other commonly used ligands, is

that TU-mercury complexes are almost pH independent, except at very low pH's, in terms of their stability. This characteristic facilitates the use of highly acidic eluants in the system and the pre-concentration of samples on a thiol resin. Also adding TU to the eluant minimizes the sorption of the solute to system components. After leaving the thiol trap the eluant enters an ion chromatography column where HgTU^{2+} and MeHgTU^+ are separated based on their respective charges.

The MeHg in the eluant stream is oxidized through photo-induced oxidation using UV light produced at 254 nm and hydrogen peroxide (UV-PCO). The photolysis of hydrogen peroxide creates hydroxyl radicals, which oxidize MeHg^{+1} to Hg^{2+} . Antioxidants are then added to the system to remove any remaining oxidant in the eluant. This is followed by the reduction of Hg^{2+} to Hg^0 by SnCl_2 (cold vapour step), separation of the cold vapour using a gas liquid separator, removal of water from the gas stream and quantification using atomic fluorescence spectroscopy. Absolute detection limits are less than 1 pg, which is comparable to detection limits obtained using GC-CVAFS and superior to results obtained from current HPLC systems.

2.4.2 Alternative methods

Ethylation coupled with GC-CVAFS is a common method of analysis for mercury (EPA 2001). This typically involves the extraction of MeHg from a solid or aqueous sample matrix, which is followed by the addition of the sample extract into a sparging flask where the MeHg is ethylated with sodium tetraethylborate and concentrated on a carbon trap. The mercury species are desorbed from the carbon trap and into the GC where they are separated on a column and analyzed using CVAFS. A drawback to this method of analysis is that the systems are somewhat expensive and the analysis requires a highly skilled operator (Shade and Hudson 2005). Electron capture detection is also commonly employed with GC applications, however, electron capture detection is not Hg specific therefore the success of analysis relies on sample preparation and retention times (Shade and Hudson 2005). GC-ICP-MS (Inductively coupled plasma- mass spectrometry) systems allow organic solvents to be used without any concern for quenching, however, the cost for these systems is high (Shade and Hudson 2005).

3.0 METHYL MERCURY PRODUCTION TRUELOVE LOWLAND, DEVON ISLAND, CANADA: A FIELD STUDY

3.1 Introduction

Mercury is being deposited to arctic environments through atmospheric deposition at polar sunrise (Carpi and Lindberg 1998) and recently it has been hypothesized that MeHg could be reaching terrestrial environments through volatilization and oxidation of dimethyl mercury from the ocean (St. Louis et al. 2005). Inevitably the mercury that remains in these environments will be deposited in the soil or water bodies. A significant amount of research has been carried out on the fate of mercury in the arctic snowpack and lakes (St. Louis et al. 2005; Hammershmidt et al. 2006; Lahoutifard et al. 2005) but little research has been carried out on arctic soil. Arctic wetlands are producing methylmercury (MeHg), however, the means by which this occurs are not yet known (Losetto et al. 2004a).

3.1.1 Truelove Lowland

The Truelove Lowland is situated on the northeastern coast of Devon Island (75° 33'N, 84° 40'N) (Bliss 1977). It is the fifth largest island in the Canadian Arctic. Most of Devon Island is a polar desert. However, the Truelove Lowland is unique in that it supports a greater biological diversity than the surrounding area and is considered a polar oasis. These areas are quite rare in the arctic, only 6% of the Arctic land mass contains these polar oases.

The climate of Truelove Lowland is similar to that of a high latitude continental land mass (Courtin and Labine 1977). Low annual temperatures (below freezing) and low precipitation characterize Devon Island. The mean annual air temperature is – 15.9°C (King 1969), in the summers the temperature can fluctuate between 2.8 and 9.6°C. The Lowland receives approximately 137 mm of snow and 42 mm of rain

(average results from 1972 – 1974). Mean annual winds are similar to temperate regions except for periods of cyclonic disturbance. Snow has a dominant influence on the hydrologic cycle. Rain accounts for a small percentage of the total precipitation for the area (approximately 23 %).

The Truelove Lowlands are covered with Pleistocene age deposits that overlay a Precambrian complex (Bliss 1977). Two geological units underlie the lowlands; the Canadian Shield and the Arctic Platform (Krupicka 1977). The lowlands are a result of postglacial rebound, which followed ice retreat resulting in uplift of portions of the Lowlands. This uplift created shallow lagoons, which eventually formed shallow lakes, some of which filled to create meadows. Raised beaches were also formed, which impeded the drainage of melt water. These raised beaches are coarse in texture and are much drier than the surrounding landscape.

The soils of the Truelove Lowland belong to the Cryosolic Great Group and are predominantly enriched in calcium (Walker and Peters 1977). Permafrost underlies the entire lowland and the arctic climate tends to retard soil development. Drainage and climate are the factors that most affect the pedogenic development of soils in the area. Generally the mineral soil (Static and Turbic Cryosols) is coarse textured with some medium to fine textured soil occurring on lacustrine and alluvial parent material. The soils of the lowland are underlain by a frozen (Cz or Oz) horizon. There are also some areas that are classified as rubble (minimal soil development). A generic diagram of the affect of drainage on soil formation along a catena can be found in Figure 3.1.1.

There are two types of organic soils, found in poorly drained depressions: Glacic Fibric Organo Cryosols and Fibric Organo Cryosols (classified by Walker and Peters 1977). However, according to the current system of Canadian soil classification they would both be classified as Histic Regosolic Static or Histic Regosolic Turbic Cryosols. The organic material is composed mostly of sedge and moss. The pH of the peat is acidic to neutral with peat found along streams being slightly acidic. Ice-cored polygons containing dry surface peat mixed with organic matter are found near streams and lakes. These materials can also contain algal cells in organic deposits resembling coprogenous or diatomaceous earth.

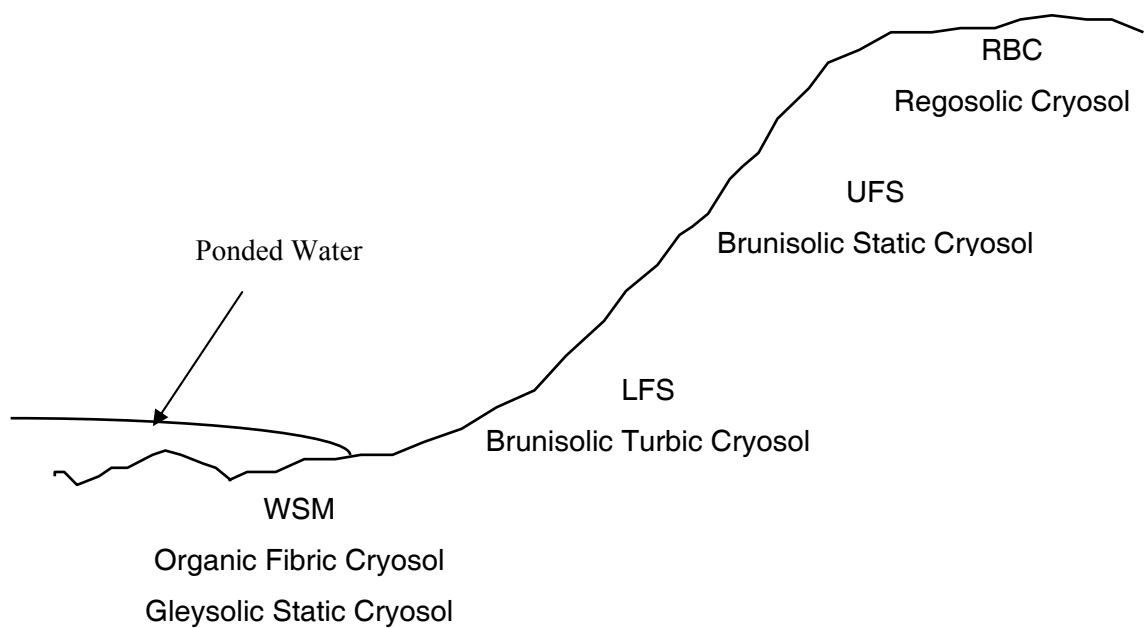


Figure 3.1.1. Typical catena on Truelove Lowland. The WSM refers to the wet sedge meadow, LFS refers to the lower foreslope, UFS refers to the upper foreslope and the RBC is representative of the raised beach crest. Information obtained from Walker and Peters (1977). Soil classification based on Walker and Peters (1977).

A cold hydrological environment characterizes the Truelove Lowland (Ryden 1977). Most overland flow, from melt water, occurs in late June and early July. Spring is characterized by a rapid decrease in snow cover and air temperatures near the soil surface rise rapidly. Snowmelt occurs mostly as overland flow, in irregular patterns, because the ground is frozen to within a few centimeters of the surface. Turbulent flow caused by snowmelt can transport and redistribute litter, typically during the non-channeled flow stage of snowmelt. During May and June soil thaw begins and the top layer fills with water, plants use this water before the melt water infiltrates. The soils active layer reaches maximum thickness in late July (<30 cm in poorly drained soils and ~80 cm in well drained soil). July and August are considered the summer season when the lowlands are snow free and the water discharge occurs through channels. The rain is frequent but the intensity is low. The remaining permafrost does not permit downward percolation and most drainage is lateral.

The vegetation communities on the Truelove Lowlands are rich in species (Muc and Bliss 1977). The productivity and percent cover of these plant communities is also much higher at this latitude than would be expected. These communities are typically composed of sedge (*Carex*), grass (*Arctagrostis*), moss, lichen along with dwarf shrubs (e.g. *Salix*) and some forbs. Plant species tolerant of poor drainage, e.g. *sphagnum*, are present further down slope; cushion plants and lichen are found on slope crests in more well drained areas. Muc and Bliss (1977) described four dominant plant communities: Frost-boil sedge moss meadow, hummocky sedge-moss meadows, cushion plant-lichen and dwarf shrub heath-moss communities.

Frost-boil sedge moss meadow communities are found in the toe slope positions and are the most widespread community (20.5 % cover). These communities have a hummocky micro-relief and are dominated by *Carex sans*. Hummocky sedge-moss meadows occur in bottom slope positions (18.4 % cover). Most of these communities are covered with cyanobacteria (blue-green algae), mosses and sedges. Cushion plant-lichen and dwarf shrub communities represent a smaller proportion of the plant communities found on the lowlands.

3.2 Objective

The objective of this study was to examine MeHg production in Cryosolic soil over an arctic summer in the hope of gaining a better understanding of the fate of mercury in polar oases. More specifically the goals of this study were to:

1. assess the effect of redox potential on MeHg production
2. assess the effects of changes in other biophysical factors such as temperature and moisture on MeHg production.

The main hypothesis is that iron reducing conditions are capable of supporting MeHg production.

To accomplish these objectives numerous physical and chemical parameters were measured along catenas on Truelove Lowland, Devon Island. The study was designed to monitor the effect of changing environmental conditions over time on redox conditions and methyl mercury production. Catena's of similar slope were randomly selected and used as replicates in the study.

3.3 Methods

The site of the field study is a coastal lowland and polar oasis situated in the high arctic on the tip of Devon Island. In an attempt to capture changes in redox conditions four catenas were selected and sampling locations were established along these catenas. Catenas were selected which were classified as wet sedge moss meadows by Walker and Peter (1977) and had an organic horizon greater than 20 cm in thickness (classified by Walker and Peter (1977) as an Fibric Organic Cryosol). Site selection was constrained to sites which could be easily accessed by foot within a day from base camp (Figure 3.3.1).

3.3.1 Sampling protocol

Five sampling locations (Figure 3.3.2) were established along each catena. Piezometers were installed in lower slope positions where soils would remain saturated and lysimeters were installed in upper slope positions where soils had the potential to become unsaturated.

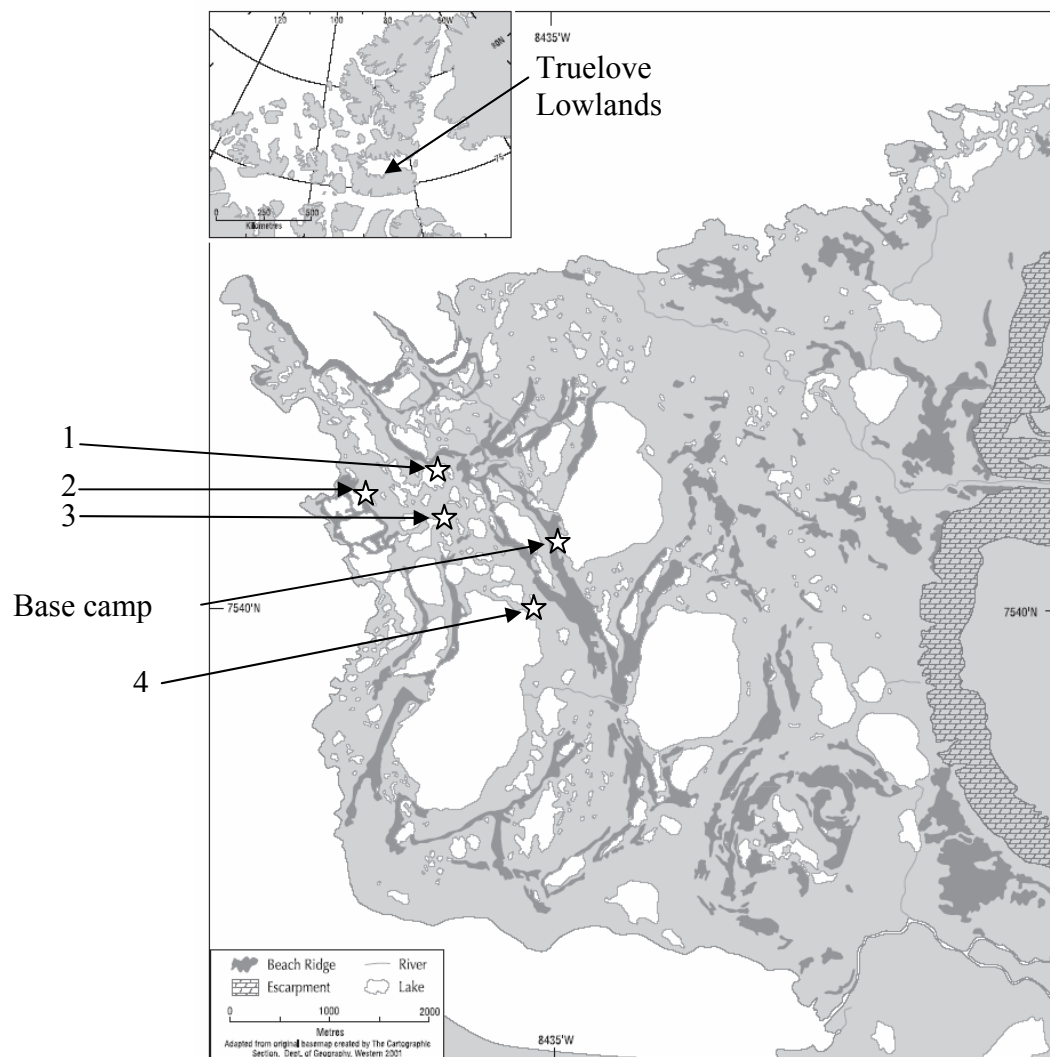


Figure 3.3.1. Map of the Truelove Lowland with locations of Catenas (obtained courtesy of the Cartography Department University of Western Ontario)

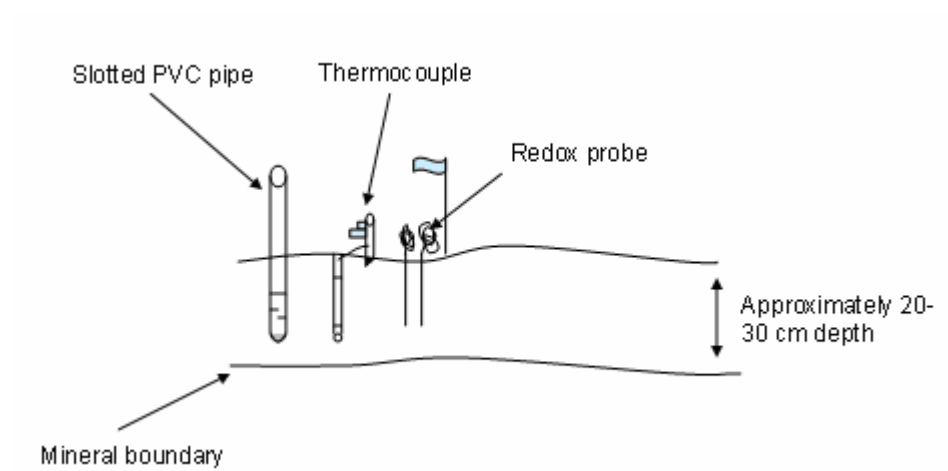


Figure 3.3.2. Diagram of instrumentation installation

Lysimeters were installed by hand augering a hole in the fibric layer using a modified aluminum root sampler. The hole was then partially filled with wet silica flour, followed by a 5 cm diameter PVC (polyvinyl chloride) lysimeter (100 Series with ceramic cup, Soil Moisture Corporation, Goleta, California). The hole was sealed with bentonite chips to prevent overland flow from entering the lysimeter especially in saturated areas. The lysimeters were purged with high purity nitrogen gas (Praxair, Edmonton, Alberta) and quickly capped and further evacuated with a hand vacuum pump to a pressure of 60 cbar and left to collect porewater.

Piezometers were installed in lower slope positions in a similar manner to the lysimeters with capped slotted PVC pipes being inserted into the soil and sealed with bentonite chips to prevent the infiltration of overland flow (Levy 2006; Regnell and Hamar 2004). Wells were capped in between sampling to prevent contamination from rain water and particulates.

Redox probes were installed by inserting platinum electrodes to a depth of ~20 cm just above the permafrost through a slit in the soil. Thermocouples were inserted through a slit in the soil to a depth of ~20 cm, soil temperature was recorded for depths of 10 and 20 cm respectively. Each location was marked with flagging tape .

3.3.2 Soil sampling

Soil was sampled to a depth of ~20 cm using a root sampler; with gloved hands the soil core was extracted, the vegetative layer removed and the remaining soil placed in trace clean HDPE (high density polyethylene) jars (VWR, West Chester, PA). Once at base camp a portion of soil was removed for gravimetric moisture determination and MeHg extraction, and the rest was frozen at -20°C.

3.3.3 Pore water sampling

Pore water was sampled for Fe(II)/Fe(III), sulfide, major anions (SO_4^{2-} , NO_3^- , NO_2^- , Cl^-), major cations (Ca^{2+} , Na^+ , Mg^{2+} , K^+), dissolved mercury (DHg), total mercury (THg), dissolved organic carbon (DOC), total organic carbon (TOC), pH and Eh. Pore water was sampled according to “clean hands dirty hands” sampling protocol. Pore water was sampled using polytetrafluoroethylene (PTFE) tubing attached to a rubber free Norm-ject™ syringe (Henke-Sass, Wolf GmbH, Tuttlingen, Germany). Samples for cation, anion, DHg and DOC analysis were filtered through a 0.45 μm PVDF (polyvinyl

difluoride) membrane filter with a polypropylene housing (Whatman Inc, Clifton, NJ). A 3 mL medical grade syringe with a 25 gauge needle (Beckton Dickinson & Co., Franklin Lake NJ) was used to inject sulfide and iron samples into 2 mL autosampler vials with Teflon septa (National Scientific Company, Rockwood, TN). Samples for THg, DHg, DOC, TOC and major anions were collected in clarified polypropylene centrifuge tubes (Becton Dickinson & Co, Franklin Lakes NJ). Solvent-Saver[®] scintillation borosilicate glass vials (VWR, West Chester, PA) were used to collect samples for cation analysis.

3.3.4 Field measurements

Platinum electrodes were installed by making a slit in the soil and pushing the probe into the bottom of the organic layer. Eh was measured by making a second slit in the organic layer, inserting an AgCl reference electrode (Thermo Orion) into the soil, ensuring good contact between the reference electrode and the soil, and connecting the copper and silver leads from the electrodes to a voltage meter (Cole Parmer). The reference electrode was attached to the positive lead and the platinum electrode was attached to the negative lead for all measurements (Ag, AgCl | KCl (sat) || Solution | Pt). The potential was taken after the rate of change, as read using a voltage meter, had plateaued ($\Delta Eh < 5 \text{ mV min}^{-1}$).

Thermocouples were installed by pushing them 30 cm into the soil with a deadblow hammer. Thermocouples were read by connecting a thermocouple reader (Cole Parmer) to a female round T-type plug (McMaster Carr, Chicago IL) on the thermocouple and recording the temperature once the reading had stabilized. pH was measured using a Quattrode[®] combination electrode (Thermo Orion) in approximately 50 mL of water in a triple rinsed HDPE cup.

3.3.5 Field equipment construction

Platinum electrodes were constructed according to Wafer et al. (2004) (Figure 3.3.3). Briefly:

1. A 1/8 inch piece of uncoated bronze brazing rod was cut to a length of 8 cm.
2. A 0.5 cm hole was drilled into one end and a 1.3 cm hole was center drilled into the other end of the brazing rod.

3. The holes were heated with a soldering iron until the brazing rod was hot enough to melt the rosin core solder (B & E Industrial Electronics, Saskatoon Sk). The solder was dipped in flux resin (B & E Industrial Electronics, Saskatoon Sk) and pressed into the hole until liquid solder filled the hole.
4. A 1.5 cm piece of 99% 18-gauge platinum wire (World Precision Instruments, Sarasota, FL) was then inserted into the 0.5 cm hole and the solder was allowed to cool. The joint was checked by tugging on the platinum wire to ensure a good connection.
5. The end of a 1 m strip of insulated 18-gauge copper wire (Radio Shack), with insulation removed from tip, was inserted into the opposite end of the brazing rod.
6. Excess solder was removed using a soldering iron and a metal file.
7. 1/8 inch insulated-thin walled-adhesive lined heat shrink tubing (B & E Industrial Electronics, Saskatoon, Sk) was then pulled over the brazing rod to within 0.5 cm of the platinum-brazing rod junction so it covered a portion of the copper wire.
8. The tubing was shrunk by slowly rotating a heat gun around the electrode. A thick walled terminal insulator (McMaster Carr, Chicago, IL Cat # 72675k51) was slid over the Pt-bronze junction and was slowly heated with a heat gun until it appeared that a water tight seal had formed.

Redox probes were tested in quinhydrone pH 4 buffer and ferric-ferrous cyanide buffer. Probes were considered acceptable if they were within ± 10 mV of the expected value for the quinhydrone solution and within ± 10 mV of the ferrous/ferric cyanide buffer. Probes were also tested in tap water and were used if they were within ± 150 mV of one another and read between 300 and 600 mV (normal Eh range of tap water) (Wafer et al. 2004). Probes that failed these tests had their terminal insulators removed and a new terminal insulator was applied and the probes were tested again. Probes that repeatedly failed these tests were disassembled and the platinum wire was re-used to make another electrode.

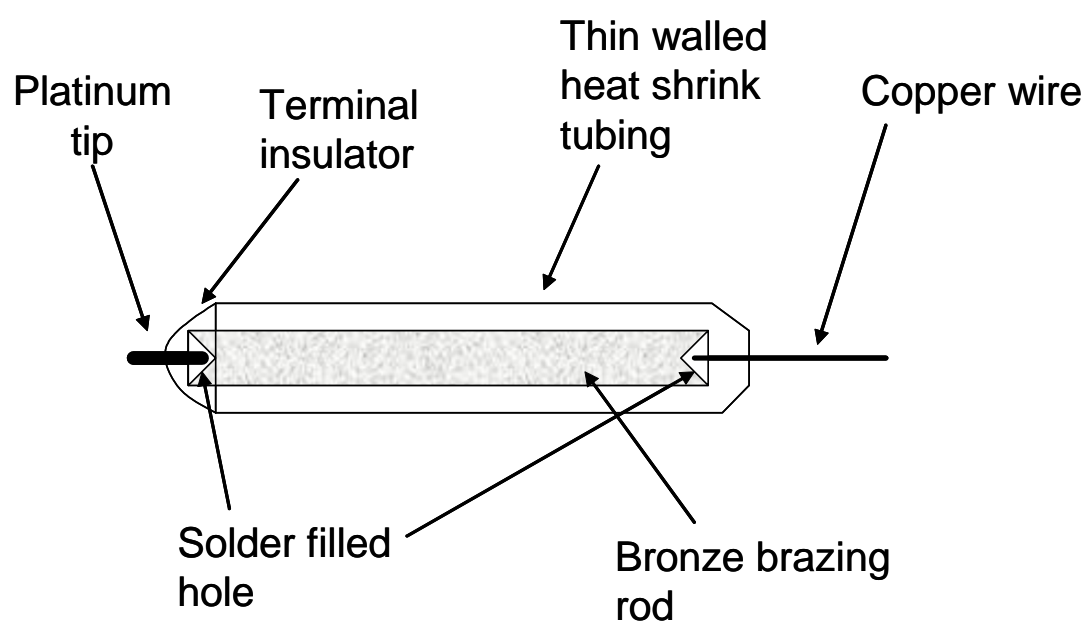


Figure 3.3.3. Diagram of fully constructed redox probe (adapted from Wafer et al. 2004).

Thermocouples were constructed using 20 gauge T-type thermocouple wire (York Wire & Cable Inc., York, PA) and 2.5 cm schedule 40 PVC pipe (Elliot 2006).

Briefly:

1. PVC pipe was cut to a length of approximately 20 cm.
2. Grooves were cut at 10 and 20 cm from the bottom of the pipe using a table saw and a hole was drilled at the groove.
4. The outer jacket was removed from a portion of the thermocouple wire exposing the insulated constantin and copper wires
5. The wire was inserted through the hole and wrapped around the groove
6. The ends of the wires were stripped exposing approximately 3 cm of bare metal and these ends were twisted together and soldered at the base of the join.
7. The excess wire was cut as close to the top of the groove as possible, soldered and sealed with marine contact adhesive (Eclectic Products Inc., Eugene, Or).
8. The opposite end of the wire was attached to a female round type plug (McMaster Carr, Chicago IL) so it could be read by a thermocouple reader. The female plug was attached to a separate piece of PVC pipe to minimize measurement error.

3.3.6 Analysis

All chemicals used in analysis were ACS grade or better. Nanopure deionized water was produced using a NANOpure DIamond Ultrapure water system, Model D11911 (Barnstead International, Dubuque IA).

3.3.7 MeHg extraction

MeHg was extracted in the field according to a method developed by Shade (2005). All acids used were of trace metal grade (Fisher Scientific Company, Edmonton, AB), all other chemicals were ACS grade or better and all water used had less than 1 ppt residual mercury. Approximately 4 g of wet organic soil was transferred to a 50 mL Falcon[®] centrifuge tube (Becton Dickinson & Co, Franklin Lakes NJ). Then 20 mL of 4.8 M nitric acid was added to each tube along with 4 mL of 1 M CuSO₄ (EMD Chemicals, San Diego CA). The tubes were capped and placed on an orbital shaker at 60 rpm for approximately one hour. Approximately 10 mL of supernatant was transferred to a 15 mL Falcon[®] centrifuge tube (Becton Dickinson & Co, Franklin Lakes

NJ) and centrifuged at 1500 rpm to allow any soil particles to settle out of solution. After centrifugation 6 mL of this solution was withdrawn, added to another 15 mL centrifuge tube, 7 mL of toluene (EMD Chemicals, San Diego CA) was added to the centrifuge tubes and they were placed on a shaker at 60 rpm for one hour. After 1 hour the toluene layer (5 ml) was removed and added to a 15 mL centrifuge tube along with 5 mL of 0.5% Omnitrace[®] HCl (EMD Chemicals, San Diego CA) and 2%, resin cleaned, Thiourea (TU) (Sigma-Aldrich, Oakville, ON). This mixture was placed on an orbital shaker for approximately 5 min. The Toluene layer was then removed and the aqueous TU-HCl layer was frozen at -20 °C until analysis. Sample duplicates and matrix spikes were extracted every ten samples to check for extraction precision and recovery.

3.3.8 MeHg analysis

MeHg was analyzed according to Shade and Hudson (2005) using HPLC-Ion Chromatography-photocatalytic oxidation-cold vapour atomic fluorescence (HPLC-IC-PCO-CVAFS) (Figure 3.3.4). Samples were run by preconcentration onto a thiol functionalized divinylbenzene resin (Jordi Associates Bellingham, MA) and eluted using an acidic thiourea solution. Samples were buffered to approximately pH 4 using 0.75 M sodium citrate (EMD Chemicals, San Diego CA) and 0.05 M sodium ascorbate solution (Alfa Aesar, Ward Hill, MA). The thiol trap was preconditioned with 0.1 M sodium borate (EMD Chemicals, San Diego CA) (also containing 0.05 M sodium ascorbate (Alfa Aesar, Ward Hill, MA)). Sample (3 mL) was injected onto the thiol trap through PTFE tubing using a modular drive pump (Cole Parmer, Cat # C-07553-70) with a rigid PTFE tubing pump head (Cole Parmer, Cat # EW-77390-00). The tubing was rinsed between samples using an acidic thiourea solution (10% HCl (EMD Chemicals, San Diego CA), 10% Ethanol and 2% thiourea (EMD Chemicals, San Diego CA)).

All reagents (Figure 3.3.4) used were pre-cleaned to remove mercury by stirring with thiol resin and filtering through a 0.45 µm PVDF filter. All reagents were made fresh except for the sodium ascorbate which was stored for approximately one week and the eluant which was stored for up to three days.

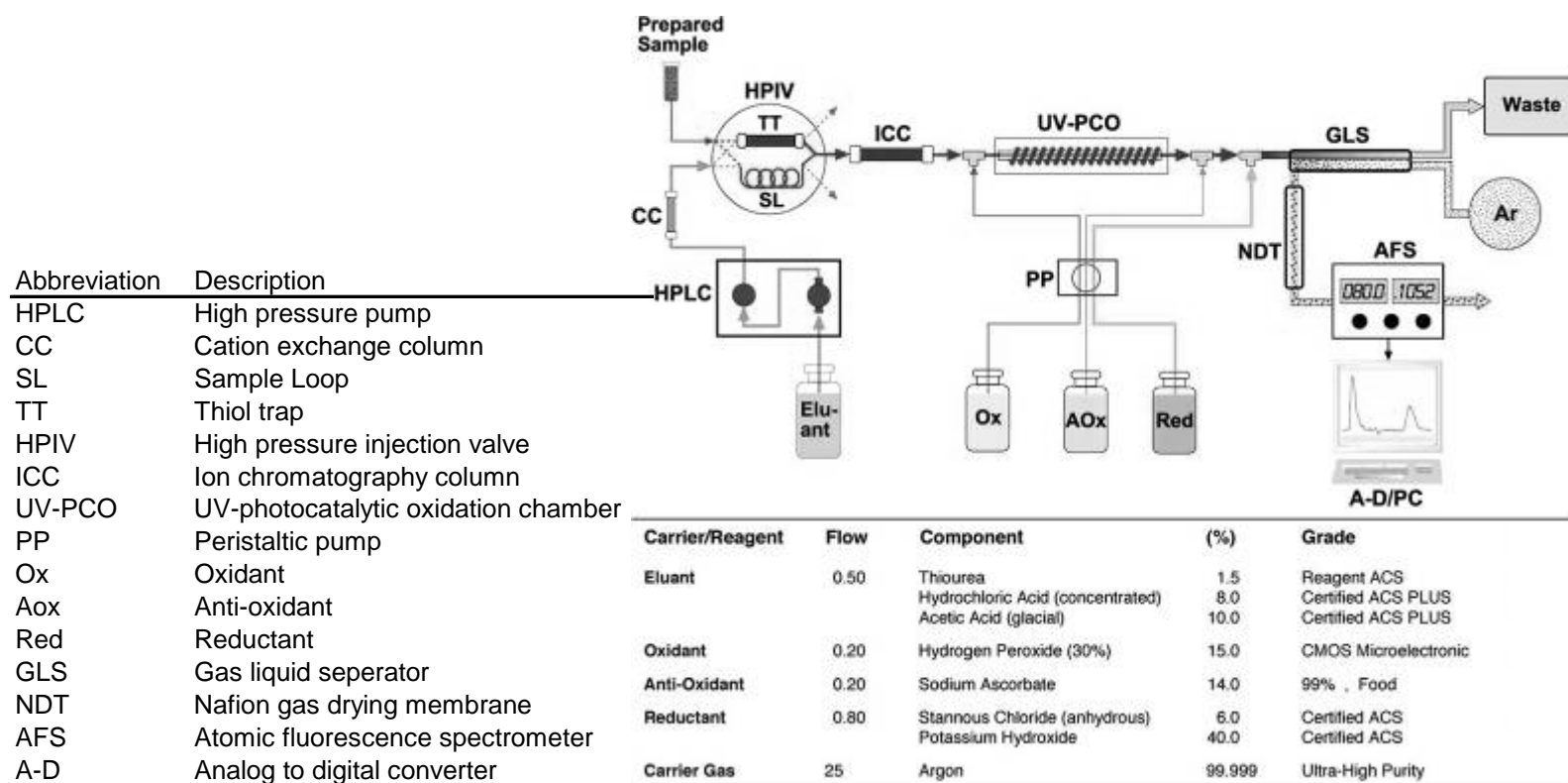


Figure 3.3.4. Overview of HPLC system (flow rate is in mL min⁻¹) adapted from Shade and Hudson (2005).

The system was run for approximately 4 hours prior to analysis to allow the baseline to stabilize. Prior to sample analysis the method detection limit (MDL) was determined based on an analysis of nine MeHg samples of low concentration according to methods outlined in (USEPA, 1998) (equation 3.1).

$$\text{MDL} = 2.602 \cdot \text{sd} \quad (3.1)$$

A 6 point calibration curve was established prior to sample analysis to ensure linearity. Standards were run every 5 samples to correct for instrument drift. Reagent blanks showed no detectable amounts of MeHg in any solutions used.

3.3.9 Hg analysis

Hg in water samples was analyzed according to EPA method 1631 (EPA 1999) using cold vapour atomic fluorescence spectroscopy (Tekran 2600 Tekran Inc., Toronto, ON). Approximately 30 mL of sample was collected in 50 mL falcon tubes (Becton Dickinson & Co, Franklin Lakes NJ). Samples were preserved at base camp by adding 250 μL BrCl (bromine chloride). BrCl was prepared by adding 5.4 g ACS grade potassium bromide (KBr) (EMD Chemicals, San Diego CA) to 500 mL of ultrapure HCl (EMD Chemicals, San Diego CA). A clean magnetic stir bar was added and the solution was stirred for 1 h. Then 7.6 g of ACS grade potassium bromate (CAS 7758-01-2, Alfa Aesar, Ward Hill, MA) was added while stirring the solution with a stir bar. Once the solution changed from yellow to orange it was loosely capped and left to stir for an hour.

Samples were kept at room temperature (4°C) until their return to the University of Saskatchewan where they were stored at 4°C until analysis. Field and lab blanks were also collected in the field (one for every 5-10 samples); these blanks were collected according to method 1631 (EPA 1999).

Prior to analysis, 30 % (w/v) hydroxyl ammonium chloride was prepared (JT Baker, Phillipsburg NJ) in a 50 mL falcon tube. The solution was sparged with ultra high purity (UHP) argon gas overnight and tested to ensure the reagent blank was within the range given in method 1631 (EPA 1999). A 3% (w/v) SnCl (stannous chloride) (J.T. Baker, Phillipsburg NJ) and 5% (v/v) HCl (Omnitrace, EMD Chemicals, San Diego CA) solution was prepared in a Teflon bottle using ultrapure water and sparged with UHP argon gas.

The Tekran 2600 was allowed to warm for at least 2 hours prior to analysis to allow the lamp to stabilize. Approximately 30 mL of sample was used for mercury analysis. Matrix duplicates and matrix spike duplicates were prepared according to Method 1631 for every 10 samples analyzed. Standards were run every 10 samples to account for instrument drift. A new standard curve was run every 30 samples. A 6 point calibration curve was used to calibrate the instrument initially. Instrument blanks were analyzed throughout the run to ensure that there wasn't any carryover between samples. The method detection limit (MDL) was determined according to EPA Part 126 Appendix B, Revision 1.1 using six replicates of a 0.2 ppt Hg Standard. All mercury standards were prepared from an NIST traceable 1000 $\mu\text{g mL}^{-1}$ stock solution.

3.3.14 Dissolved (DOC) and total organic carbon (TOC) analysis

Samples were analyzed for DOC and TOC using methods outlined in both the Shimadzu TOC-5050A manual and Bird et al. (2003). DOC and TOC samples were stored in 15 mL high clarity falcon tubes (Becton Dickinson & Co., Franklin Lakes NJ). An organic carbon stock standard was prepared from ACS grade potassium hydrogen phthalate (Nacalai Tesque, Inc., Kyoto, Japan). This solution can be stored for months at 4 °C. Serial dilutions of this stock solution were made in Nanopure water each day. Prior to analysis 5 mL of sample was withdrawn and transferred to a 9 mL glass autosampler vial (Shimadzu Scientific Instruments, Columbia, MD). Samples were acidified prior to analysis with 2 M HCl (EMD Biosciences Inc., La Jolla CA) to a pH of approximately 2 and sparged with CO₂ free air to remove any inorganic carbon in the sample. Samples were run with a 50 μL injection volume. Two injections per sample were analyzed with a maximum of three to meet QAQC parameters listed below:

- A sample value was accepted if the maximum standard deviation of peak area between replicate injections was below 200 and maximum coefficient of variation was below 2%.

The catalyst was regenerated daily and all tubing was cleaned with a series of blank runs until the blank stabilized prior to the samples being run and sample blanks, duplicates and standards were run every 10 samples

3.3.10 Sulfide analysis

Sulfide was analyzed from soil water extracts following the procedure of Cline (1969) and Goulet et al. (2007). Briefly, N,N-dimethyl-p-phenylenediamine sulfate (2 g) and 3 g ferric chloride $\text{FeCl}_3 \cdot 6\text{H}_2\text{O}$ were added to cool Hydrochloric Acid (EMD Biosciences, La Jolla CA) diluted to 50% v/v. A small amount (100 μL) of diamine reagent was placed in 2 mL autosampler vials (VWR CAT # 66030-442) and sealed anaerobically under a nitrogen atmosphere. In the field, 1.5 mL of sample was added to each vial using a 2 mL syringe with a 25 ga needle (Becton Dickinson & Co., Franklin Lakes NJ) and the hole was sealed with clear silicone.

200 μL of sample was pipetted onto a 96 well tissue culture plate (Becton Dickinson & Co., Franklin Lakes NJ) and read on a spectrophotometer. Standards were prepared using $\text{Na}_2\text{S} \cdot 9\text{H}_2\text{O}$ crystals (Alfa Aesar, Ward Hill, MA) and dissolved in oxygen free water. Then 1.5 mL of standard was added to 100 μL of diamine reagent in the glove box. The samples and standards were analyzed spectrophotometrically using an Emax Precision Microplate Reader. The difference in absorbance can be used to calculate the concentration using the following formula

$$C_{\Sigma s^{-2}} = F(A - A_b) \quad (3.2)$$

where C is the concentration as function of F, a factor derived from the standard curve; A the measured absorbance at 650 nm; and A_b , which is the blank absorbance at 650 nm. Goulet et al. (2007) achieved spike recoveries >95% using this method of sample preservation, without preserving with zinc acetate.

3.3.11 Iron analysis

Dissolved iron Fe(III) and Fe(II) were measured simultaneously in a solution with two separate colourimetric complexing agents. This procedure follows a method modified from Takagai and Igarashi (2003) by Levy (2006). This method is based on the assumption that the absorbance of Fe(II) will be constant at 405 and 450 nm (Figure 3.3.5) and that Fe(III) does not absorb at 405 but does absorb at 450 nm (Figure 3.3.5). Fe(III) and Fe(II) are complexed with bathophenanthrolinedisulfonic acid disodium salt (Bap) (Sigma-Aldrich, Oakville, ON), and deferoxamine mesylate B (DFB) (Sigma-Aldrich, Oakville, ON). The siderophore solution contains 3×10^{-3} μM Bap, 1.5×10^{-3} μM DFB and 0.038 M KH_2PO_4 (EMD Chemicals, San Diego CA) which is

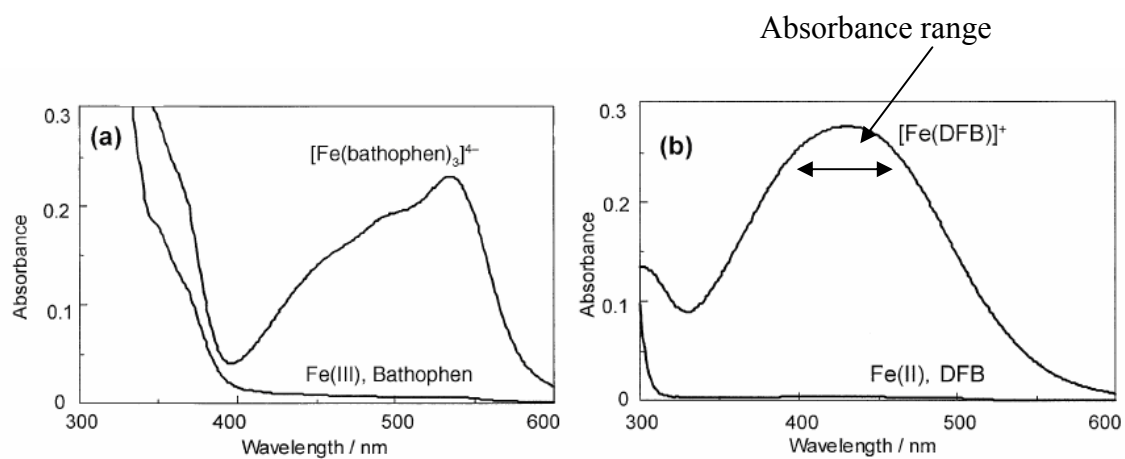


Figure 3.3.5. Absorbance of bathophenanthrolinedisulfonic acid disodium salt (Bap) and deferoxamine mesylate B (DFB) complexes over a range of wavelengths (adapted from Takagi and Igarashi (2003)).

added (1.5 mL) to a 2 mL autosampler vial (VWR CAT # 66030-442) in an anaerobic nitrogen environment.

In the lab these samples were analyzed by pipetting into a 96 well culture plate (Becton Dickinson & Co., Franklin Lakes NJ). Standards were prepared by making serial dilutions of ferric chloride (EM Science, USA) or ferrous ammonium sulfate hexahydrate (EM Science, USA). Stock solutions of Fe(II) and Fe(III) were prepared daily by dissolving ferric chloride or ferrous ammonium sulfate in 1% HCl. These solutions were then diluted in the complexing solution to make standards for the five point calibration curve. The solutions were allowed to sit for 30 min to allow the colour to develop. Ferrous and ferric iron standards were analyzed separately at absorbance's of 405 and 450 nm. The separate curves for each species were constructed according to Levy (2006):

1. Standard curves are expressed as $y = mx + b$, for each wavelength, where m is the slope, x is the concentration, b is the intercept and y is the absorbance.
2. Mixed standards of Fe(II)/Fe(III) are then analyzed and the absorbance corrected using the following two formulas (reproduced from Levy 2006)

$$Fe(III) = abs_{450nm} - \left[\left(\frac{1}{1 - \frac{Fe(II)m_{abs405nm}}{Fe(II)m_{abs450nm}}} \right) (abs_{450nm} - abs_{405nm}) \right] \quad (3.3)$$

$$Fe(II) = \frac{abs_{450} - abs_{405}}{1 - \left(\frac{Fe(II)m_{abs405nm}}{Fe(II)m_{abs450nm}} \right)} \quad (3.4)$$

3. m_{abs} is the slope of the corresponding regression equation, e.g. $Fe(II)m_{abs405nm}$ is the slope of the regression line for the Fe(II) standards analyzed at 405 nm. The subscript abs corresponds to the absorbance of the mixed standard at 405 or 450 nm. This corrected absorbance (Fe(II) and Fe(III) in the above equations) is then plotted against the known concentrations of the mixed standards to obtain a second mixed regression curve that is used to calculate the concentrations of Fe(II)/Fe(III) in the samples.

3.3.12 Major cation analysis

Cations were analyzed using a model 1200 Varian atomic absorption spectrometer with an air-acetylene flame (Varian Inc., Palo Alto, CA). Samples and standards were diluted in a lanthanum – hydrochloric acid mixture to minimize ionization and complexation interferences (EPA 1998). A six point calibration curve, spanning the relevant range of sample concentrations, was prepared from NIST traceable Na, Ca, K and Mg standards (VWR International, West Chester, PA). Samples were not run unless the r^2 value of the standard curve was greater than 0.997. Duplicates were analyzed every 10 samples and 1 blank was analyzed every 20 samples to ensure no carryover was occurring. The calibration curve was re-sloped every 20 samples and the whole calibration curve was re-run every 80 samples. Selected samples were run in duplicate over two analysis periods to ensure system reproducibility. The software included with the model 1200 was used to calculate concentrations automatically from the calibration curve using a linear curve fitting function.

3.3.13 Major anion analysis

Anions were analyzed according to Swallow and Low (1994) using a Waters Quanta 4000 capillary electrophoresis system (Waters Corporation, Millford, MA). Separations were achieved using a 60 cm x 75 μm (i.d.) fused silica column. Samples were introduced using a 30 second hydrostatic injection from a height of 10 cm. The electrolyte buffer was composed of 5 mM sodium chromate, 0.4 mM OFM-BT[®] (Waters Corporation, Millford, MA) which was adjusted to pH 8 with lactic acid and filtered using a 0.45 μm Millipore membrane filter (Millipore, Billerica, MA). Anions were detected at 254 nm using indirect UV detection. Samples and standards were analyzed according to the following sequence: 30 s hydrostatic injection; 3 min run time at 25 Kv; 1.5 min 0.1 M NaOH rinse; 4 min nanopure deionized water rinse; and purge 5 min with buffer.

A five point standard curve was prepared daily from a mixed stock solution. The mixed stock solution was prepared by dissolving appropriate amounts of ACS grade NaSO_4 , NaNO_3 and a stock solution of 1000 $\mu\text{g L}^{-1}$ Cl^- (VWR International) in nanopure water and kept at 4 °C. Standards were not run unless the r^2 for the calibration curve exceeded 0.997.

3.3.15 Statistics

For time period analysis catenas were used as replicates ($n=4$) and sample locations were treated as subsamples to avoid pseudo replication (Hulbert 1984). Sample locations and time periods were used as replicates to evaluate the differences between catenas. All data was evaluated for normality and heterogeneity prior to statistical analysis. Those data which were not normally distributed were transformed using a log normal transformation. Those data which remained non-normal after log transformation were analyzed non-parametrically using the un-transformed data. Distributions of log normal data were expressed using the geometric mean and confidence intervals for each group (indicated by \pm symbol). Normal data distributions were expressed using the mean and standard error for the group. The standard error was chosen to express the variability of the sample mean because it is an indicator of the precision with which the sample mean represents the population mean (Field 2005). Non-normal distributions were expressed using the median and the first and third quartiles of the distribution.

Repeated measures ANOVAs were used to examine differences between dependent variables over time (Field 2005). The assumption of sphericity was tested using the Mauchly test. Groups that did not meet the assumptions of sphericity were corrected using the Greenhouse-Geisser correction. The Friedman test was used to perform repeated measures analysis on non-parametric statistics (reported as X^2). Analysis of variance (general linear model) was used to determine differences between groups (test statistic denoted by an F), data was tested for homogeneity of variance using Levene's test prior to analysis. Differences between groups of non-parametric data were assessed using the Kruskal-Wallis test (test statistic denoted with an H). The Kruskal-Wallis test was used because it is less sensitive to differences in distributions between groups. The strengths of relationships between normally distributed data were assessed using Pearson Correlation Coefficients (r). Correlations of non-normal data sets were performed using the Spearman rank correlation test (r_s). SPSS 15.0 (Chicago, IL, USA) was used to analyze time series data and Minitab 14 Statistical Analysis software (Minitab Inc., State College, PA, USA) was used for all statistical calculations.

3.4 Results

Samples for the first four time periods were collected over a 48 h period (Calendar day 207, 210, 213, 216) and samples for the final four time periods were collected within a 24 h period (days 219, 221, 223, 225) during the Arctic summer of 2006.

3.4.1 MeHg concentration in Of horizon

MeHg was log transformed to normalize its distribution. MeHg had a mean concentration of 3.51 pmol g^{-1} (dry weight) ($\pm 0.77 \text{ pmol g}^{-1}$) over the study period. MeHg concentration in the soil was different ($F=2.349$, $p=0.075$) and decreased over time (Figure 3.4.1). MeHg concentration differed by catena over the study period ($F=17.88$, $p<0.001$) (Figure 3.4.2). MeHg was not correlated to Fe(II) ($r_s=0.273$), DHg ($r=-0.010$), temperature ($r=0.11$) and DOC ($r=-0.020$).

3.4.2 Dissolved mercury

Mercury was log transformed to normalize its distribution. Mercury averaged 18.5 pM ($\pm 2.25 \text{ pM}$) over the study period. There was no significant difference ($F=0.84$, $p=0.573$) by time period (Figure 3.4.3). The initial (25.12 pM , $\pm 10.97 \text{ pM}$) and final (21.87 pM , $\pm 3.17 \text{ pM}$) time periods both had slightly higher mercury concentrations than other sampling periods. Mercury was different between catenas ($F=7.34$, $p<0.001$) (Figure 3.4.4); catena 1 and 2 had the highest concentration of mercury. Although the trend in MeHg decline was similar between catenas.

3.4.3 Dissolved organic carbon

Dissolved organic carbon (DOC) data was log transformed to normalize its distribution. DOC concentrations exhibited a mean concentration of 20 mg L^{-1} ($\pm 1.54 \text{ mg L}^{-1}$). DOC concentrations did not exhibit a trend over time ($F=1.491$, $p=0.224$) (Figure 3.4.5). DOC concentrations between catenas were quite similar with only catena 4 showing a higher DOC concentration (Figure 3.4.6). Catena 1 (19.22 mg L^{-1} , $\pm 2.1 \text{ mg L}^{-1}$) and 2 (19.67 mg L^{-1} , $\pm 2.93 \text{ mg L}^{-1}$) had similar DOC concentrations. Catena 3 (14.93 mg L^{-1} , $\pm 0.84 \text{ mg L}^{-1}$) and 4 (31.89 mg L^{-1} , $\pm 5 \text{ mg L}^{-1}$) represented the extremes of the DOC concentration range.

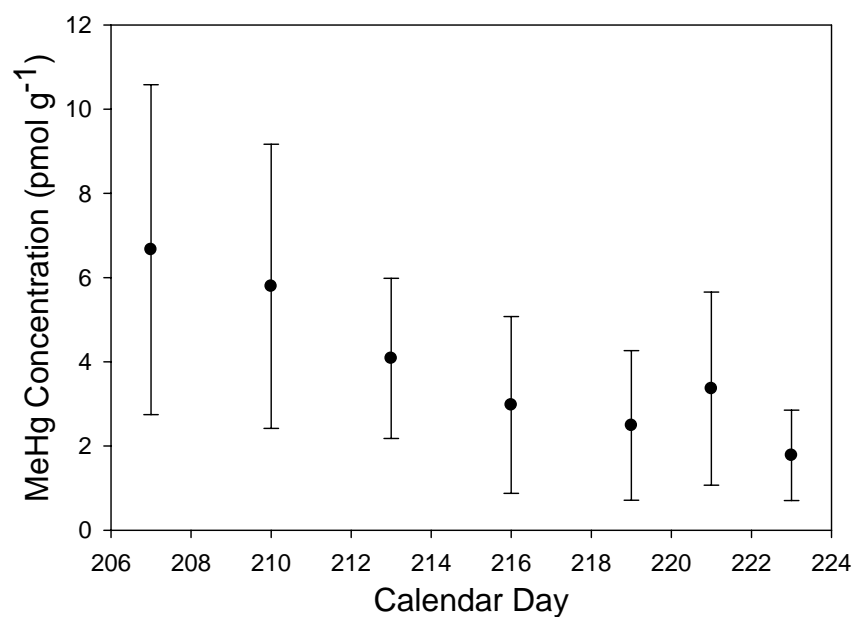


Figure 3.4.1. Mean MeHg concentrations in wetland soil over time. Error bars represent 95% confidence intervals.

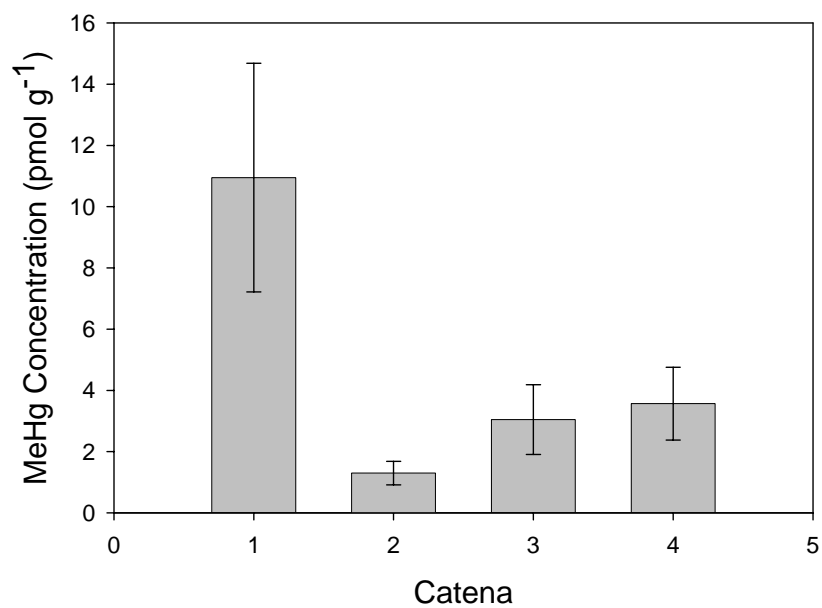


Figure 3.4.2. Mean MeHg concentration at each catena. Error bars represent 95% confidence intervals.

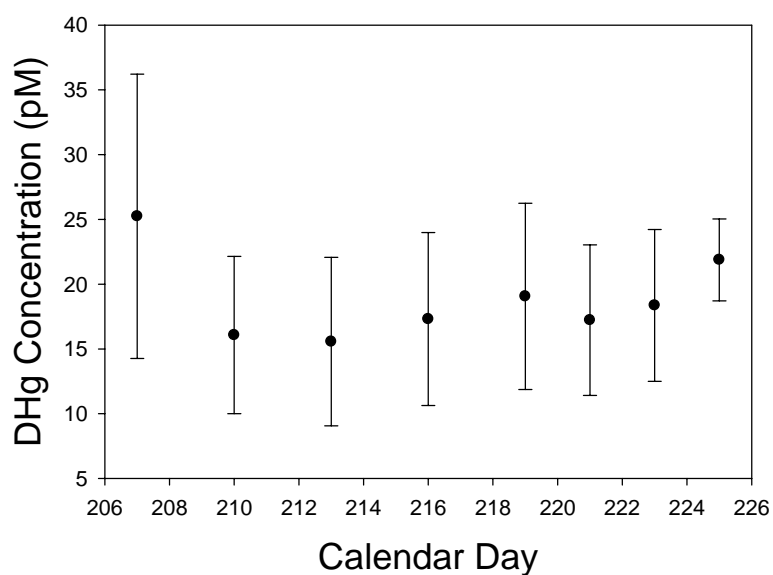


Figure 3.4.3. Mean dissolved mercury (DHg) over the course of the summer sampling period. Error bars represent 95% confidence intervals. DHg is mercury which remains after filtration with a 0.45 μm PVDF membrane.

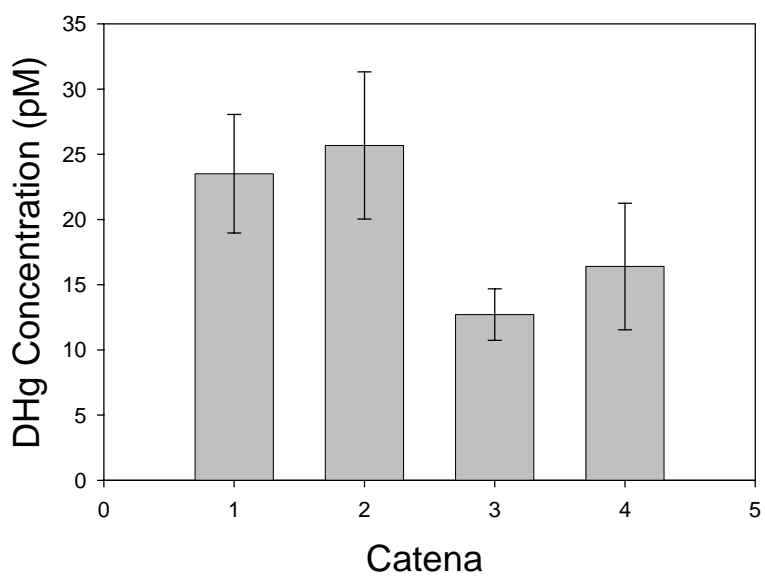


Figure 3.4.4. Mean concentrations of dissolved mercury in pore water at each catena. Error bars represent 95% confidence interval for mean DHg concentrations. DHg is mercury remaining after filtration with a 0.45 μm PVDF membrane.

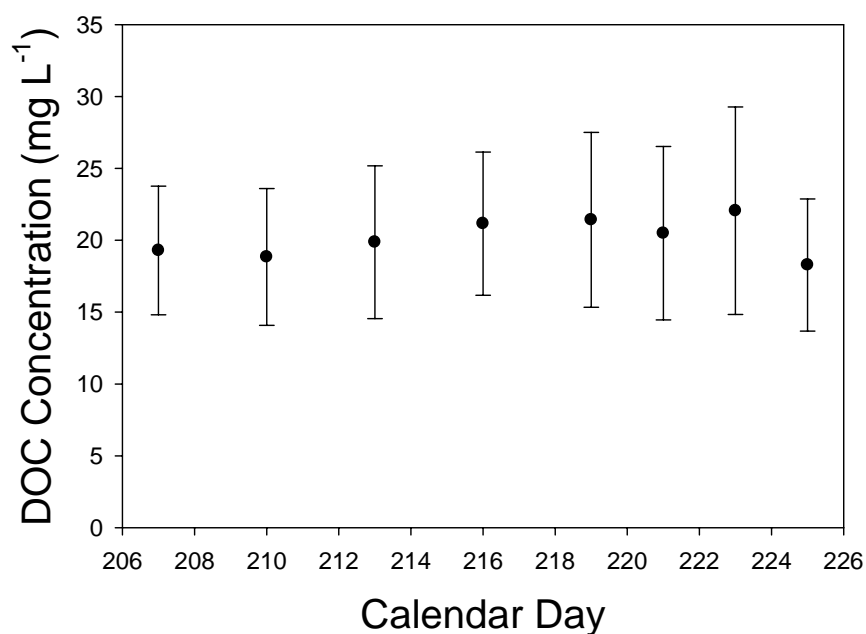


Figure 3.4.5. Mean DOC concentration over sampling period. Error bars represent 95% confidence intervals. DOC defined as organic carbon fraction which can pass through a 0.45 μm filter.

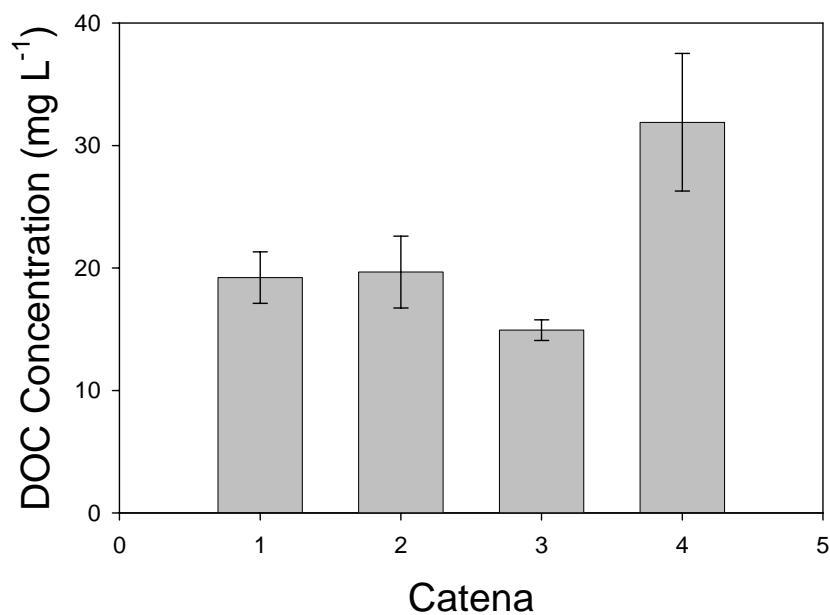


Figure 3.4.6. Mean DOC concentration by catena. Error bars represent 95% confidence intervals. DOC defined as fraction of organic carbon which can pass through a 0.45 μm filter.

There were moderate to weak correlations between DOC and DHg ($r = 0.402$), Fe(II) ($r_s = 0.345$), Fe(III) ($r = 0.333$) during the study period.

3.4.4 Sulfide data

Sulfide was undetectable ($<3 \mu\text{M}$, MDL Cline Method) in most samples. Sample location 21 (catena 2, position 1) showed an increase in detectable sulfide from August 9 to August 13 2006 [sampling days 221 ($7 \mu\text{M}$), 223 ($8.5 \mu\text{M}$) and 225 ($11.5 \mu\text{M}$)]. See Appendix I for sulfide data by location.

3.4.5 Iron data

Only Fe data from lysimeters (filtered to $1 \mu\text{m}$) was used because the samples from the piezometers had not been filtered. Ferrous iron concentration did not change significantly over time ($X^2 = 2.92$, $p = 0.893$) (Figure 3.4.7). Median ferrous iron concentrations over the study period averaged ($99.78 \mu\text{M}$, Q1 $41.84 \mu\text{M}$ /Q3 $140.73 \mu\text{M}$). Ferric iron averaged $183 \mu\text{M}$ (SE $11 \mu\text{M}$) over the sampling period (only water samples obtained from lysimeters were used for analysis). Ferric iron was different over time ($F = 5.526$, $p = 0.001$) (Figure 3.4.8). Ferric and ferrous iron were significantly different by catena ($F = 13.57$, $p = 0.004$ and $H = 39.87$, $p < 0.001$ respectively) (Figure 3.4.9 and 3.4.10).

3.4.6 Dissolved cations and anions

Sodium and potassium were log transformed to normalize their distributions. Calcium (0.79 mM , SE 0.031 mM), sodium (0.51 mM , $\pm 0.034 \text{ mM}$) and magnesium (0.84 mM , SE 0.029 mM) were present in elevated concentrations over the study period. Potassium was present but at lower concentrations (0.024 mM , $\pm 0.0032 \text{ mM}$). The distribution of these elements, by catena can be found in Figure 3.4.11.

Dissolved sulfate was virtually undetectable ($<3 \mu\text{M}$) except for a small portion of samples which had sulfate concentrations above the MDL ($n = 33$). The average sulfate concentrations of those samples which exhibited detectable peaks was $20 \mu\text{M}$ (SE 5). Nitrate was also undetectable (MDL $9 \mu\text{M}$) during the study. Chloride changed significantly over time (Figure 3.4.13), however, chloride concentrations were quite similar between catenas (Figure 3.4.12).

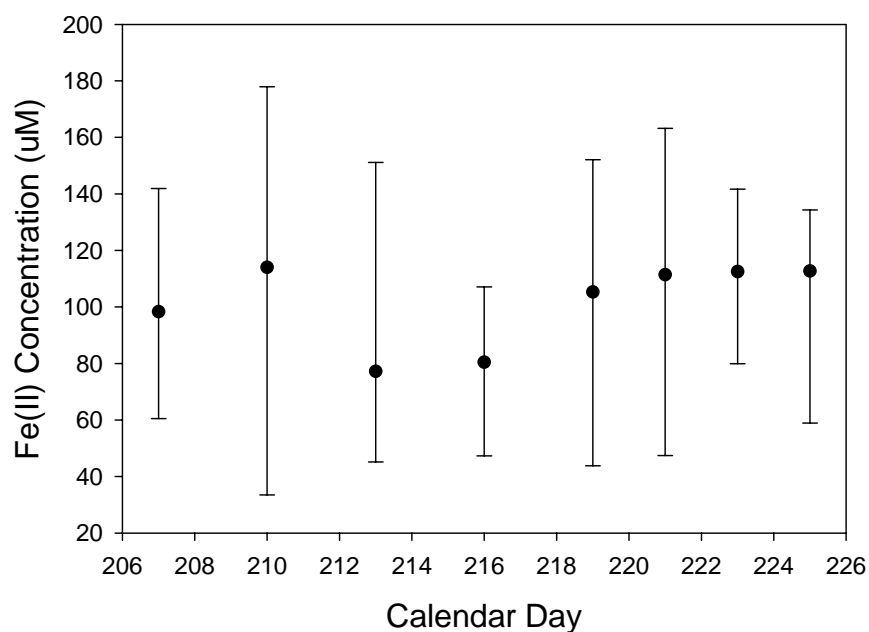


Figure 3.4.7. Median Iron(II) concentrations over time (data from lysimeters only). Error bars represent 1st and 3rd quartiles of distribution.

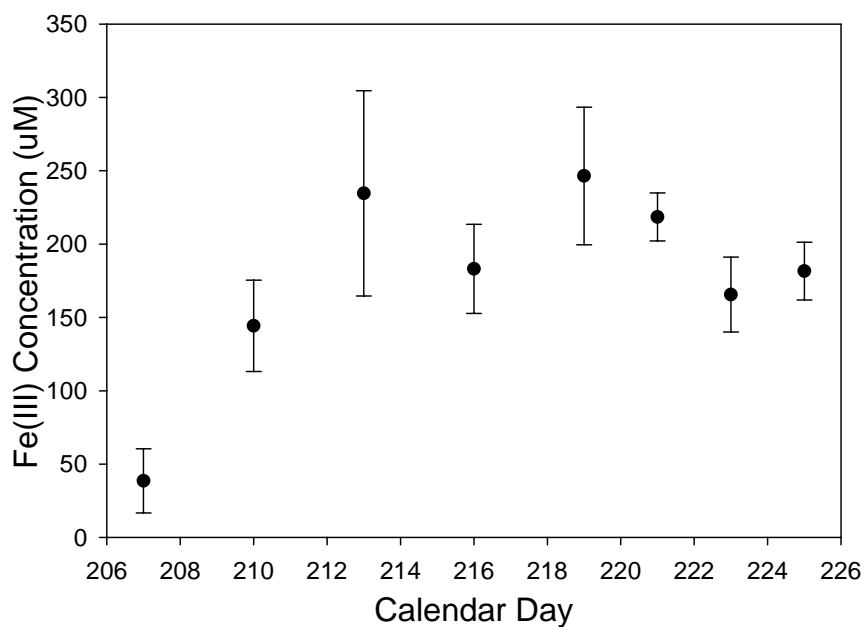


Figure 3.4.8. Mean Iron(III) concentrations over time (data from lysimeters only). Error bars represent standard error of mean.

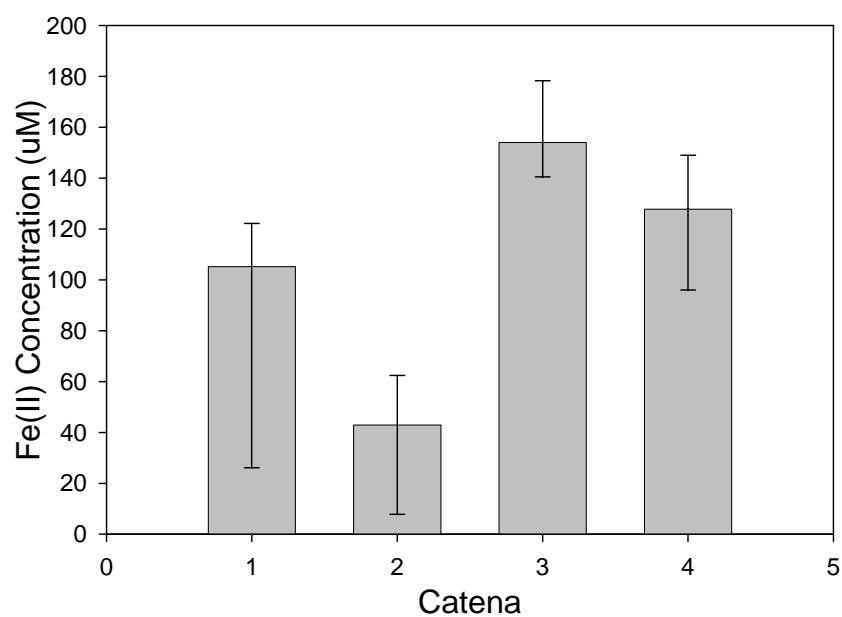


Figure 3.4.9. Median Fe(II) concentration by catena (data from lysimeters only). Error bars represent 1st and 3rd quartiles of distribution.

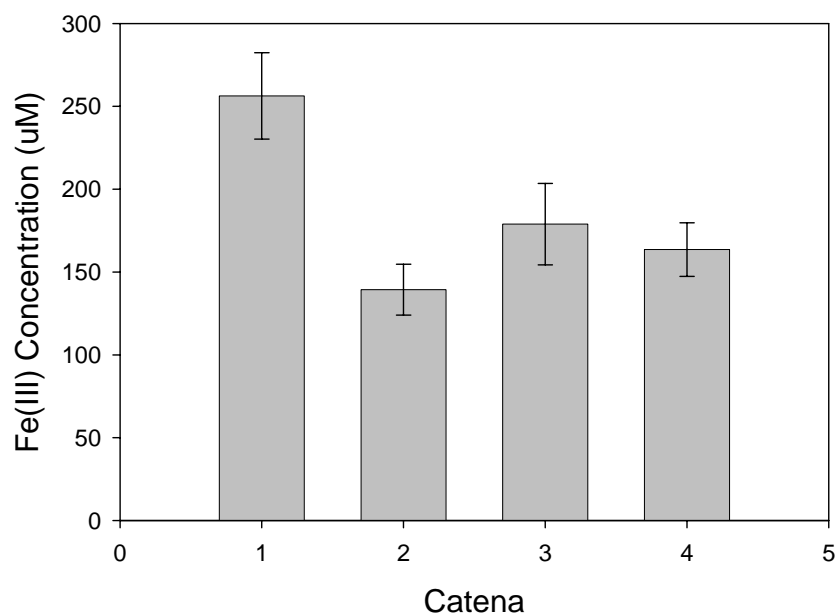


Figure 3.4.10. Mean Fe(III) concentration by catena (data from lysimeters only). Error bars represent standard error of mean.

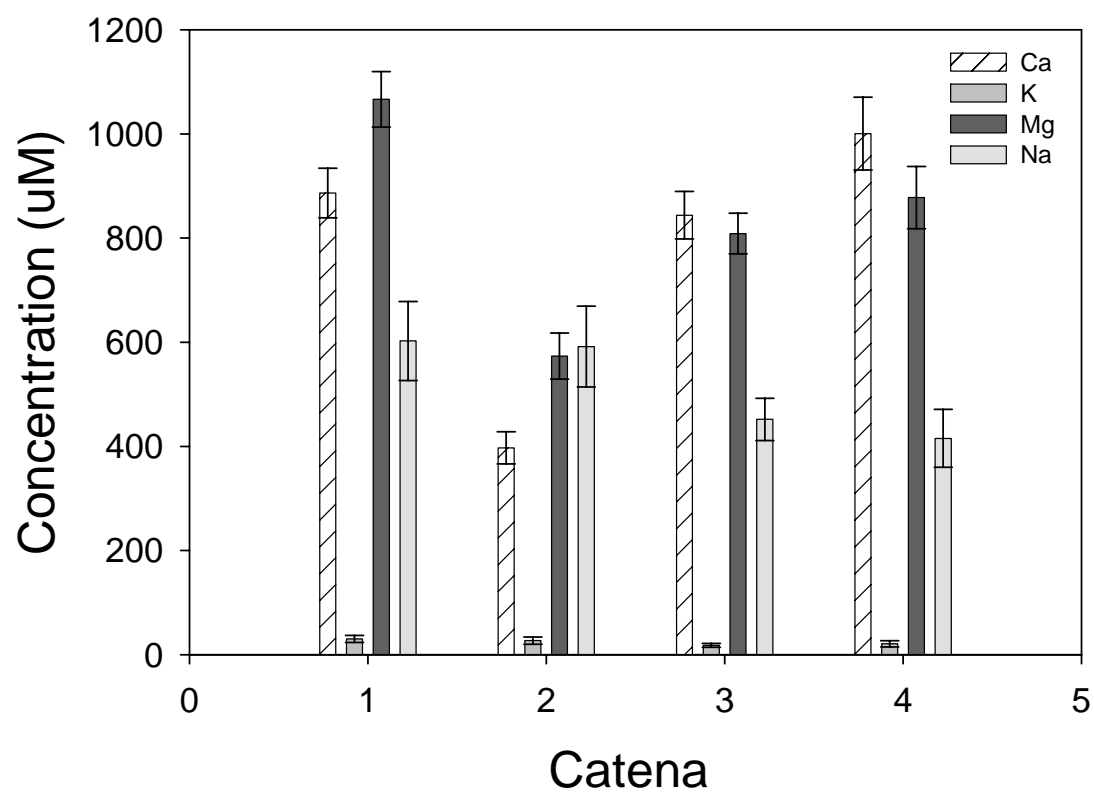


Figure 3.4.11. Mean concentration of calcium (Ca), magnesium (Mg), potassium (K) and sodium (Na) in soil water. Error bars represent standard error for untransformed data (Ca and Mg) and 95% confidence intervals for log transformed data (K and Na).

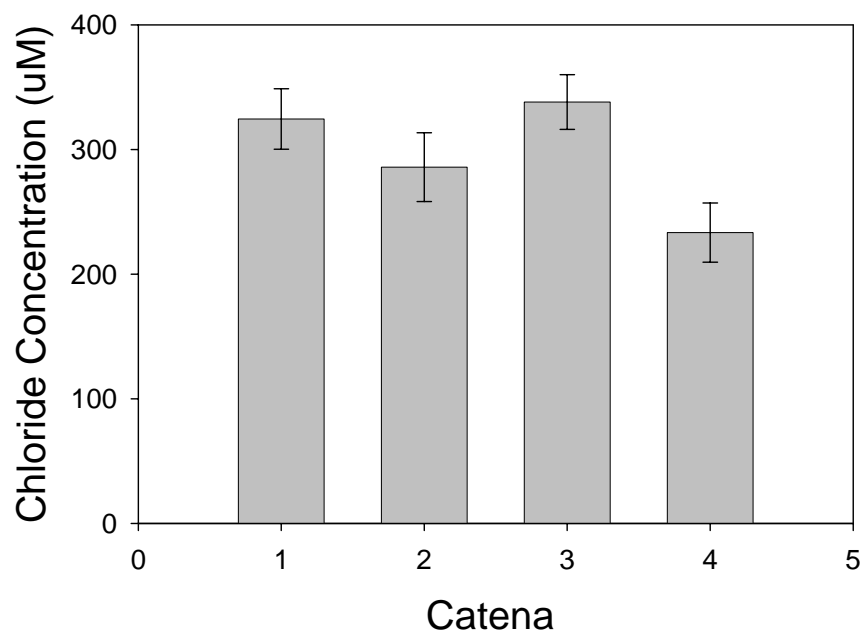


Figure 3.4.12. Mean chloride concentration by catena. Error bars represent standard error of mean.

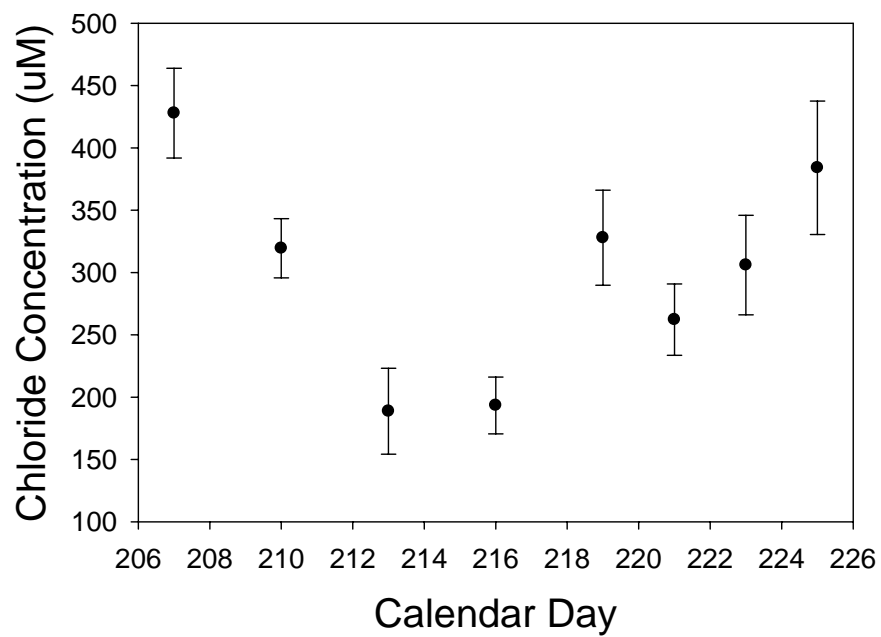


Figure 3.4.13. Mean chloride concentration by calendar day. Error bars represent standard error of the mean.

Chloride averaged 0.30 mM (SE 0.013 mM) during the study and there was a weak correlation between chloride and mercury ($r = 0.152$).

3.4.7 Field measured parameters

Eh was in the iron reducing range (162 mV, SE 5.31) throughout the study and was fairly constant over the study period, except for an initial increase in Eh from CD 210 to 212 (Figure 3.4.14).

Temperature was highest between the period of CD 214 and CD 220 (Figure 3.4.15). The pH over the entire sampling period was 7.04 (SE 0.05) and was not significantly different by time period ($F=0.615$, $p = 0.622$) (Figure 3.4.16). Soil moisture did not show any significant trend over time ($F=1.15$, $p=0.338$) and averaged 83% (SE 0.6%). There was a decreasing trend from lower to upper slope for all catena's except catena 2 (data not shown).

3.4.8 Results of modeling in Visual Minteq

Those samples from T1-T4 which had pH data and dissolved mercury concentrations associated with them were inputted into Visual Minteq (Gustafson 2006). The models default parameters were used to model the speciation of mercury in pore water. The NICA-Donnan model, with current DOC-metal binding parameters (Milne et al. 2003), was used in speciation calculations. Sulfide for the most part was undetectable throughout the study and any estimate of sulfide concentration would be a guess at best. The model was run with and without sulfide, assuming a sulfide concentration of 1.5 μM (half of detection limit for cline method), to simulate the speciation of mercury when sulfide is and is not present. The MINTEQ database was also updated using current complexation data for mercury and sulfide (Appendix C).

Results show that in the presence of sulfide all the mercury is complexed to sulfide species. In the absence of sulfide all the mercury was present as Hg-fulvic acid complexes, the concentration of all other complexes was not within four orders of magnitude of the Hg-fulvic acid complex.

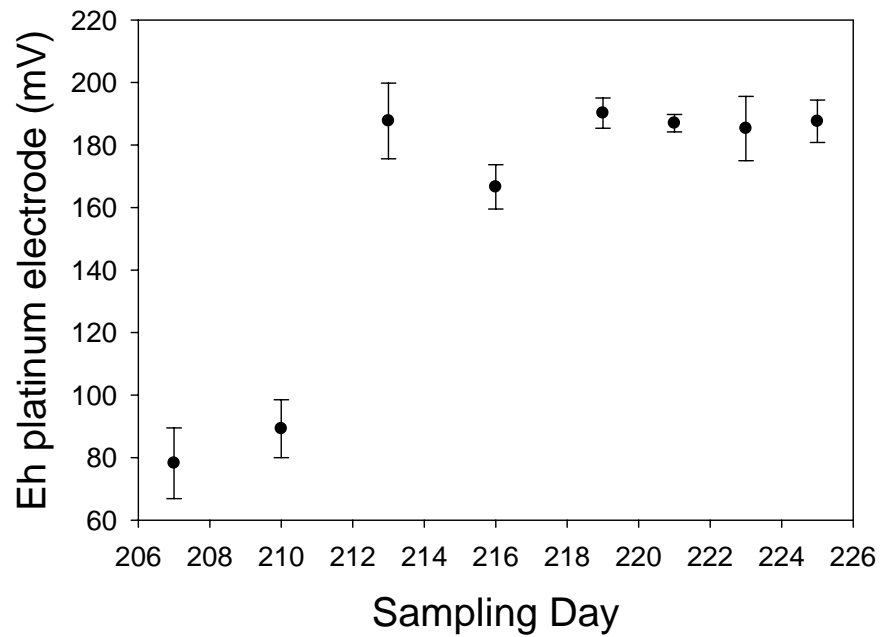


Figure 3.4.14. Eh measurement (mV) over sampling period. Points indicate average redox potential for the calendar day at all four locations. Error bars represent the standard error of the mean.

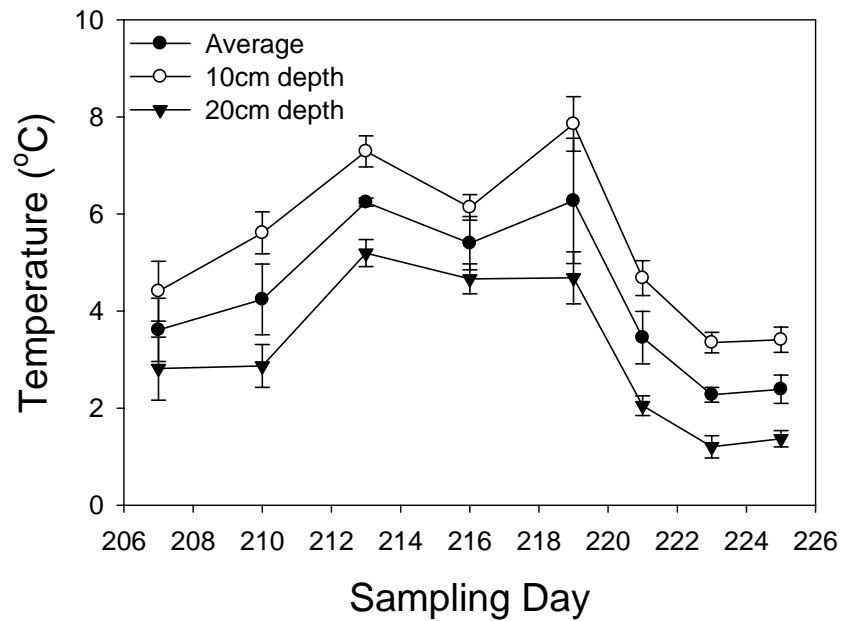


Figure 3.4.15. Mean temperatures over time for the soil profile. Error bars represent standard error of the mean.

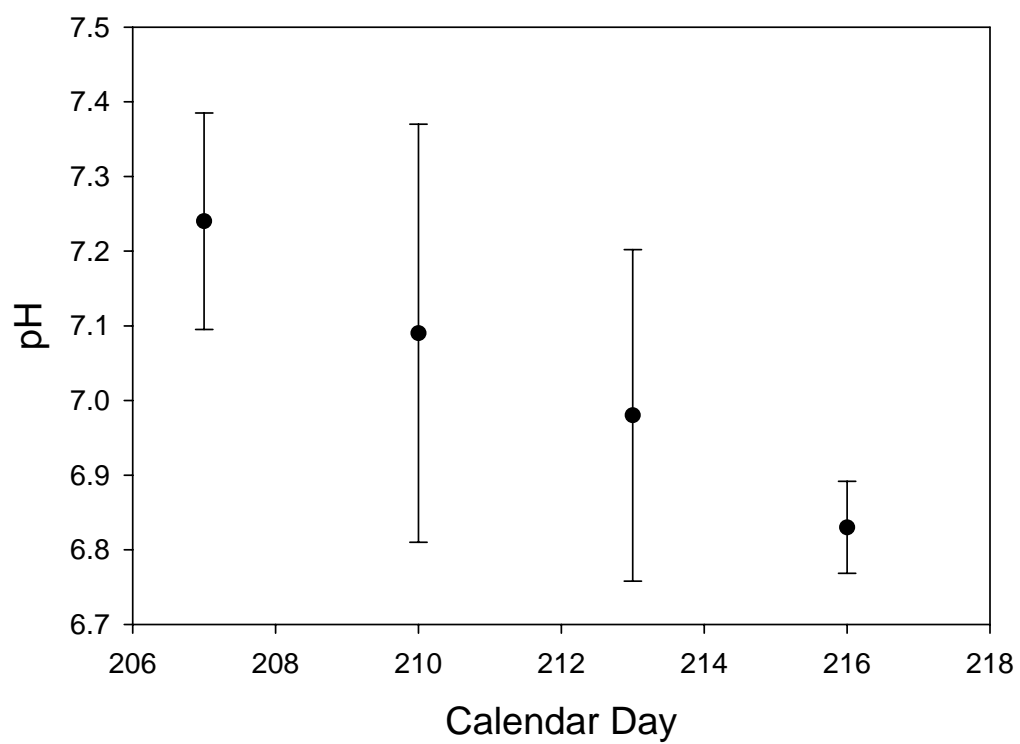


Figure 3.4.16. pH as a function of time for the Truelove Lowlands; data was only collected for the first four time periods because the pH meter malfunctioned. Error bars represent the standard error.

3.5 Discussion

3.5.1 Geochemical conditions during study

Redox potential showed a large initial increase (80 mV) after the second sampling period. This increase does seem to be reflected somewhat by the increase in Fe(III) over the first two sampling periods. However, the increased Eh may also be due to an error caused by a switch in redox meters on day 212 (due to a malfunction in the original meter). Although both redox meters showed similar results for electrodes in buffers, readings of natural waters are higher for the redox meter used after time 2 (data not shown). Elevated concentrations of Fe(II) and Fe(III) in solution most likely reflect complexation to dissolved organic matter which prevents the precipitation of iron (Milne et al. 2003). Geochemical models were not used to estimate the Eh because of the uncertainty of the DOM-metal complexes (Goulet et al. 2007) and because pH data was only available for the first four sampling periods.

Levy (2006) found constant detectable amounts of sulfide in the groundwater flowing through the WSM at melt, although a change in sulfide concentration during the sampling period was not noted (Levy 2006). It is possible that when Levy (2006) sampled the groundwater on the Truelove Lowlands the system was not in equilibrium. The redox measured in the groundwater and the presence of Fe(III), in their study, would seem to indicate that the groundwater was not sulfate reducing. It is possible for sulfide to be present in oxidizing conditions due to its slow oxidation kinetics (Morse 1987). However, sulfide would have shown a decrease over the sampling period as it oxidized. It seems that conditions during snow melt and springtime were reducing which would have maintained the concentration of sulfide in the groundwater.

Sulfate is known to be quite limited in some wetlands (bogs), and is typically present in micro molar concentrations in the pore water (Steinmann and Shotyk 1997). During this study (2006) sulfate was undetectable except for some sporadic pore water samples which had sulfate concentrations that were just above the detection limit. It would seem that sulfate in these organic soils is limited at least during the summer period. Nitrate was undetectable during our study period, but was detectable during snowmelt in a previous study (Dickson 2006) and may be depleted during the spring.

Stutter and Billet (2003) found low levels of sulfate and nitrate in soil porewater in arctic soil. Elevated chloride concentrations may be due to the deposition of chloride from marine sources on the arctic landscape (Davidson et al. 1987; Stutter and Billet 2003). The elevated levels of sodium in the porewater may also be due to marine sources; sodium and chloride levels in the porewater were present in similar concentration ranges in most samples. The change in chloride concentrations over time could be due to changes in the source concentration of chloride, followed by a decrease in groundwater flow and an increase in evaporation leading to increased concentrations of chloride.

3.5.2 Methyl mercury dynamics

Methyl mercury showed a steady decrease in concentration over the sampling period. The high variability in methyl mercury concentrations is most likely caused by the heterogeneity of the substrate analyzed. The soils were extracted wet in the field and could only be homogenized by hand which introduced more unsystematic error into the study. The steady decrease in methyl mercury can not be directly explained by other parameters measured during this study. From the redox couples (Fe , $\sum \text{S}^{-2}$) and the Eh data it appears that the soil was under iron reducing conditions throughout the study period. Fleming et al. (2006) found that iron reducers could produce MeHg at levels comparable to sulfate reducing bacteria. However, Warner et al. (2003) found that iron reducing conditions suppressed methylation and attributed this either to limited mercury bioavailability or the suppression of sulfate reducer activity. Delaune et al. (2004) found that an increase in redox potential, in lake sediment microcosms, lead to a decrease in methylation, however, when mercury was added to the microcosms methylation increased significantly. This is perhaps indicative of mercury availability being limited under oxidizing conditions.

The decline in MeHg over time could be because of desorption and leaching of MeHg from the soil. Organic matter has a high affinity for mercury and even in the presence of elevated pore water DOM concentrations, limited MeHg would desorb into solution $K_{\text{peat-porewater}} = 10^3 - 10^5$ (Heyes et al. 2000). Although the hydraulic conductivity of fibric organic material is relatively high compared to more decomposed organic matter (10^{-4} m s^{-1} vs 10^{-7} m s^{-1}) (Letts et al. 1999), the wetlands appeared to be

drying out when we were sampling and the relatively subdued topography (< 2% slopes) should reduce interflow rates and preclude desorption as a possible mechanism for MeHg loss.

It seems more likely that the loss of MeHg during the study was caused by demethylation reactions in the soil. Demethylation through photo-oxidative pathways does not seem likely in arctic soil, therefore biotic demethylation seems likely. It is thought that biotic demethylation can occur both oxidatively (CO₂ and a small amount of CH₄ produced) or reductively (CH₄ produced) (Barkay and Poulain 2007). Oxidative demethylation is dominant under reducing conditions and reductive demethylation is dominant under more oxidative conditions (Barkay and Poulain 2007). Although studies have been conducted on the biotic pathways of demethylation, little research has been done on the environmental factors which affect demethylation and on demethylation in arctic environments (Barkay and Poulain 2007).

Speciation modeling using Visual Minteq illustrates the dominance of DOM-Hg complexes in wetlands. In the absence of sulfide, Hg is almost completely complexed to DOM. This is also evident from the complexation constant for DOM-Hg complexes (Log K 22 – 28) (Ravichandran 2004). In the presence of sulfide the model gives the impression that sulfide is the dominant ligand in solution. Although recent field studies in the Florida everglades have found that DOM complexes do exist under sulfate reducing conditions and that DOM may actually bind Hg-sulfide complexes (Miller et al. 2007). In the presence of DOM and in the absence of sulfide, mercury is thought to be primarily complexed to thiol groups on DOM molecules. This reduces the bioavailability of mercury due to the size and charged nature of these complexes (Kelly et al. 2003; Ravichandran 2004). Miskimmin et al. (1992) found that lakes with high DOM concentrations at circumneutral pH inhibited MeHg production. High DOM levels in solution could be leading to the formation of primarily Hg-DOM complexes in the porewater and inhibiting methylation by limiting mercury availability.

Methyl mercury concentration can be thought of as being the net product of methylation and demethylation reactions (Hintelmann et al. 2000). An increase in MeHg is the result of an increase in the ratio of the rate of methylation to demethylation (Hintelmann et al. 2000). MeHg is considered to be more bioavailable than Hg and this

could be due to the decreased residence time of MeHg in the environment, which would alter its distribution and speciation (Hintelmann et al. 2000). Methyl mercury has less time to adsorb to soil particles or to speciate with ligands in solution so it may be more bioavailable than mercury (Hintelmann et al. 2000). Heyes et al. (2006) noted that during their experiments most of the stable mercury isotope (^{199}Hg) added to estuarine sediment was as available as ambient MeHg. Little is known about the response of demethylation to temperature, however, the slight change in temperature (observed in this study) could have caused little change in the rate of MeHg degradation. MeHg is thought to be produced and degraded through first order reactions (Heyes et al. 2006). Therefore if the ratio of bioavailable Hg to MeHg decreased the net rate of MeHg accumulation would decrease, if this ratio decreased substantially the net rate of MeHg production would become negative (Figure 3.6.1).

Sulfide was only sporadically detectable; however, Levy (2006) measured sulfide consistently at concentrations of $4.8\ \mu\text{M}$. These elevated concentrations of sulfide may have been indicative of an initial period of microbial activity which drove conditions in the water anaerobic. Sulfide, however, was below detection limits throughout this study indicating increasingly oxidizing conditions or a loss of sulfide from solution combined with a decline in sulfate availability in these wetlands. Although it has been suggested that sulfate reducing bacteria may not be important mediators of methyl mercury production in arctic environments (Loseto et al. 2004a); recent evidence suggests that sulfate reducers may play a role in methylation in arctic environments (Barkay and Poulain 2007). MeHg production could occur at spring thaw when sulfate is present and the lowlands are saturated with water, which may favour sulfide reduction.

3.6 Conclusions

The objectives of this study were to determine the factors affecting MeHg production in Arctic wetland soils. However, we saw a significant decline during the sampling period indicating that Arctic soils do not produce MeHg in the summer. The data collected from the field also indicate that mercury was limited over the

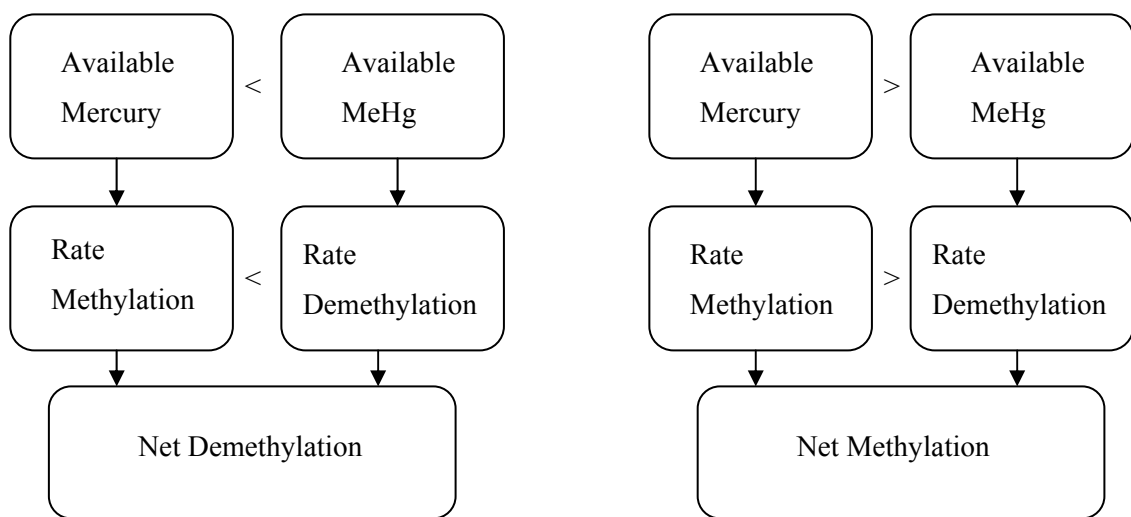


Figure 3.6.1. Flow chart depicting the effect of available mercury and MeHg on methylation/demethylation.

summer and that this led to a decrease in the rate of methylation and the subsequent loss of mercury from the soil (inputs less than outputs). I also hypothesized that iron reducers would stimulate MeHg production, however, this study indicates that iron reducing conditions are not associated with the accumulation of methyl mercury in the soil. MeHg can not decline indefinitely in the soil so there must be a pulse of MeHg in the spring. There appears to be three plausible hypotheses that can explain the presence of methyl mercury in the soil:

1. A pulse of microbial activity/sulfate at spring thaw lowers the redox potential of the soil and facilitates a spike in methyl mercury production. The low sulfide concentrations during the spring detected by Levy (2006) are in the range that is thought to promote methylation (Benoit et al. 1999).
2. Divalent mercury is limited and methyl mercury production is dependant on atmospheric inputs of mercury which occur at polar sunrise. For example Hammerschmidt et al. (2006) found that mercury was limiting methyl mercury production in Alaskan watersheds.
3. There is an external source for methyl mercury (St. Louis et al. 2005) and arctic wetlands act only as a sink for methyl mercury.

These hypotheses will be examined in more detail in the following chapter.

4.0 USING SOIL MICROCOSMS TO ELUCIDATE THE MECHANISMS OF MeHg PRODUCTION IN ARCTIC SOIL

4.1 Introduction

Previous results from a field study on the Truelove Lowlands indicate that MeHg declined over a two week period during the arctic summer, however, how MeHg accumulates in this soil during the spring is not known. Loseto et al. (2004a) found that when frozen soil, collected prior to snow melt, was incubated at 4°C MeHg concentrations increased 100 fold over an initial 30 day period and then declined slightly after 30 days. Previous investigators have found that spring thaw leads to a pulse of microbial activity due to a sudden pulse of nutrients (Schimel and Clein 1996). Levy (2006) found sulfide at micromolar concentrations in the groundwater on the Truelove Lowlands which declined to below detection limits during the 2006 field season. It is possible that an initial pulse of microbial activity rapidly reduces the Eh in soil microsites and creates conditions favorable for mercury methylation. Hammerschmidt et al. (2006) found that mercury was a limiting factor in mercury methylation in arctic sediments. Mercury may also be limited in arctic soil and a pulse of mercury to these lowlands from atmospheric deposition could promote MeHg production. However, MeHg may also be deposited directly to the Lowlands from the atmosphere; St. Louis et al. (2005) found that MeHg was being deposited directly to the Arctic snow pack and did not photodegrade.

4.2 Objectives

The objectives of this experiment were to determine whether available mercury was limiting the production of MeHg or whether a pulse of MeHg was being produced, in-situ, at spring thaw on the Truelove lowlands.

4.3 Methods

4.3.1 Microcosm Experiment

Soils collected from catena two over the last five sampling periods (T3-T8) were homogenized in a large Rubbermaid container for one hour. The soil was homogenized by hand by mixing and ripping apart large aggregates of organic soil until the soil was relatively homogenous. The homogenized soil was stored at 4°C and sub samples of the soil were taken and dried in an oven to a constant weight at 85 °C to determine the gravimetric water content.

The following day, 22 g of wet soil was packed into 50 mL clarified polypropylene Falcon[®] centrifuge tubes (Becton Dickinson & Co., Franklin Lakes NJ) and 6 mL of autoclaved water was added to the microcosms in a glove box under oxygen limited conditions to saturate the soil. The amount of water needed to saturate the soil was determined by slowly adding and mixing water into the soil until it became ponded on the surface. The soil and water were mixed using a clean metal spatula and then capped with a HDPE cap containing a butyl rubber septum. A nitrile rubber o-ring (Kinecor Inc., Saskatoon, Sk) was inserted into the cap to form an airtight seal between the cap and the tube. The tubes were checked for leaks by over pressurizing the containers with air while holding the container in either, ethanol at -20°C, water at 4°C or water at room temperature. All microcosms were frozen at -20°C prior to the experiment commencing. All treatments were capped under an oxygen limited atmosphere inside a nitrogen filled glove box. The natural treatment was kept at 4°C for 1 day prior to freezing because it took two days to prepare the microcosm experiment.

Mercury was added into the spiked treatments to achieve a concentration of 1 µg g⁻¹ dry weight of mercury (4.2 µg mercury added). The spike was prepared fresh from a 1000 µg l⁻¹ mercury chloride/water stock solution. The stock solution was diluted in the glove box using cool autoclaved water. Sterile treatments were gamma irradiated at the Cross Cancer Institute (Edmonton, Alberta). The samples were exposed to two doses of 30 KGy with a 1 week rest period in between to allow any spores to sporulate prior to the second treatment. The strength of the source was 0.44 Krads min⁻¹ and each dose lasted approximately 4 days and 20 hours. The samples were stored frozen (-20°C)

prior to the initial radiation treatment, after which the samples were kept at 4°C until they were packed into centrifuge tubes. Once the samples had been irradiated they were packed into Falcon[®] centrifuge tubes (Becton Dickinson & Co., Franklin Lakes NJ) in a biosafety cabinet using aseptic techniques. The samples were then loosely capped (caps were soaked in 10% bleach for 30 min and allowed to dry in a sterile cabinet), and placed inside a nitrogen filled glove box, which had been wiped out with ethanol, and capped under a nitrogen atmosphere. The samples were closed inside the glove box and then kept for 3 days at 4°C prior to freezing at -20°C.

To ensure that samples had been successfully sterilized, approximately 2 g of wet soil was added to sterile water and thoroughly shaken. Aliquots (100 µL) of this solution were withdrawn and spread on an agar plate (VWR, West Chester, PA) containing tryptic soy medium. Five separate containers were plated with some containers subsampled and plated twice as replicates. Blanks, consisting of sterile water only, were plated to ensure that the pipetting technique and biosafety cabinet were not contributing to contamination. These plates were checked for growth periodically over a three week period. Only one plate, from one of the soil containers, showed some growth and it was considered minimal [22 cfu g⁻¹ (wet soil)].

Thermocouples were placed in three Falcon[®] centrifuge tubes with soil packed to a specific bulk density (0.18 g cm⁻³) for temperature measurements. Thermocouples consisted of T-type wire (York Wire & Cable Inc., York, PA) which was inserted into a pipette tip and the ends of the constantin and copper wires were soldered together and waterproofed with a marine adhesive. Surrogates for redox potential were prepared by packing soil into a HDPE container (VWR, West Chester, PA), to the same bulk density and soil moisture content as the microcosms, in an anaerobic chamber. The surrogates were then capped, sealed with silicone tape and frozen at -20°C prior to the experiment. After 40 days when the soil had thawed a salt bridge (constructed according to Vepraskas (2002)) was inserted into the soil as well as two platinum electrodes (constructed as discussed previously). A lid with holes drilled through it was placed over the container, sealed with silicone and silicone tape was used to seal around the lid. The soil was at room temperature for less than one hour and was kept in a cooler when not in the glove box.

4.3.2 Sampling Methods

At beginning of the experiment soil was removed from the -20°C freezer and moved to a -5°C walk-in freezer. The soil remained at this temperature in the dark for 40 days with microcosms being sampled at day 10 and 40 of the incubation. After 40 days the soil was moved to a 4°C walk in fridge and stored in plastic coolers for the duration of the experiment. Soil was sampled at day 45, 50, 70 and 99 days to capture MeHg changes during thaw and beyond. Four replicate containers from each treatment were removed at each time period and sampled destructively. During the -5°C incubation the headspace was sampled for CO_2 , N_2O and CH_4 , after gas sampling the soil was frozen at -20°C until lyophilization. Gas was sampled using a rubber tipped 10 mL Mono-jectTM syringe (Henke-Sass, Wolf GmbH, Tuttlingen, Germany) with 25 gauge needle (Beckton Dickinson & Co., Franklin Lake NJ). The needle was inserted through the septum in the sample container and air from the container headspace was withdrawn and subsequently expelled three times to ensure mixing of the headspace, after which the plunger was withdrawn to 5.2 mL and the air was allowed to flow into the syringe for approximately 30 seconds. The needle was then withdrawn from the septum, 0.2 mL of gas was expelled, and then used to pierce the septum of a 20 mL glass Exetainer[®] vial (uncoated soda glass vials, Labco Limited, United Kingdom). The sample was evacuated into the exetainer vial and diluted at room temperature with 15 mL of UHP argon gas (Praxair, Saskatoon, Saskatchewan). Samples were analyzed, within a week, at the University of Saskatchewan (Saskatoon, Sk) using a gas chromatograph equipped with an electron capture detector (Varian Inc., Palo Alto, CA).

Thermocouples were also measured at each sampling period to ensure that the temperature on the chamber was accurate. Redox measurements were taken once the soil had thawed using methods mentioned in the previous chapter, except the reference electrode was inserted into the salt bridge rather than directly into the soil. Porewater was sampled by squeezing the porewater out of the soil using a plunger from a clean Norm-jectTM syringe (Henke-Sass, Wolf GmbH, Tuttlingen, Germany) the pore water was then withdrawn into a rubber free 2 mL Norm-jectTM syringe (Henke-Sass, Wolf GmbH, Tuttlingen, Germany) and filtered through a $0.45\ \mu\text{m}$ PVDF (polyvinyl difluoride) membrane filter with a polypropylene housing (Whatman Inc, Clifton, NJ).

Porewater was quickly injected into autosampler vials for sulfide and iron analysis using methods describe previously and the remaining liquid was filtered into 7 mL borosilicate glass vials with teflon lined lids (VWR, West Chester, PA). All porewater samples were stored at 4°C prior to analysis. Anions were analyzed using capillary electrophoresis as described in the previous chapter. Colour was determined at 420 nm as an estimate of humic and fulvic acids in solution (Regnell and Hammar 2004, Cuthbert and Giorgio 1992).

Samples from the microcosms were lyophilized in a manifold style freeze dryer (Labconco, Kansas City, USA). The soil was then ground and mixed using a spatula, 0.5 g was extracted and analyzed for MeHg using methods described previously, except only 5 mL of HNO₃ and 1 mL of CuSO₄ were used. Artifactual formation of MeHg was determined to be 0.015% of inorganic mercury (based on a 1 µg g⁻¹ inorganic mercury spike). Soil was also extracted for poorly crystalline iron oxides using an ammonium oxalate extraction (Land Resource Research Unit 1984). Briefly 0.25 g of freeze dried soil was weighed into a 50 mL Falcon[®] centrifuge tube (Becton Dickinson & Co., Franklin Lakes NJ) and the acid oxalate extracting solution (made from ACS grade chemicals (BDH, Toronto, ON)) was added at a ratio of 1 part soil to 40 parts water (weight:volume). The mixture was extracted in the dark for four hours and then centrifuged at 3500 rpm for 20 minutes. The supernatant was withdrawn using a Norm-ject[™] syringe (Henke-Sass, Wolf GmbH, Tuttlingen, Germany) and filtered through a 0.45 µm PVDF (polyvinyl difluoride) membrane filter with a polypropylene housing (Whatman Inc, Clifton, NJ). The solution was stored in the dark at 4 °C until analysis. Prior to analysis the solution was diluted 50 fold with a 2000 µg l⁻¹ NaCl solution to give a concentration within the linear range of the Spectra AA atomic absorption spectrometer (Varian Inc., Palo Alta, California). Samples were analyzed using an air-acetylene flame at 248.3 nm. Standards were prepared in the same matrix as the samples using a stock 1000 µg l⁻¹ Fe solution in nitric acid (VWR, West Chester, PA)).

The soil was extracted sequentially for water soluble and exchangeable mercury. Water soluble mercury was determined, according to Bloom et al. (2003), by mixing 40 mL of Nanopure deionized water with 0.4 g of dry soil in a polypropylene Falcon[®] centrifuge tube (Becton Dickinson & Co., Franklin Lakes NJ). Centrifuge tubes

exhibited similar recoveries to borosilicate glass for water solutions spiked with mercury. The mixture was shaken on reciprocating shaker for four hours and then centrifuged at 3500 rpm for 20 min. The supernatant was withdrawn using a Norm-ject™ syringe (Henke-Sass, Wolf GmbH, Tuttlingen, Germany) and filtered with a 0.45 µm PVDF (polyvinyl difluoride) membrane filter with a polypropylene housing (Whatman Inc, Clifton, NJ). The filtrate was preserved with BrCl and analyzed using methods described in the previous chapter (Section 3.3.6.1). Exchangeable mercury was extracted using 0.1 M BaCl₂ (EMD Chemicals, San Diego CA) using methods described above, except the extraction was only shaken for ~30 min (Renneberg and Dudas 2001).

4.3.3 Statistical Analysis

The experiment was established using a randomized complete design. The treatments (spiked, natural, sterile) and sampling times were considered as factors for analysis. There were 4 replicates per treatment for each time period. Statistical analysis was conducted using statistical methods described in section 3.3.7. All gas sampling data was analyzed assuming it was non-parametric. The Dunnett multiple comparison test was used to compare differences between levels of a treatment.

4.4 Results

Once thawed, MeHg concentrations increased in the active soils (Figure 4.4.1). There was an interaction between treatment and time for MeHg ($F=49.46$, $p<0.001$). MeHg concentration did not change in the sterile treatment over time ($F=0.14$, $p=0.989$). MeHg in the spiked and natural treatments changed over time ($F=11.57$ $p<0.001$, for natural and $F=59.68$ $p<0.001$ for spiked treatments). MeHg, in the natural treatment, declined slightly from an initial concentration of 7.16 pmol g⁻¹ (SE 0.67 pmol g⁻¹) to 5.38 pmol g⁻¹ (SE 0.151) during the 40 day incubation at -5 °C ($p<0.05$ Dunnett test). Once the soil thawed the spiked treatment increased at a much greater rate than the natural treatment (0.82 pmol g⁻¹ day⁻¹ in the spiked treatment versus a maximum of 0.074 pmol g⁻¹ day⁻¹ in the natural treatment). MeHg concentrations in the natural treatment did not increase during the initial 10 days after the soil was thawed but at Day 70 and 99 MeHg increased significantly ($p<0.05$ Dunnett test). The rate of increase in

MeHg was $0.074 \text{ pmol g}^{-1} \text{ day}^{-1}$ over the last 29 days of the experiment versus $0.042 \text{ pmol g}^{-1} \text{ day}^{-1}$ during the initial 30 days after the soil was thawed (sampling day 40-70). The spiked treatment did not reach a plateau in MeHg production and produced MeHg at a constant rate. Sequential extractions for water soluble mercury did not change over time in the natural treatment ($F=2.18$, $p = 0.1$) and extracts for exchangeable mercury were lower than the reagent blank.

The redox potential corrected to the SHE (standard hydrogen electrode) decreased over time; on sampling day 45 Eh was 281 mV (SE 53 mV) which declined to 62 mV (SE 17 mV) on the final sampling day (Figure 4.4.2). Eh was not recorded for day 10 and day 40 because the soil was frozen and the agar salt bridge would have frozen at these temperatures. Mottling was also observed along the polypropylene walls of the tubes after the final time period indicating the reduction and solubilization of iron and its redistribution. No mottling was observed within the soil core in the centrifuge tube. There was also an increase in oxalate extractable iron from $190 \text{ } \mu\text{mol g}^{-1}$ (SE 11 $\mu\text{mol g}^{-1}$) after thaw to $257 \text{ } \mu\text{mol g}^{-1}$ (SE 25 $\mu\text{mol g}^{-1}$) on sampling day 99 ($F = 2.48$, $p = 0.069$). MeHg concentrations in the natural treatment were correlated with both oxalate extractable iron ($r = 0.523$) and colour ($r = 0.765$).

Sulfate concentrations changed only in the natural treatment ($F = 17.15$, $p < 0.001$) where it decreased from $664 \text{ } \mu\text{M}$ (SE $80 \text{ } \mu\text{M}$) on sampling day 70 to $234 \text{ } \mu\text{M}$ (SE $79 \text{ } \mu\text{M}$) during the last time period. Nitrate (MDL $9 \text{ } \mu\text{M}$), sulfide (MDL $3 \text{ } \mu\text{M}$) and iron (MDL $20 \text{ } \mu\text{M}$ and $5 \text{ } \mu\text{M}$ for Fe(III) and Fe(II) respectively) were not detected in soil porewater after thaw. Colour which is an estimate of the dissolved humic and fulvic acid in water was used to qualitatively describe DOM production (Regnell and Hammar 2004). Colour (absorbance at 420 nm) increased in the porewater from thaw (day 45) to sampling day 99 in both spiked and natural treatments (Figure 4.4.3). There was a significant difference in colour by time period in both the spiked ($F = 9.52$, $p = 0.002$) and natural treatments ($F = 13.26$, $p < 0.001$).

The gas sampling data was non-normally distributed and was analyzed non-parametrically using the Kruskal-Wallis test. Gas samples were analyzed for N_2O , CH_4 and CO_2 production.

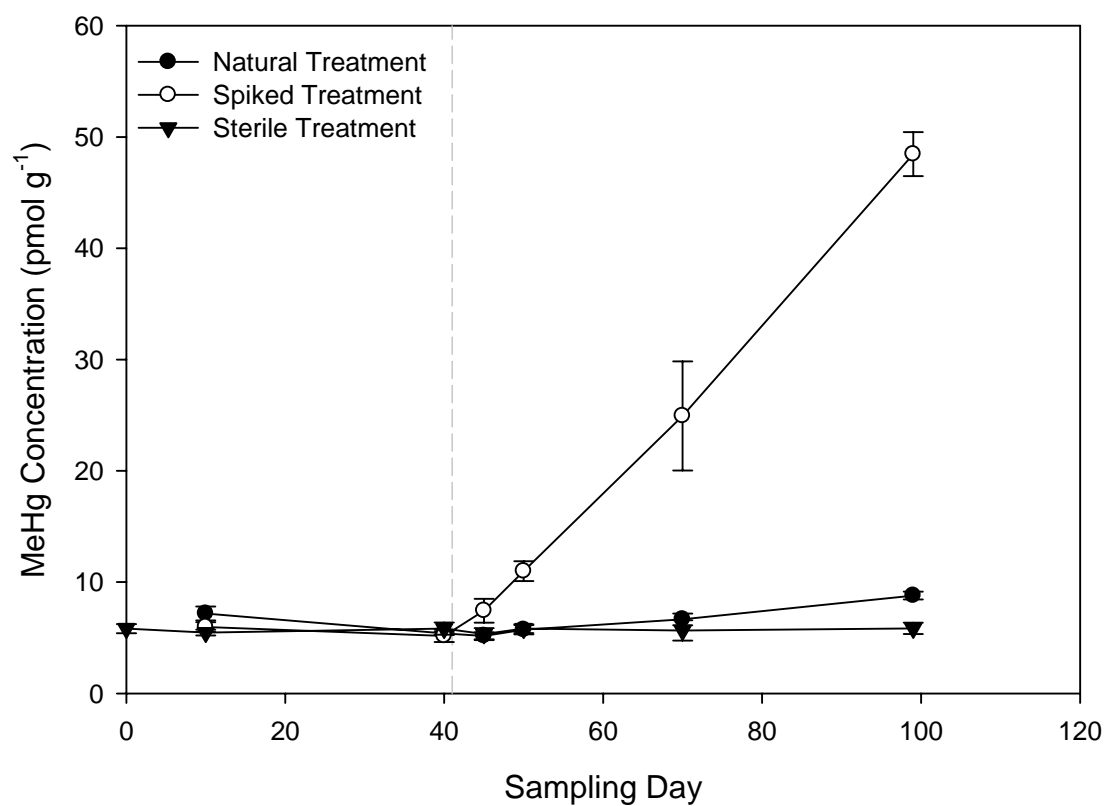


Figure 4.4.1. MeHg concentration as a function of treatment (mercury spiked (4.4 μg mercury), natural or gamma radiation sterilized) over time. Error bars represent standard error of mean concentration ($n = 4$, except natural treatment (sampling day 99) where $n = 5$). Dashed line indicates the beginning of the 4 °C incubation.

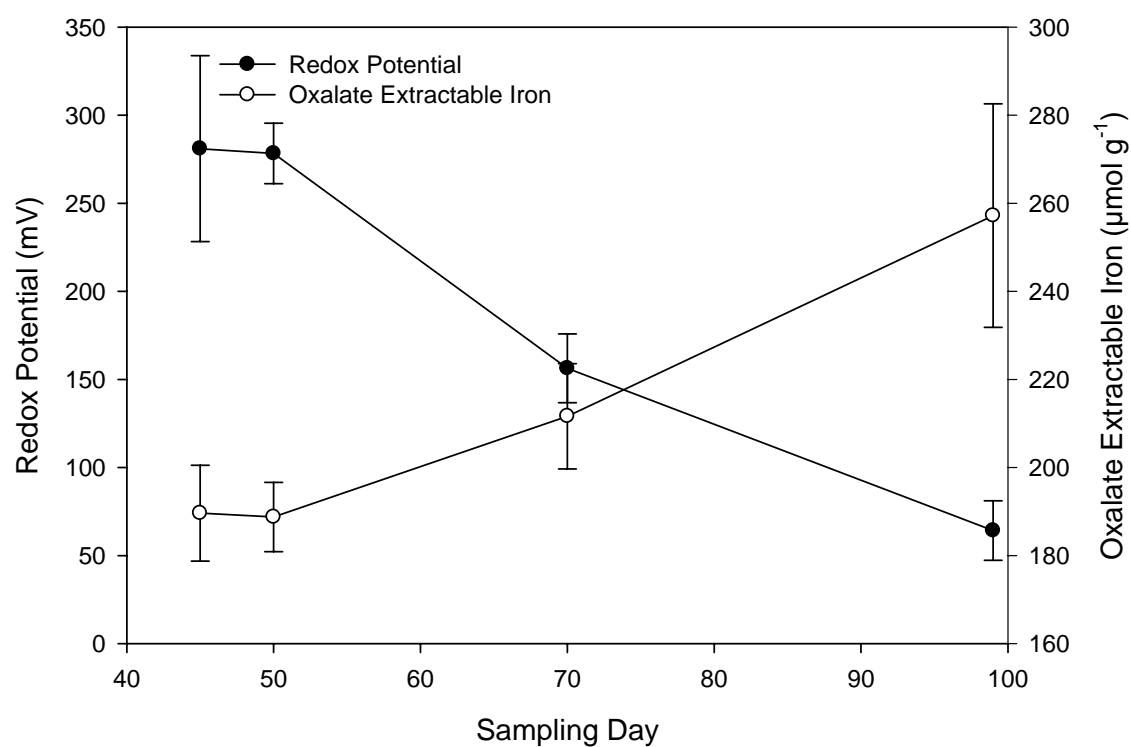


Figure 4.4.2. Average redox potential (corrected to SHE) as measured in surrogate microcosms over time. Error bars represent standard error of sample mean ($n = 3$ except sampling day 40 where $n = 2$). Open circles correspond to the average oxalate extractable iron in the natural treatment over time. Error bars represent standard error of sample mean ($n = 4$ except sampling day 99 where $n = 5$).

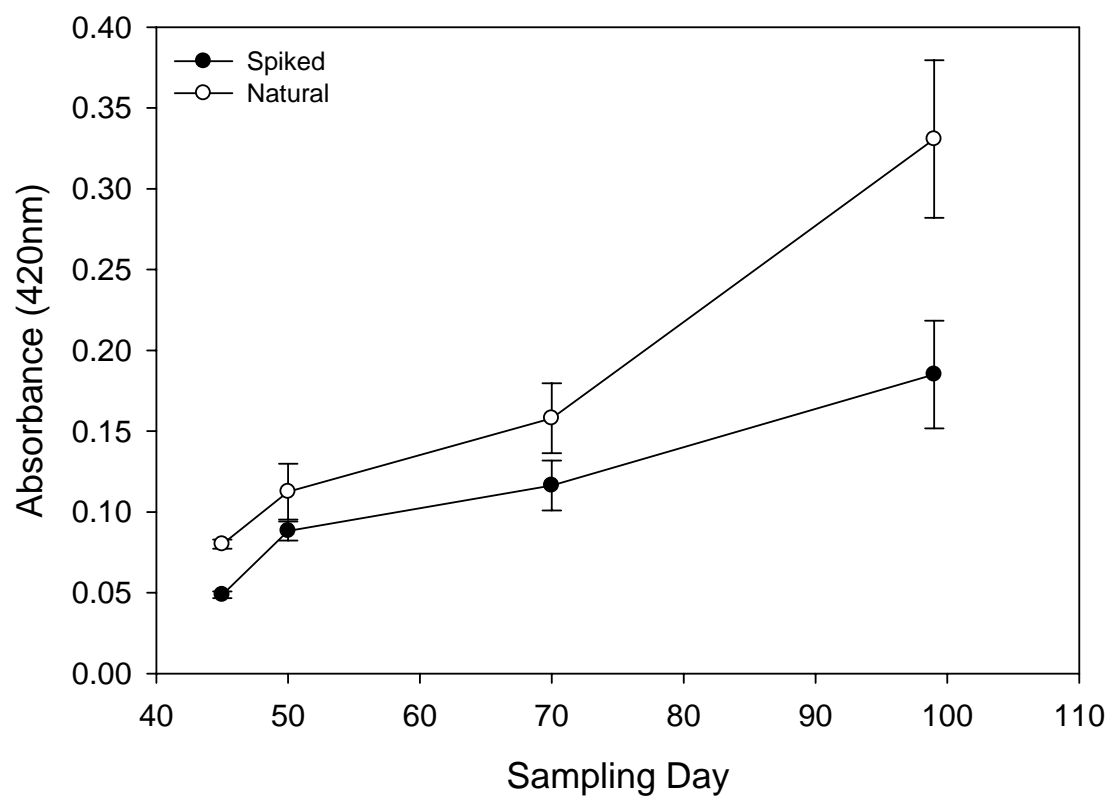


Figure 4.4.3. Mean colour (absorbance (unitless) at 420 nm) of porewater as a function of sampling day in the spiked and natural treatments. Error bars represent standard error of absorbance (n=4 except natural treatment (sampling day 99) where n = 5).

Nitrous oxide was low in all treatments throughout the experiment and did not change over time (Figure 4.4.4). There were differences for the CO₂ and CH₄ emissions between the treatments (Figure 4.4.5 and 4.4.6). Gas samples were high for CH₄ and CO₂ in the sterile treatment and increased after thaw (Figure 4.4.5 and 4.4.6). There was significant difference in CO₂ emitted from the natural and spiked treatments over time ($p < 0.001$) (Figure 4.4.5). CO₂ production was low when the soils were frozen at – 5°C and increased rapidly after thaw. The rate of CO₂ production was 1.2 nmol g soil⁻¹ day⁻¹ prior to thaw and increased to 155 nmol g soil⁻¹ day⁻¹ after thaw in the natural treatment. There was a sudden increase in CH₄ production and variance during the last time period in the natural treatment (Figure 4.4.6). However, CH₄ production was not significant in the spiked treatment ($H = 6.94, p = 0.173$) but was significant in the natural treatment ($H = 13.18, p = 0.017$).

4.5 Discussion

MeHg in the spiked treatment increased eight fold over the experiment with a constant rate of MeHg production of 0.88 pmol g⁻¹ day⁻¹. Loseto et al. (2004a) found 100 fold increases in soil MeHg concentrations after a 30 day incubation at 4°C, which is greater than the increase reported in this study. However, MeHg production in their study was site specific with significant differences in the rates of methylation depending on where the soil was collected. The increase in MeHg production in the spiked treatment is most likely indicative of mercury being much more bioavailable. Delaune et al. (2004) found that sediment slurries spiked with mercury under oxic and anoxic conditions both produced MeHg although methylation occurred to a lesser extent in the oxic treatment in some of the sediment types incubated. Delaune et al. (2004) concluded that input of mercury into lakes from external sources could stimulate methylation. The rate of methylation in the spiked treatment also did not change as the experiment progressed and the redox potential declined suggesting that mercury bioavailability is the primary factor affecting MeHg production in Arctic wetland soils.

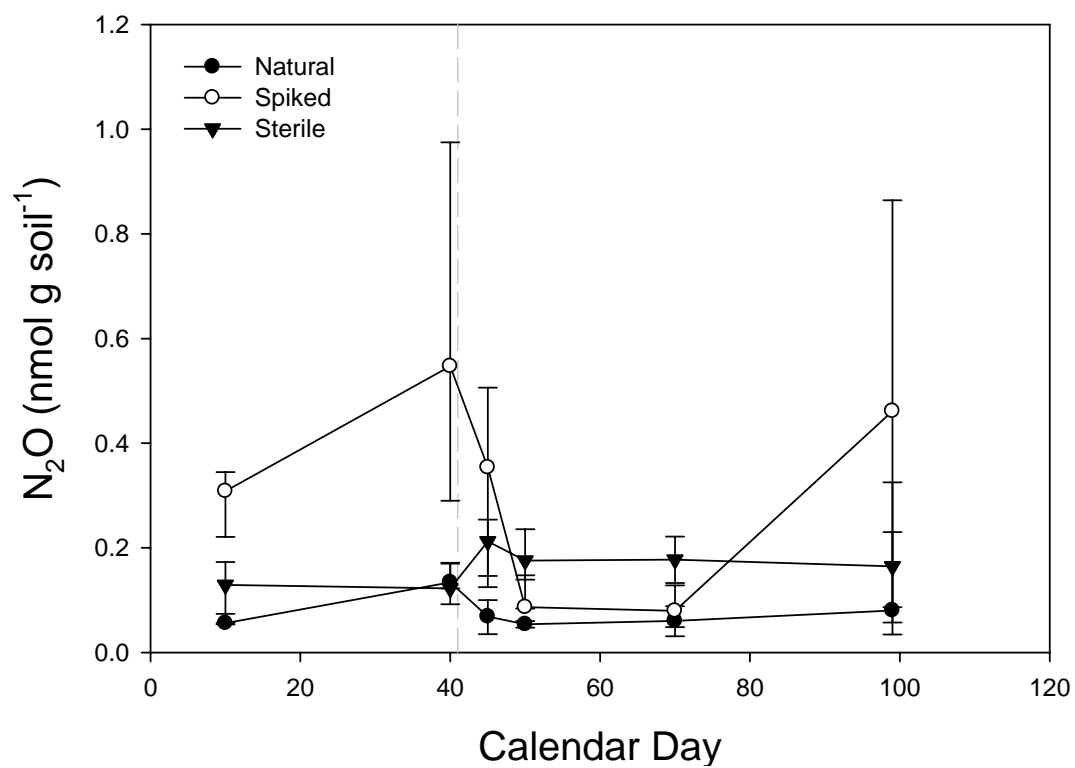


Figure 4.4.4. Median cumulative N₂O release over time standardized to one gram of dry soil. Error bars represent 1st and 3rd quartiles of distribution (n = 4). Dashed line indicates beginning of 4°C incubation

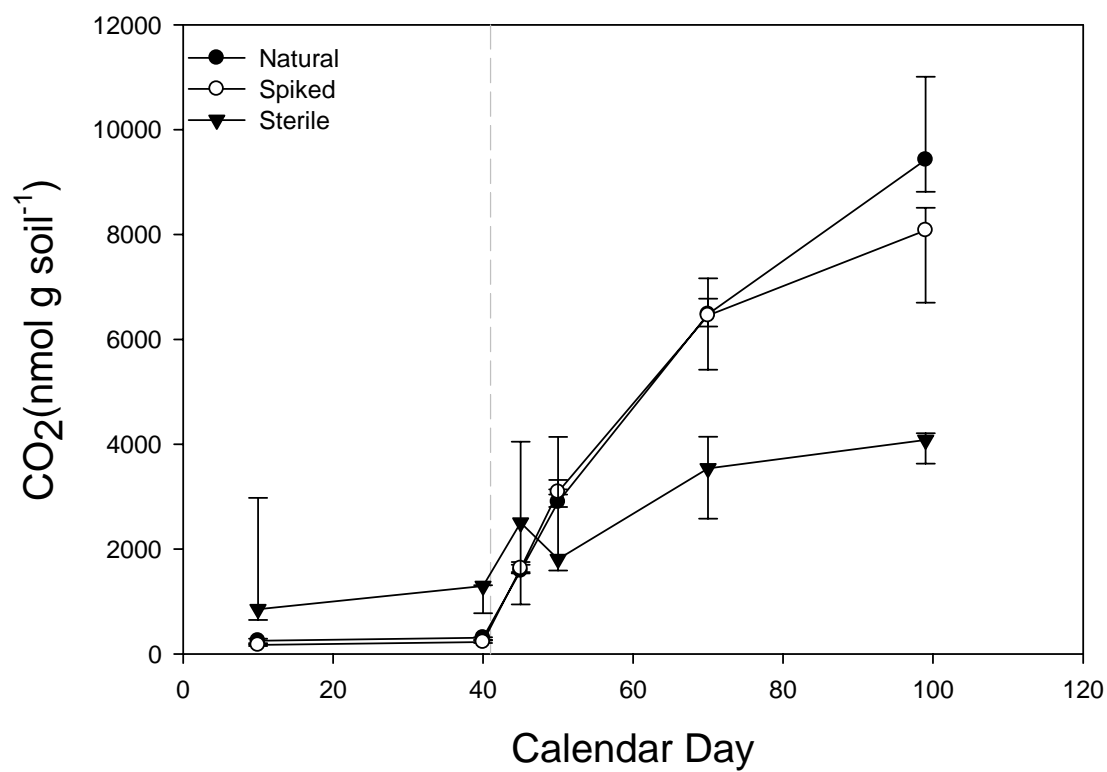


Figure 4.4.5. Median cumulative CO₂ release over time standardized to one gram of dry soil. Error bars represent 1st and 3rd quartiles of distribution (n = 4). Dashed line indicates beginning of 4°C incubation.

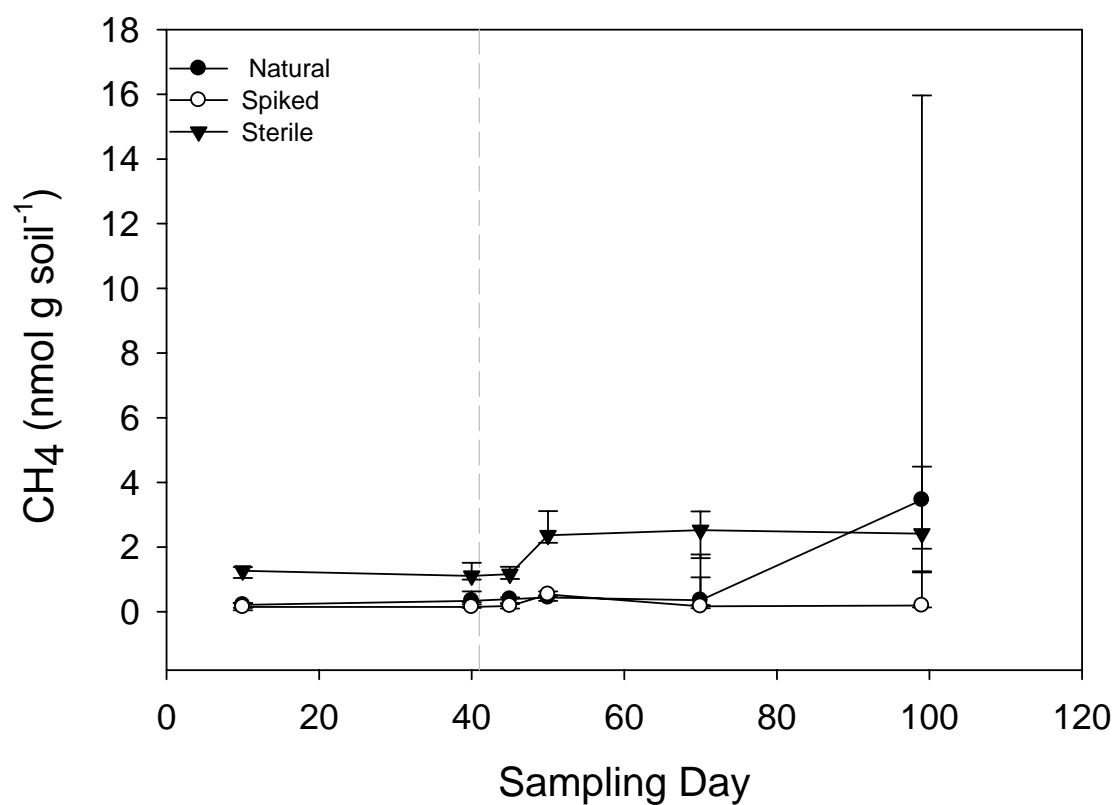


Figure 4.4.6. Median cumulative CH₄ release over time standardized to one gram of dry soil. Error bars represent 1st and 3rd quartiles of distribution (n = 4). Dashed line indicates beginning of 4°C incubation.

In contrast, MeHg concentration in unspiked microcosms did not increase until the final time period which exhibited a doubling in the rate of net MeHg produced. However, the microcosms are closed systems with little gas or air exchange and are much more reducing than the redox conditions we measured in the field. Nor did the re-saturation of the soil result in increased MeHg production unlike what has been found at the Experimental Lakes Area in Ontario (St. Louis et al. 2004). Mercury concentrations were lower in the barium chloride extract than the blank, most likely due to re-adsorption of aqueous mercury onto the soil. This indicates that most mercury is not bound in outer sphere complexes on the soils cation exchange sites because it was not displaced by the extracting solution (Stumm and Morgan 1996). Most of the mercury that was dissolved in the water soluble portion was most likely associated with soluble organic matter because the extract had a slight yellow colour.

There was a sudden appearance of mottles on the outside of the sample containers used in the microcosm study, which was most likely due to the reductive dissolution and mobilization of iron (the polypropylene is slightly permeable to oxygen). Analysis of oxalate extractable iron showed an increase in amorphous iron oxides, which is indicative of the dissolution of crystalline iron oxides, and the subsequent re-precipitation of amorphous iron oxides. The high concentrations of iron in the soil (~1% by weight Fe) are consistent with elevated levels of oxalate extractable iron reported by Walker and Peters (1977) for Fibric Organic Cryosols on the Truelove Lowlands. Iron reducers have been shown to be capable of methylating mercury in the environment and in the laboratory (Warner et al. 2003; Fleming et al. 2006; Kerin et al. 2006). Iron reduction was occurring in these soils but MeHg production was likely limited by low mercury bioavailability.

Although definite conclusions on the cause of the increase in MeHg in the natural treatment can not be determined without further manipulative studies, it would appear that iron reduction or organic matter dissolution could have been stimulating this increase in methylation because both were correlated to MeHg production in the natural treatment. However, DOM has not been found to increase mercury bioavailability but rather for the most part inhibits uptake through the formation of large charged molecules (Kelly et al. 2003). The increased concentration of DOM in solution could

have stimulated microbial activity (Ravichandran 2004) or simply may be auto correlated to MeHg production as both are a result of microbial activity. Sulfate decreased in the natural treatment, however, there was no corresponding detectable increase in sulfide. The decrease in sulfate only in the natural and not the spiked treatment may be because of errors sampling or analyzing the porewater. There is also some evidence that indicates that methanogenesis is not stimulating MeHg production because samples which had high CH₄ production did not demonstrate a corresponding increase in MeHg concentration. However, this experiment can only offer a general indication of the correlation between redox potential and MeHg production. More specific manipulative experiments are needed to determine the potential of arctic soils to produce MeHg under specific geochemical conditions.

MeHg did not change significantly in the sterile treatment over the course of the study. This is the first study to examine the methylation potential of sterilized arctic soil and therefore no comparisons are available. From this study it appears that abiotic methylation is not a significant source of MeHg production in arctic soil. Mercury is thought to be methylated abiotically via residual biotically produced compounds in soil and sediments (e.g. methylcobalamin, methyltin and other methyl compounds) (Weber 1993; Celo et al. 2006). However, Celo et al. (2006) found that methylcobalamin was inhibited from methylating mercury by moderate to high levels of chloride and other organo methyl compounds are most likely not present in arctic soils at significant concentrations. Conversely numerous studies have found that a variety of compounds and conditions can methylate mercury abiotically (Celo et al. 2006; Weber 1993; Hintelmann 1999). It is still possible that abiotic methylation does occur in soils, perhaps, in combination with biological activity and further studies could be carried out on sterile soil poised under different geochemical conditions.

Results from gas sampling did not show any significant increases in nitrous oxide emissions and nitrate was not detected in the porewater. Indicating that perhaps these soils are limited in nitrate and denitrifiers may not be directly associated with methylation. This is not surprising given that of all the common nitrogen species found in soil, mercury shows only an affinity for ammonia (Morel et al. 1998). There would not seem to be a mechanism whereby methylation would occur unless denitrifiers are

capable of methylating mercury at elevated rates. CO₂ showed a steady increase over the experiment with little carbon dioxide being emitted while soil was incubated at -5°C (1.2 nmol g⁻¹ d⁻¹) indicating lower microbial activity during the sub-zero portion of the experiment. Schimel and Clein (1996) also found that soil frozen at -5°C emitted minimal amounts of CO₂ (~ 0 µg CO₂ g OM⁻¹ h⁻¹). Panikov et al. (2006) found low rates of CO₂ production (~tens of nmol CO₂ g⁻¹ d⁻¹) in arctic soil subjected to temperatures between 0°C and -39°C. The authors (Panikov et al. 2005) also found that soil collected in the spring and summer had much lower respiration rates at subzero temperatures than soil collected during the winter. Levels of CO₂ and CH₄ were higher for the sterile treatment most likely due to chemical reactions catalyzed by the gamma irradiation of the soil (McNamara et al. 2003).

4.6 Conclusion

Overall MeHg was produced at a much greater rate in the spiked treatment than the natural treatment and production in the spiked treatment did not seem to be affected by changes in redox potential. Contrary to observations in the field MeHg production was observed, in the natural treatment, when iron appeared to be the dominant terminal electron acceptor. However, MeHg did not show a significant increase in concentration until the soil had become much more reducing than what was observed in the field. CO₂ production seemed to increase at a steady rate throughout the experiment, which does not indicate that there was a pulse of microbial activity at thaw. This correlates with the redox data which showed a steady decline in redox potential after thaw. The absence of a pulse of microbial activity at thaw could be because the soil had undergone two brief freeze thaw cycles prior to the experiment. Schimel and Clein (1996) have found that tundra soils tend to have a less pronounced pulse of CO₂ at thaw if they have undergone prior freeze thaw cycles after the soil is collected. However, this dampening effect occurred after numerous freeze thaw cycles. In the absence of a pulse of microbial activity at thaw it seems that the soil would not achieve the redox conditions necessary for a significant net MeHg production, during the course of an Arctic summer. The results of the field study indicate that these wetlands soils are not capable of producing MeHg at high enough levels to be a source of MeHg to the Arctic ecosystem without

anthropogenic inputs of inorganic mercury or a change in microbial activity/porewater chemistry (e.g. change in porewater speciation of Hg^{+2}) at thaw due to snowmelt.

5.0 GENERAL CONCLUSION

The field and laboratory experiments demonstrated that the organic soils on the Truelove Lowlands do not have the potential to produce significant amounts of MeHg without external inputs of mercury. In the field MeHg declined steadily and the soils only seemed to be mildly reducing. During the incubation of wetland soil, under ambient conditions, the soil's biological community was not more active at thaw than at any other point during the experiment and MeHg did not increase until the end of the experiment. However, upon the addition of inorganic mercury, the rate of MeHg production was ~20x the rate of MeHg production in the natural (ambient) treatment.

It is unclear how MeHg is being maintained in the soils of Truelove Lowland. One possibility is that atmospherically deposited mercury is a labile mercury pool that is more readily available for methylation than ambient mercury. Mercury from atmospheric mercury depletion events is highly bioavailable (Constant et al. 2007) and may stimulate MeHg production in the soil. However, the inorganic mercury adsorbed from snowmelt would be present at concentrations below that used in our spiked treatment and thus potentially have less of an effect on MeHg production. MeHg deposited directly in the snowmelt (St. Louis et al. 2005) may also be a source of organic mercury to these soils. Scott et al. (2004) found that mercury in the snowpack was highly bioavailable (bioavailable Hg(II) represented 50 % of total Hg), and therefore may be readily methylated during snowmelt and provide a source of MeHg to these soils. Assuming that 8 km² of the Lowland is terrestrial and that the snowmelt with a DHg concentration of 5-10 pM drains entirely into the wet sedge meadows (1 km²) (Guillemette 1998) and that all of this DHg is converted to MeHg, atmospheric mercury would account for less than 10 % of the total MeHg lost during the field study. These calculations suggest that atmospheric deposition can not be the sole driver of MeHg in Truelove Lowland.

Our data suggests that a combination of atmospheric and in-situ processes maintain a cycle of MeHg production (spring) and loss (summer) in arctic soils. Atmospheric Hg may be a long term source of mercury to the soil and in-situ production initially in the soil may drive MeHg production. However, regardless of the initial source of soil MeHg it appears that Arctic soils do not export significant amounts of MeHg and that snowmelt is the major source of MeHg to arctic freshwater ecosystems.

6.0 BIBLIOGRAPHY

- Alberts, J.J., J.E. Schindler, R.W. Miller and D.E. Nutter. 1974. Elemental mercury evolution mediated by humic acid. *Science* 184:895-897.
- ATSDR. 1999. Toxicological profile for mercury. Atlanta, GA.
- Barkay, T. and A.J. Poulain. 2007. Mercury (micro)biogeochemistry in polar environments. *FEMS Microbiol. Ecol.* 59:232-241.
- Benoit, J.M., R.P. Mason and C.C. Gilmour. 1999. Estimation of mercury-sulfide speciation in sediment pore waters using octanol-water partitioning and implications for availability to methylating bacteria. *Environ. Toxicol. Chem.* 18:2138-2141.
- Berg, P., S. Rysgaard and B. Thamdrup. 2003. Dynamic modeling of early diagenesis and nutrient cycling. A case study in an arctic marine sediment. *Am. J. Sci.* 303:905-955.
- Bird, S.M., M.S. Fram, K.L. Crepeau. 2003. Method of analysis by the U.S. Geological Survey California District Sacramento Laboratory-determination of dissolved organic carbon in water by high temperature catalytic oxidation, method validation, and quality-control practices. Report No. 03-366. US Geological Survey, Sacramento, CA.
- Bliss, L.C. 1977. Introduction. p. 1-11. *In* L. C. Bliss (ed.) Truelove Lowland, Devon Island, Canada: A High Arctic Ecosystem. The University of Alberta Press, Edmonton, AB.
- Bloom, N.S., E. Preus, J. Katon and M. Hiltner. 2002. Selective extractions to assess the biogeochemically relevant fractionation of inorganic mercury in sediments and soils. *Anal. Chim. Acta.* 479: 233-248.
- Carpi, A. and S.E. Lindberg. 1998. Application of a Teflon dynamic flux chamber for quantifying soil mercury flux: tests and results over a background soil. *Atmos. Environ.* 32: 873-882.

- Celo, V., D.R.S. Lean and S.L. Scott. 2006. Abiotic methylation of mercury in the aquatic environment. *Sci. Total Environ.* 368:126-137.
- Childers, S.E., S. Ciufo and D.R. Lovley. 2002. *Geobacter metallireducens* accesses insoluble Fe(III) oxide by chemotaxis. *Nature* 416:767-769.
- Chipperfield, J.R. and C. Ratledge. 2000. Salicylic acid is not a bacterial siderophore: a theoretical study. *BioMetals* 13:165-168.
- Choi, S.C., T. Chase and R. Bartha. 1994. Enzymatic catalysis of mercury methylation by *Desulfovibrio desulfuricans* LS. *Appl. Environ. Microbiol.* 60:1342-1346.
- Cline, J.D. 1969. Spectrophotometric determination of hydrogen sulfide in natural waters. *Limnol. Oceanogr.* 14:454-458.
- Collins, R.C., D.M. Sherman and K.V. Ragnarsdottir. 1999. Surface complexation of Hg²⁺ on goethite: mechanism from EXAFS spectroscopy and density functional calculations. *J. Colloid Interface Sci.* 219:345-350.
- Compeau, G. C. and R. Bartha. 1985. Sulfate-reducing Bacteria: Principal Methylators of Mercury in Anoxic Estuarine Sediment. *Appl. Environ. Microbiol.* 50:498-502.
- Constant, P., L. Poissant, R. Villemur, E. Yumvihoze and D. Lean. 2007. Fate of inorganic mercury and methyl mercury within the snow cover in the low arctic tundra on the shore of Hudson Bay. *J. Geophys. Res., [Atmos.]* 112: 1-10.
- Courtin, G.M., and C.L. Labine. 1977. Microclimatological studies on Truelove Lowland. p. 73-106. *In* L. C. Bliss (ed.) Truelove Lowland, Devon Island, Canada: A High Arctic Ecosystem. The University of Alberta Press, Edmonton, AB.
- Cuthbert, I.D. and P.D. Giorgio. 1992. Toward a standard method of measuring color in freshwater. *Limnol. Oceanogr.* 37:1319-1326.
- Das, A. and F. Caccavo. 2000. Dissimilatory Fe(III) oxide reduction by *Shewanella alga* BrY requires Adhesion. *Curr. Microbiol.* 40:344-347.
- Davidson, C.L. and R.E. Honrath. 1987. The scavenging of atmospheric sulfate by arctic snow. *Atmos. Environ.* 21:871-882.
- Delaune, R.D., A. Jugsujinda, I. Devai and W.H. Patrick Jr.. 2004. Relationship

- of sediment redox conditions to methyl mercury in surface sediments of Louisiana Lakes. *J. Environ. Sci. Health, Part A* 39:1925-1933.
- Dickson, A. 2006. MSc candidate. Personal communication. February 25, 2006.
- Dispaquale, M.C.M. and R.S. Oremland. 1998. Bacterial methylmercury degradation in Florida Everglades peat sediment. *Environ. Sci. Technol.* 32:2556-2563.
- Ekstrom, E.B., F.M.M. Morel and J.M. Benoit. 2003. Mercury methylation independent of the acetyl-coenzyme A pathway in sulfate-reducing bacteria. *Appl. Environ. Microbiol.* 69:5414-5422.
- Elliot, K. 2006. Field Technician. Personal communication. March 20, 2006.
- EPA. 1998. Method 7000B, Revision 2: Flame atomic absorption spectrophotometry. United States Environmental Protection Agency, Washington, DC.
- EPA. 1999. Method 1631, Revision B: Mercury in water by oxidation, purge and trap, and cold vapor atomic fluorescence spectrometry. Rep No. EPA-821-R-99-005. United States Environmental Protection Agency, Washington, DC.
- EPA. 2001. Draft Method 1630: Methyl mercury in water by distillation, aqueous ethylation, purge and trap, and CVAFS. Rep No. EPA-821-R-01-020. United States Environmental Protection Agency, Washington, DC.
- Evers, D.C. 2005. Mercury connections: the extent and effects of mercury pollution in northeastern North America. BioDiversity Research Institute. Gorham, MN.
- Falter, R. 1999. Experimental study on the unintentional abiotic methylation of inorganic mercury during analysis: part 1: localization of the compounds effecting the abiotic mercury methylation. *Chemosphere* 39:1051-1073.
- Field, A. 2005. *Discovering statistics using SPSS*. 2nd ed. SAGE Publication Inc. Thousand Oaks, CA, USA.
- Fleming, E.J., E.E. Mack, P.G. Green and D.C. Nelson. 2006. Mercury methylation from unexpected sources: molybdate-inhibited freshwater sediments and an iron-reducing bacterium. *Appl. Environ. Microbiol.* 72:457-464.
- Fortin, D. and S. Langley. 2005. Formation and occurrence of biogenic iron-rich

- minerals. *Earth-Sci. Rev.* 72:1-19.
- Gabriel, M.C. and D.G. Williamson. 2004. Principal biogeochemical factors affecting the speciation and transport of mercury through the terrestrial environment. *Environ. Geochem. Health* 26:421-434.
- Gilmour, C.C., E.A. Henry and R. Mitchell. 1992. Sulfate stimulation of mercury methylation in freshwater sediments. *Environ. Sci. Technol.* 26:2281-2287.
- Gilmour, C.C., G.S. Riedel, M.C. Ederington, J.T. Bell, J.M. Benoit, G.A. Gill and M.C. Stordal. 1998. Methylmercury concentrations and production rates across a trophic gradient in the northern Everglades. *Biogeochemistry* 40:327-345.
- Goulet, R.R., J. Holmes, A. Tessier, F. Wang, S.D. Siciliano, B. Page, D.R.S. Lean, M. Amyott and L. Poissant. 2007. Mercury methylation in sediments of a riverine marsh: the role of redox conditions sulfur chemistry and microbial communities. *Geochim. Cosmochim. Acta* 71:3396-3406.
- Guillemette, S. 1998. Arctic plant community-soil associations mapping using spot imagery: Truelove Lowland, Devon Island, N.W.T. MSc Thesis. University of Western Ontario, London, ON.
- Gustafsson, J. P. 2006. Visual Minteq. Version 2.51. Division of Land and Water Resources, Royal Institute of Technology. Stockholm, SWE.
- Hammerschmidt, C.R., W.F. Fitzgerald, C.H. Lamborg, P.H. Balcom and C.M. Tseng. 2006. Biogeochemical cycling of methylmercury in lakes and tundra watersheds of arctic Alaska. *Environ. Sci. Technol.* 40:1204-1211.
- Heyes, A., R.P. Mason, E.H. Kim and E. Sunderland. 2006. Mercury methylation in estuaries: insights from using measuring rates using stable mercury isotopes. *Mar. Chem.* 102:134-147.
- Heyes, A., T.R. Moore, J.W.M. Rudd and J.J. Dugoua. 2000. Methyl mercury in pristine and impounded boreal peatlands, Experimental Lakes Area, Ontario. *Can. J. Fish. Aquat. Sci.* 57:2211-2222.
- Hintelmann, H. 1999. Comparison of different extraction techniques used for methylmercury analysis with respect to accidental formation of methylmercury during sample preparation. *Chemosphere* 39:1093-1105.

- Hintelmann, H., K. Keppel-Jones and R.D. Evans. 2000. Constants of mercury methylation and demethylation rates in sediments and comparison of tracer and ambient mercury availability. *Environ. Toxicol. Chem.* 19:2204-2211.
- Hintelmann, H., P.M. Welbourn and R.D. Evans. 1995. Binding of methylmercury compounds by humic and fulvic acids. *Water, Air, Soil Pollut.* 80:1031-1034.
- Hulbert, S.H. 1984. Pseudoreplication and the design of ecological field experiments. *Ecological Monographs* 54:187-211.
- Jackson, T.A. 1998. Mercury in aquatic ecosystems. In: Langston W.J., M.J. Bebianno (eds.). *Metal metabolism in aquatic environments*. London: Chapman and Hall Publishers. Pp. 76 – 157. As cited in Gabriel and Williamson 2004.
- Kelly, C.A., J.W.M. Rudd and M.H. Holoka. 2003. Effect of pH on mercury uptake by an aquatic bacterium: implications for Hg cycling. *Environ. Sci. Technol.* 37:2941-2946.
- Kerin, E.J., C.C. Gilmour, E. Roden, M.T. Suzuki, J.D. Coates and R.P. Mason. 2006. Mercury methylation by dissimilatory iron-reducing bacteria. *Appl. Environ. Microbiol.* 72:7919-7921.
- King, R.H. 1969. Periglaciation on Devon Island, N.W.T. Unpublished Ph.D. thesis, Department of Geography, University of Saskatchewan. As cited in Guillemette (1998).
- Kirk, G.A. 2004. *The Biogeochemistry of Submerged Soils* John Wiley & Sons, Ltd. West Sussex, UK.
- Kostka, J.E., B. Thamdrup, R.N. Glud and D.E. Canfield. 1999. Rates and pathways of carbon oxidation in permanently cold arctic sediments. *Mar. Ecol- Prog. Ser.* 180:7-21.
- Krupicka, J. 1977. Bedrock geology of the Truelove River area. p. 73-106. In L. C. Bliss (ed.) *Truelove Lowland, Devon Island, Canada: A high Arctic ecosystem*. The University of Alberta Press, Edmonton, AB.
- Lahoutifard, N., M. Sparling and D. Lean. 2005. Total and methyl mercury patterns in arctic snow during springtime at Resolute, Nunavut, Canada. *Atmos. Environ.* 39:7597-7606.

- Lalonde, J.D., M. Amyot, A.M.L. Kraepiel and F.M.M. Morel. 2001.
Photooxidation of Hg(0) in artificial and natural waters. *Environ. Sci. Technol.* 35:1367-1372.
- Land Resource Research Unit. 1984. Method 84-011 Ammonium Oxalate extractable Fe and Al. *In* B.H. Sheldrick (ed.) *Analytical Methods Manual*. Agriculture Canada, Ottawa, ON.
- Letts, M.G., N.T. Roulet, N.T. Comer, M.R. Skarupa and D.L. Versegny. 1999.
Parametrization of peatland hydraulic properties for the Canadian Land Surface Scheme. *Atmos. Ocean* 38:141-160.
- Levy, S. 2006. Arsenic in a high arctic soil ecosystem on Devon Island, Nunavut. MSc Thesis. University of Saskatchewan, Saskatoon, Sk.
- Lindberg, S.E., S. Brooks, C.J. Lin, K.J. Scott, M.S. Landis, R.K. Stevens, M. Goodsite, and A. Richter. 2002. Dynamic oxidation of gaseous mercury in the Arctic troposphere at polar sunrise. *Environ. Sci. Technol.* 36:1245-1256.
- Loseto, L.L., S.D. Siciliano and D.R.S. Lean. 2004a. Methylmercury production in high arctic wetlands. *Environ. Toxicol. Chem.* 23:17-23.
- Loseto, L.L., D.R.S. Lean and S.D. Siciliano. 2004b. Snowmelt sources of methylmercury to high arctic ecosystems. *Environ. Sci. Technol.* 38:3004-3010.
- Lovley, D.R. 1991. Dissimilatory Fe(III) and Mn(IV) reduction. *Microbiol. Rev.* 55:259-287.
- Lovley, D.R. 1993. Dissimilatory metal reduction. *Annu. Rev. Microbiol.* 47:263-290.
- Lovley, D.R. 2000. Fe(III) and Mn(IV) reduction. *In* environmental microbe-metal interactions ed. Lovley, D.R. pp. 3-30. Washington: ASM. ISBN 1555811957.
As cited in Luu and Ramsay 2003.
- Lovley, D.R., J.D. Coates, E.L. Blunt-Harris, E.J.P. Phillips and J.C. Woodward. 1996. Humic substances as electron acceptors for microbial respiration. *Nature* 382:445-448.
- Lovley, D.R. and E.J.P. Phillips. 1988. Novel mode of microbial energy metabolism: organic carbon oxidation coupled to dissimilatory reduction of iron and manganese. *Appl. Environ. Microbiol.* 54:1472-1480.
- Luu, Y.S. and J.A. Ramsay. 2003. Review: microbial mechanisms of accessing

- insoluble Fe(III) as an energy source. *World J. Microbiol. Biotechnol.* 19:215-225.
- Macdonald, R.W. 2005. Climate change, risks and contaminants: a perspective from studying the arctic. *Hum. Ecol. Risk Assess.* 11:1099-1104.
- Magnuson, T.S., N. Isoyama, A.L. Hodges-Myerson, G. Davidson, M.J. Maroney, G.G. Geesey and D.R. Lovley. 2001. Isolation characterization and gene sequence analysis of a membrane associated 89 kDa Fe(III) reducing-cytochrome c from *Geobacter sulfurreducens*. *Biochem. J.* 359:147-152.
- McNamara, N.P., H.I.J. Black, N.A. Beresford and N.R. Parekh. 2003. Effects of acute gamma irradiation on chemical physical and biological properties of soils. *Appl. Soil. Ecol.* 24:117-132.
- Meier, J., R. Costa, K. Smalla, B. Boehrer and K. Wendt-Potthoff. 2005. Temperature dependence of Fe(III) and sulfate reduction rates and its effect on growth and composition of bacterial enrichments from an acidic pit lake neutralization experiment. *Geobiology* 3:261-274.
- Miller, C.L., R.P. Mason, C.C. Gilmour and A. Heyes. 2007. Influence of dissolved organic matter on the complexation of mercury under sulfidic conditions. *Environ. Toxicol. Chem.* 26:624-633.
- Milne, C.J., D.G. Kinniburgh, W.H. Van Riemsdijk and E. Tipping. 2003. Generic NICA-Donnan model parameters for metal-ion binding by humic substances. *Environ. Sci. Technol.* 37:958-971.
- Miskimmin, B.M., J.W.M. Rudd and C.A. Kelly. 1992. Influence of dissolved organic carbon, pH, and microbial respiration rates on mercury methylation and demethylation in lake water. *Can. J. Fish Aquat. Sci.* 49:17-22.
- Morel, F.M.M., A.M.L. Kraepiel and M. Amyot. 1998. The chemical cycle and bioaccumulation of mercury. *Annu. Rev. Ecol. Syst.* 29:543 –566.
- Morse, J.W., F.J. Millero, J.C. Cornwell and D. Rickard. 1987. The chemistry of the hydrogen sulfide and iron sulfide systems in natural waters. *Earth-Sci. Rev.* 24:1-42.
- Muc, M., and L.C. Bliss. 1977. Plant communities of the Trulove Lowland. p.

- 143-154. In L. C. Bliss (ed.) Truelove Lowland, Devon Island, Canada: A high Arctic Ecosystem. The University of Alberta Press, Edmonton, AB.
- Nealson, K.H. and D. Saffarini. 1994. Iron and manganese in anaerobic respiration: environmental significance, physiology, and regulation. *Annu. Rev. Microbiol.* 48:311-343.
- Nevin, K.P. and D.R. Lovley. 2002. Mechanisms for accessing insoluble Fe(III) oxide during dissimilatory Fe(III) reduction by *Geothrix fermentans*. *Appl. Environ. Microbiol.* 68:2294-2299.
- Newman, D.K. and R. Kolter. 2000. A role for excreted quinones in extracellular electron transfer. *Nature* 405:94-97.
- Onat, E. 1974. Solubility studies of metallic mercury in pure water at various temperature. *J. Inorg. Nucl. Chem.* 36:2029-2032.
- Oremland, R.S., C.W. Culbertson, M.R. Winfrey. 1991. Methylmercury decomposition in sediments and bacterial cultures: involvement of methanogens and sulfate reducers in oxidative demethylation. *Appl. Environ. Microbiol.* 57:130 -137.
- Pak, K. and R. Bartha. 1998a. Products of mercury demethylation by sulfidogens and methanogens. *Bull. Environ. Contam. Toxicol.* 61:690-694.
- Pak, K. and R. Bartha. 1998b. Mercury methylation and demethylation in anoxic lake sediments and by strictly anaerobic bacteria. *Appl. Environ. Microbiol.* 64:1013-1017.
- Panikov, N.S., P.W. Flanagan, W.C. Oechel, M.A. Mastepanov and T.R. Christensen. 2005. Microbial activity in soils frozen to below -39°C. *Soil Biol. Biochem.* 38:785-794.
- Ravichandran, M. 2004. Interactions between mercury and dissolved organic matter - a review. *Chemosphere* 55:319-331.
- Regnell, O. and T. Hammar. 2004. Coupling of methyl and total mercury in a minerotrophic peat bog in southeastern Sweden. *Can. J. Fish. Aquat. Sci.* 61:2014-2023.
- Renneberg, A.J. and M.J. Dudas. 2001. Transformation of elemental mercury to

- inorganic and organic forms in mercury and hydrocarbon co-contaminated soils. *Chemosphere* 45:1103-1109.
- Roden, E.E. and J.M. Zachara. 1996. Microbial reduction of crystalline iron (III) oxides: influence of oxide surface area and potential for cell growth. *Environ. Sci. Technol.* 30:1618-1628.
- Roychoudhury, A.N. 2006. Time dependent calibration of a sediment extraction scheme. *Mar. Pollut. Bull.* 52:397-403.
- Royer, R.A., W.D. Burgos, A.S. Fisher, B.H. Jeon, R.F. Unz and B.A. Dempsey. 2002. Enhancement of hematite bioreduction by natural organic matter. *Environ. Sci. Technol.* 36:2897-2904.
- Ryden, B.E. 1977. Hydrology of Truelove Lowland. p. 107-136. *In* L. C. Bliss (ed.) Truelove Lowland, Devon Island, Canada: A high Arctic Ecosystem. The University of Alberta Press, Edmonton, AB.
- Schimel, J.P. and J.S. Clein. 1996. Microbial response to freeze-thaw cycles in tundra and taiga soils. *Soil Biol. Biochem.* 28:1061-1066.
- Schluter, K. 2000. Review: evaporation of mercury from soils. An integration and synthesis of current knowledge. *Environ. Geol.* 39:249-271.
- Schroeder, W., K.G. Anlauf, and L.A. Barrie. 1998. Arctic springtime depletion of mercury. *Nature* 394:331-332.
- Schwertmann, U. and R.M. Taylor. 1989. Iron oxides. p.379-438. *In* J.B. Dixon and S.B. Weed (eds.). Minerals in soil environments. 2nd ed. SSSA Book Series. 1. SSSA, Madison, WI. As cited in: Liu, C. 1999. Surface chemistry of iron oxide minerals formed in different ionic environments. PhD Thesis. University of Saskatchewan, Saskatoon, SK.
- Schuster, E. 1991. The behaviour of mercury in the soils with special emphasis on complexation and adsorption processes-a review of the literature. *Water, Air, Soil Pollut.* 56:667 – 680.
- Scott, K. J. 2001. Bioavailable mercury in Arctic snow determined by a light-emitting mer-lux bioreporter. *Arctic* 54:92-101.
- Semkin, R.G., G. Mierle and R.J. Neureuther. 2005. Hydrochemistry and mercury cycling in a high arctic watershed. *Sci. Total Environ.* 324:199-221.

- Senko, J.M., T.A. Dewers and L.R. Krumholz. 2005. Effect of oxidation rate and Fe(II) state on microbial nitrate-dependent Fe(III) mineral formation. *Appl. Environ. Microbiol.* 71:7172-7177.
- Shade, C. W. 2005. Hg-Thiourea complex ion chromatography with on-line cold vapor generation and atomic fluorescence spectrometric detection (HGTU/IC-CVAFS). PhD thesis. University of Illinois, Urbana-Champaign, IL.
- Shade, C.W. and R.J.M. Hudson. 2005. Determination of MeHg in environmental sample matrices using Hg-thiourea complex ion chromatography with on-line cold vapour generation and atomic fluorescence spectrometric detection. *Environ. Sci. Technol.* 39:4974-4982.
- Siciliano, S.D. and D.R.S. Lean. 2002. Methyltransferase: an enzyme assay for microbial methylmercury formation in acidic soils and sediments. *Environ. Toxicol. Chem.* 21:1184-1190.
- Siciliano, S.D., N.J. O'Driscoll and D.R.S. Lean. 2002. Microbial reduction and oxidation of mercury in freshwater lakes. *Environ. Sci. Technol.* 36:3064-3068.
- St. Louis, V.L., J.W.M. Rudd, C.A. Kelly, R.A. Bodaly, M.J. Paterson, K.G. Beaty, R.H. Hesslein, A. Heyes and A.R. Majewski. 2004. The rise and fall of mercury methylation in an experimental reservoir. *Environ. Sci. Technol.* 38:1348-1358.
- St. Louis, V.L., M.J. Sharp, A. Steffen, A. May, J. Barker, J.L. Kirk, D.J.A. Kelly, S.E. Arnott, B. Keatley and J.P. Smol. 2005. Some sources and sinks of monomethyl and inorganic mercury on Ellesmere Island in the Canadian high arctic. *Environ. Sci. Technol.* 39:2686-2701.
- Steinmann, P. and W. Shotyk. 1997. Chemical composition, pH, and redox state of sulfur and iron in complete vertical porewater profiles from two *Sphagnum* peat bogs, Jura Mountains, Switzerland. *Geochim. Cosmochim. Acta* 61:1143-1163.
- Stumm, W. and J.J. Morgan. 1996. Aquatic chemistry: chemical equilibria and rates in natural waters. 3rd ed. Wiley Interscience, New York, NY.
- Stutter, M.I. and M.F. Billet. 2003. Biogeochemical controls on streamwater and soil solution chemistry in a high arctic environment. *Geoderma* 113:127-146.

- Swallow, K.W. and N.H. Low. 1994. Capillary zone electrophoretic analysis of the minor anions present in orange juice and orange pulpwash. *J. Agric. Food Chem.* 42:2808-2811.
- Takagai, Y. and S. Igarashi. 2003. Simultaneous determination of Iron(II) and Iron(III) by micellar electrokinetic chromatography using an off-line selective complexing reaction. *Anal. Sci.* 19:1207-1209.
- Tchounwou, P.B., W.K. Ayensu, N. Ninashvili and D. Sutton. 2003. Environmental exposure to mercury and its toxicopathologic implications for public health. *Environ. Toxicol.* 18:149 –175.
- Temple, K.L. and A.R. Colmer. 1951. The autotrophic oxidation of iron by a new bacterium: *Thiobacillus Ferrooxidans*. *J. Bacteriol.* 62:605-611.
- Vandieken, V., C. Knoblauch and B.B. Jorgensen. 2006. *Desulfovibrio frigidus* sp. Nov. and *Desulfovibrio ferrireducens* sp. Nov., psychrotolerant bacteria isolated from Arctic fjord sediments (Svalbard) with the ability to reduce Fe(III). *Int. J. Syst. Evol. Microbiol.* 56:681-685.
- Vepraskas, M.J. 2002. Redox Potential Measurements. <http://www.soil.ncsu.edu/wetlands/wetlandsoils/RedoxWriteup.pdf>. Accessed December 2006.
- Wafer, C.C., J.B. Richards and D.L. Osmond. 2004. Construction of platinum-tipped redox probes for determining soil redox potential. *J. Environ. Qual.* 33:2375-2379.
- Walker, B.D., and T.W. Peters. 1977. Soils of Truelove Lowland and Plateau. p. 31-62. *In* L. C. Bliss (ed.) Truelove Lowland, Devon Island, Canada: A high Arctic ecosystem. The University of Alberta Press, Edmonton, AB.
- Warner, K.A., E.E. Roden and J.C. Bonzongo. 2003. Microbial mercury transformation in anoxic freshwater sediments under iron-reducing and other electron-accepting conditions. *Environ. Sci. Technol.* 37:2159-2165.
- Weber, J.H. 1993. Review of possible paths for abiotic methylation of mercury(II) in the aquatic environment. *Chemosphere* 26:2063-2077.
- Yamamoto, M. 1996. Stimulation of elemental mercury oxidation in the presence of chloride ion in aquatic environments. *Chemosphere* 32:1217-1224.

APPENDIX A. RESULTS FROM FIELD STUDY

Table A.1 Results from field measurements Truelove Lowland, Devon Island

Sampler type**	Sampling Day	Sample Location	GPS Location		Eh	Temperature**			pH
			Longitude	Latitude		B	T	Average	
			—Decimal degrees—		mV	———— °C —————			
P	207	11	-84.622816	75.6812507	129.00	1.30	3.60	2.45	7.51
P	207	12	-84.622722	75.6812413	70.00	0.80	2.80	1.80	7.36
L	207	13	-84.622271	75.6812097	201.00	3.70	1.20	2.45	7.42
L	207	14	-84.622229	75.6811851	92.80	8.70	9.10	8.90	7.65
L	207	15	-84.621967	75.6811125	18.50	8.00	8.30	8.15	6.56
P	207	21	-84.64836	75.6804635	198.10	3.20	3.20	3.20	7.06
P	207	22	-84.647741	75.6804043	12.35	0.30	1.70	1.00	-
L	207	23	-84.647613	75.6803795	2.60	0.30	1.70	1.00	-
L	207	24	-84.647687	75.680357	55.95	2.90	2.90	2.90	7.04
L	207	25	-84.647399	75.6803239	19.80	0.10	2.20	1.15	6.21
P	207	31	-84.621361	75.6759364	55.00	3.80	6.20	5.00	7.74
P	207	32	-84.621144	75.6759352	73.15	1.90	3.30	2.60	7.49
P	207	33	-84.620989	75.6758779	16.00	2.10	4.70	3.40	7.14
L	207	34	-84.620708	75.6758443	109.00	2.20	5.20	3.70	6.86
L	207	35	-84.620366	75.6758917	48.00	1.30	3.50	2.40	7.67
P	207	41	-84.591229	75.6666319	48.30	1.30	3.50	2.40	7.67
P	207	42	-84.591274	75.6666564	161.70	1.80	3.40	2.60	7.11
L	207	43	-84.590894	75.6667141	20.00	0.30	2.30	1.30	-
L	207	44	-84.590769	75.6667287	78.55	10.30	10.70	10.50	7.12
L	207	45	-84.590327	75.6667859	154.20	2.00	8.70	5.35	7.52

Sampler type*	Sampling Day	Sample Location	GPS Location		Eh	Temperature**			pH
			Longitude	Latitude		B	T	Average	
			—Decimal degrees—		mV	———— °C —————			
P	210	11	-84.622816	75.6812507	74.00	3.20	6.50	4.85	7.50
P	210	12	-84.622722	75.6812413	36.00	2.50	5.60	4.05	7.61
L	210	13	-84.622271	75.6812097	-	2.50	5.80	4.15	7.03
L	210	14	-84.622229	75.6811851	112.00	2.80	7.80	5.30	7.03
L	210	15	-84.621967	75.6811125	-	2.80	7.80	5.30	6.54
P	210	21	-84.64836	75.6804635	55.50	4.30	8.30	6.30	-
P	210	22	-84.647741	75.6804043	176.00	2.20	4.60	3.40	-
L	210	23	-84.647613	75.6803795	33.00	1.60	4.80	3.20	5.94
L	210	24	-84.647687	75.680357	48.25	0.30	3.10	1.70	6.36
L	210	25	-84.647399	75.6803239	101.50	0.30	3.22	1.76	6.33
P	210	31	-84.621361	75.6759364	85.00	7.70	9.10	8.40	7.77
P	210	32	-84.621144	75.6759352	-	5.00	7.00	6.00	7.56
P	210	33	-84.620989	75.6758779	-	4.80	6.20	5.50	7.71
L	210	34	-84.620708	75.6758443	-	4.20	6.20	5.20	7.20
L	210	35	-84.620366	75.6758917	-	4.30	6.20	5.25	7.34
P	210	41	-84.591229	75.6666319	-	0.30	2.60	1.45	7.18
P	210	42	-84.591274	75.6666564	287.00	0.50	2.50	1.50	7.19
L	210	43	-84.590894	75.6667141	-	1.40	3.90	2.65	7.37
L	210	44	-84.590769	75.6667287	39.00	1.70	4.40	3.05	6.92
L	210	45	-84.590327	75.6667859	23.50	5.00	6.60	5.80	-
P	213	11	-84.622816	75.6812507	212.30	6.10	8.10	7.10	7.47
P	213	12	-84.622722	75.6812413	171.00	5.20	7.30	6.25	7.77
L	213	13	-84.622271	75.6812097	208.00	5.00	7.60	6.30	7.44

Sampler type*	Sampling Day	Sample Location	GPS Location		Eh	Temperature**			pH
			Longitude	Latitude		B	T	Average	
			—Decimal degrees—		mV	———— °C —————			
L	213	14	-84.622229	75.6811851	142.35	5.30	8.30	6.80	7.30
L	213	15	-84.621967	75.6811125	197.80	4.80	7.00	5.90	7.35
L	213	21	-84.64836	75.6804635	215.05	6.20	7.70	6.95	-
P	213	22	-84.647741	75.6804043	223.00	5.60	7.50	6.55	-
L	213	23	-84.647613	75.6803795	210.10	4.50	7.00	5.75	6.92
L	213	24	-84.647687	75.680357	-	4.50	7.10	5.80	7.29
L	213	25	-84.647399	75.6803239	-	4.50	7.20	5.85	7.33
P	213	31	-84.621361	75.6759364	241.30	0.80	1.60	1.20	7.23
P	213	32	-84.621144	75.6759352	-	5.70	8.00	6.85	6.64
P	213	33	-84.620989	75.6758779	-	6.80	8.30	7.55	6.65
L	213	34	-84.620708	75.6758443	46.00	6.30	8.00	7.15	6.58
L	213	35	-84.620366	75.6758917	184.00	6.60	8.70	7.65	6.96
P	213	41	-84.591229	75.6666319	130.00	4.70	6.80	5.75	6.75
P	213	42	-84.591274	75.6666564	226.00	5.00	7.00	6.00	6.43
L	213	43	-84.590894	75.6667141	221.00	5.50	7.50	6.50	6.39
L	213	44	-84.590769	75.6667287	-	5.20	7.50	6.35	6.21
L	213	45	-84.590327	75.6667859	-	5.60	7.60	6.60	-
P	216	11	-84.622816	75.6812507	74.00	5.00	5.80	5.40	7.17
P	216	12	-84.622722	75.6812413	161.50	4.20	5.70	4.95	-
L	216	13	-84.622271	75.6812097	222.00	4.60	5.70	5.15	6.20
L	216	14	-84.622229	75.6811851	217.00	4.20	5.70	4.95	6.45
L	216	15	-84.621967	75.6811125	160.00	4.30	6.20	5.25	7.25
L	216	21	-84.64836	75.6804635	175.00	4.60	6.50	5.55	7.07

Sampler type*	Sampling Day	Sample Location	GPS Location		Eh	Temperature**			pH
			Longitude	Latitude		B	T	Average	
			—Decimal degrees—		mV	———— °C —————			
P	216	22	-84.647741	75.6804043	174.50	5.00	6.20	5.60	6.89
L	216	23	-84.647613	75.6803795	205.00	5.00	6.80	5.90	6.99
L	216	24	-84.647687	75.680357	152.50	5.00	7.90	6.45	6.74
L	216	25	-84.647399	75.6803239	206.00	3.80	5.60	4.70	7.30
P	216	31	-84.621361	75.6759364	207.00	7.60	8.70	8.15	6.79
P	216	32	-84.621144	75.6759352	30.00	5.90	6.80	6.35	6.80
P	216	33	-84.620989	75.6758779	195.00	5.70	6.60	6.15	6.80
L	216	34	-84.620708	75.6758443	213.00	5.50	7.00	6.25	6.51
L	216	35	-84.620366	75.6758917	95.00	6.20	7.30	6.75	-
P	216	41	-84.591229	75.6666319	100.00	3.00	4.00	3.50	6.98
P	216	42	-84.591274	75.6666564	219.00	4.50	5.30	4.90	6.83
L	216	43	-84.590894	75.6667141	197.00	0.50	3.50	2.00	-
L	216	44	-84.590769	75.6667287	212.50	4.20	5.60	4.90	6.50
L	216	45	-84.590327	75.6667859	116.00	4.50	5.80	5.15	-
P	219	11	-84.622816	75.6812507	202.50	6.50	10.30	8.40	-
P	219	12	-84.622722	75.6812413	167.50	7.10	9.50	8.30	7.41
L	219	13	-84.622271	75.6812097	181.00	7.00	10.00	8.50	7.36
L	219	14	-84.622229	75.6811851	164.50	7.80	13.20	10.50	7.39
L	219	15	-84.621967	75.6811125	166.50	7.00	10.30	8.65	-
L	219	21	-84.64836	75.6804635	128.00	7.30	9.90	8.60	-
P	219	22	-84.647741	75.6804043	230.50	7.10	8.30	7.70	-
L	219	23	-84.647613	75.6803795	193.00	6.70	9.30	8.00	6.38
L	219	24	-84.647687	75.680357	208.50	6.40	9.50	7.95	-

Sampler type*	Sampling Day	Sample Location	GPS Location		Eh	Temperature**			pH
			Longitude	Latitude		B	T	Average	
			—Decimal degrees—		mV	———— °C —————			
L	219	25	-84.647399	75.6803239	200.50	6.50	10.10	8.30	7.60
P	219	31	-84.621361	75.6759364	199.00	4.50	7.60	6.05	-
P	219	32	-84.621144	75.6759352	195.00	2.70	5.30	4.00	-
P	219	33	-84.620989	75.6758779	184.00	2.50	4.30	3.40	-
L	219	34	-84.620708	75.6758443	221.00	1.60	4.00	2.80	-
L	219	35	-84.620366	75.6758917	196.00	2.50	5.70	4.10	-
P	219	41	-84.591229	75.6666319	196.00	1.70	5.00	3.35	-
P	219	42	-84.591274	75.6666564	179.00	2.30	6.20	4.25	-
L	219	43	-84.590894	75.6667141	204.00	2.50	6.70	4.60	-
L	219	44	-84.590769	75.6667287	205.50	1.70	5.80	3.75	-
L	219	45	-84.590327	75.6667859	182.50	2.30	6.10	4.20	-
P	221	11	-84.622816	75.6812507	187.50	2.30	7.50	4.90	-
P	221	12	-84.622722	75.6812413	172.00	2.20	5.00	3.60	-
L	221	13	-84.622271	75.6812097	214.00	2.30	5.70	4.00	-
L	221	14	-84.622229	75.6811851	176.50	2.70	7.70	5.20	-
L	221	15	-84.621967	75.6811125	161.50	3.20	7.30	5.25	-
L	221	21	-84.64836	75.6804635	161.00	2.80	4.70	3.75	-
P	221	22	-84.647741	75.6804043	244.50	2.40	4.60	3.50	-
L	221	23	-84.647613	75.6803795	161.00	2.10	5.10	3.60	-
L	221	24	-84.647687	75.680357	213.50	1.60	5.60	3.60	-
L	221	25	-84.647399	75.6803239	193.00	-	5.50	5.50	-
P	221	31	-84.621361	75.6759364	211.50	4.30	5.70	5.00	-
P	221	32	-84.621144	75.6759352	155.00	1.90	3.40	2.65	-

Sampler type*	Sampling Day	Sample Location	GPS Location		Eh	Temperature**			pH
			Longitude	Latitude		B	T	Average	
			—Decimal degrees—		mV	———— °C —————			
P	221	33	-84.620989	75.6758779	187.00	2.00	3.20	2.60	-
L	221	34	-84.620708	75.6758443	156.00	1.10	3.50	2.30	-
L	221	35	-84.620366	75.6758917	208.00	2.10	4.00	3.05	-
P	221	41	-84.591229	75.6666319	192.00	0.30	1.90	1.10	-
P	221	42	-84.591274	75.6666564	173.50	0.80	2.60	1.70	-
L	221	43	-84.590894	75.6667141	212.00	1.90	3.70	2.80	-
L	221	44	-84.590769	75.6667287	207.50	1.30	3.40	2.35	-
L	221	45	-84.590327	75.6667859	152.50	1.70	3.50	2.60	-
P	223	11	-84.622816	75.6812507	199.50	1.10	3.70	2.40	-
P	223	12	-84.622722	75.6812413	184.00	0.80	2.70	1.75	-
L	223	13	-84.622271	75.6812097	206.00	1.20	4.00	2.60	-
L	223	14	-84.622229	75.6811851	185.00	1.20	3.80	2.50	-
L	223	15	-84.621967	75.6811125	170.00	2.00	4.70	3.35	-
L	223	21	-84.64836	75.6804635	213.00	2.10	3.40	2.75	-
P	223	22	-84.647741	75.6804043	259.50	1.50	3.50	2.50	-
L	223	23	-84.647613	75.6803795	191.00	0.70	3.20	1.95	-
L	223	24	-84.647687	75.680357	210.50	0.70	3.60	2.15	-
L	223	25	-84.647399	75.6803239	185.00	0.50	3.10	1.80	-
P	223	31	-84.621361	75.6759364	194.00	5.00	6.20	5.60	-
P	223	32	-84.621144	75.6759352	164.00	1.00	2.60	1.80	-
P	223	33	-84.620989	75.6758779	185.00	1.10	2.70	1.90	-
L	223	34	-84.620708	75.6758443	132.00	0.30	2.50	1.40	-
L	223	35	-84.620366	75.6758917	212.00	0.70	2.80	1.75	-

Sampler type*	Sampling Day	Sample Location	GPS Location		Eh	Temperature**			pH
			Longitude	Latitude		B	T	Average	
			—Decimal degrees—			———— °C —————			
P	223	41	-84.591229	75.6666319	295.00	0.50	2.10	1.30	-
P	223	42	-84.591274	75.6666564	0.50	0.10	2.00	1.05	-
L	223	43	-84.590894	75.6667141	187.00	1.20	3.50	2.35	-
L	223	44	-84.590769	75.6667287	162.50	1.00	3.30	2.15	-
L	223	45	-84.590327	75.6667859	170.00	1.40	3.60	2.50	-
P	225	11	-84.622816	75.6812507	211.00	0.70	2.00	1.35	-
P	225	12	-84.622722	75.6812413	207.00	0.30	2.10	1.20	-
L	225	13	-84.622271	75.6812097	149.00	1.20	3.60	2.40	-
L	225	14	-84.622229	75.6811851	183.00	0.70	2.60	1.65	-
L	225	15	-84.621967	75.6811125	182.50	1.20	3.60	2.40	-
L	225	21	-84.64836	75.6804635	167.00	2.00	3.40	2.70	-
P	225	22	-84.647741	75.6804043	268.50	1.10	3.10	2.10	-
L	225	23	-84.647613	75.6803795	200.50	0.30	2.50	1.40	-
L	225	24	-84.647687	75.680357	183.50	0.50	3.10	1.80	-
L	225	25	-84.647399	75.6803239	173.00	1.20	2.70	1.95	-
P	225	31	-84.621361	75.6759364	211.50	2.80	4.10	3.45	-
P	225	32	-84.621144	75.6759352	176.00	1.60	2.80	2.20	-
P	225	33	-84.620989	75.6758779	180.00	1.80	3.20	2.50	-
L	225	34	-84.620708	75.6758443	208.00	1.00	3.30	2.15	-
L	225	35	-84.620366	75.6758917	207.00	2.50	6.20	4.35	-
P	225	41	-84.591229	75.6666319	174.00	0.60	1.30	0.95	-
P	225	42	-84.591274	75.6666564	99.50	2.10	4.50	3.30	-
L	225	43	-84.590894	75.6667141	203.00	1.60	4.00	2.80	-

Sampler type*	Sampling Day	Sample Location	GPS Location		Eh	Temperature**			pH
			Longitude	Latitude		B	T	Average	
			—Decimal degrees—			———— °C —————			
L	225	44	-84.590769	75.6667287	194.00	1.70	5.00	3.35	-
L	225	45	-84.590327	75.6667859	173.50	2.50	5.10	3.80	-

* Sampler type piezometer (P) and lysimeters (L)

** Temperature taken at 20 cm (B) and 10 cm (T)

Table A.2 Summary of results for mercury and organic carbon (DOC/TOC) present in pore water, and methylmercury in soil on Truelove Lowland, Devon Island

Sampler type*	Sampling Day	Sample Location	THg	DHg	pHg	MeHg	DOC	TOC
			-----pM-----			pmol g ⁻¹	-----mg L ⁻¹ -----	
P	207	11	68.25	9.11	59.15	24.60	13.59	15.68
P	207	12	-	12.34	-	3.74	16.23	18.95
L	207	13	110.17	60.97	49.21	24.37	35.21	30.58
L	207	14	156.05	89.59	66.47	64.06	24.21	20.48
L	207	15	-	28.60	-	59.56	22.66	18.04
P	207	21	7.60	7.56	0.04	5.06	10.34	7.54
P	207	22	114.42	4.88	109.53	2.91	14.21	13.44
L	207	23	86.68	77.50	9.18	3.12	25.61	19.76
L	207	24	17.77	18.23	-	2.19	21.61	19.10
L	207	25	65.65	46.71	18.94	3.72	18.62	17.64
P	207	31	228.04	9.67	218.37	8.04	16.54	14.10
P	207	32	-	9.67		3.77	16.28	15.48
P	207	33	183.03	11.40	171.63	-	10.42	8.89
L	207	34	18.47	15.72	2.75	-	12.48	11.03
L	207	35	48.36	33.12	15.24	3.09	20.32	14.19
P	207	41	115.38	-	-	4.36	17.56	19.59
P	207	42	175.94	10.66	165.28	21.57	18.77	18.43
L	207	43	83.19	-	-	3.64	-	-
L	207	44	75.87	59.12	16.75	2.06	45.55	43.88
L	207	45	249.69	251.02	-	3.16	38.29	34.09
P	210	11	21.76	15.95	5.82	19.38	11.32	13.00

Sampler type*	Sampling Day	Sample Location	THg	DHg	pHg	MeHg	DOC	TOC
			—————pM—————			pmol g ⁻¹	—— mg L ⁻¹ ——	
P	210	12	8.26	14.40		13.95	16.96	15.87
L	210	13	97.90	51.38	46.51	21.59	32.60	26.14
L	210	14	79.42	50.84	28.58	24.92	21.91	17.53
L	210	15	35.49	24.35	11.14	16.49	14.30	14.04
P	210	21	7.64	5.32	2.33	1.86	7.38	6.41
P	210	22	-	-	-	3.53	-	-
L	210	23	74.59	53.87	20.73	1.11	27.55	19.12
L	210	24	25.20	20.67	4.53	1.72	20.28	17.46
L	210	25	46.07	36.90	9.17	3.93	18.89	16.40
P	210	31	174.27	9.36	164.91	5.51	14.18	12.46
P	210	32	60.90	9.20	51.70	0.52	13.75	11.81
P	210	33	82.45	6.48	75.97	14.98	11.76	7.62
L	210	34	17.32	17.34	-0.02	6.03	22.09	10.01
L	210	35	29.96	19.51	10.45	21.59	15.28	14.56
P	210	41	-	4.37	-	5.58	17.62	16.53
P	210	42	133.18	8.97	124.20	20.89	18.99	18.16
L	210	43	34.58	25.98	8.59	1.09	45.21	43.06
L	210	44	34.65	-	-	5.94	49.86	46.03
L	210	45	-	-	-	3.62	-	-
P	213	11	-	-	-	28.43	13.05	11.61
P	213	12	7.37	-	-	0.35	15.51	15.21
L	213	13	-	-	-	26.51	32.00	27.12
L	213	14	-	-	-	24.11	20.66	18.42

Sampler type*	Sampling Day	Sample Location	THg	DHg	pHg	MeHg	DOC	TOC
			-----pM-----			pmol g ⁻¹	---- mg L ⁻¹ ----	
L	213	15	-	-	-	18.09	17.67	17.18
L	213	21	-	-	-	2.76	-	-
P	213	22	-	-	-	0.28	-	-
L	213	23	42.40	38.55	3.86	2.50	22.32	22.00
L	213	24	22.43	20.55	1.87	7.57	22.61	20.96
L	213	25	38.67	30.93	7.74	5.15	18.86	20.65
P	213	31	61.43	9.84	51.59	-	14.43	14.84
P	213	32	46.18	11.34	34.84	2.94	14.76	14.70
P	213	33	81.30	10.64	70.65	3.00	11.81	10.57
L	213	34	17.43	14.82	2.61	0.42	13.37	11.30
L	213	35	19.44	19.32	0.12	30.96	17.43	15.83
P	213	41	43.97	5.92	38.05	4.86	17.21	16.38
P	213	42	123.35	7.86	115.49	21.64	19.04	17.84
L	213	43	17.95	13.01	4.94	3.96	49.42	48.79
L	213	44	20.10	17.48	2.63	3.47	54.54	50.95
L	213	45	-	-	-	0.28	-	-
P	216	11	69.89	16.16	53.73	38.917	13.74	11.37
P	216	12	-	10.96	-	2.671	16.40	14.57
L	216	13	36.00	23.72	12.28	-	35.04	30.14
L	216	14	49.92	-	-	47.220	24.66	19.76
L	216	15	28.77	21.49	7.27	5.299	23.38	19.73
L	216	21	76.43	58.21	18.22	0.478	15.37	10.73
P	216	22	-	-	-	2.308	-	-

Sampler type*	Sampling Day	Sample Location	THg	DHg	pHg	MeHg	DOC	TOC
			—————pM—————			pmol g ⁻¹	—— mg L ⁻¹ ——	
L	216	23	43.38	40.62	2.75	0.292	27.28	27.75
L	216	24	29.40	22.57	6.83	1.950	28.38	26.60
L	216	25		25.78		0.873	28.20	23.52
P	216	31	49.03	9.73	39.30	8.367	13.89	13.00
P	216	32	57.07	9.13	47.94	7.379	15.92	15.00
P	216	33	45.71	8.85	36.86	15.835	12.76	7.34
L	216	34	19.54	16.13	3.41	2.524	16.82	14.28
L	216	35	-	-	-	-	-	-
P	216	41	12.15	-	-	0.508	19.46	15.53
P	216	42	111.75	12.29	99.46	5.077	19.08	18.24
L	216	43	-	-	-	2.201	-	-
L	216	44	18.91	-	-	0.820	59.62	55.11
L	216	45	134.13	16.43	117.70	2.054	-	-
P	219	11	36.66	10.86	25.80	62.267	12.32	12.31
P	219	12	105.08	34.13	70.95	3.581	14.30	12.33
L	219	13	94.02	-	-	14.825	35.34	30.06
L	219	14	68.15	50.78	17.36	16.799	23.94	21.76
L	219	15	-	-	-	7.340	-	-
L	219	21	41.72	21.59	20.13	0.270	10.77	7.06
P	219	22	-	-	-	1.532	-	-
L	219	23	-	51.68	-	1.149	29.49	30.85
L	219	24	42.95	29.24	13.71	1.554	31.70	-
L	219	25	67.74	26.46	41.28	2.052	22.54	22.74

Sampler type*	Sampling Day	Sample Location	THg	DHg	pHg	MeHg	DOC	TOC
			—————pM—————			pmol g ⁻¹	—— mg L ⁻¹ ——	
P	219	31	215.52	3.34	212.19	0.703	18.11	13.59
P	219	32	92.89	-	-	0.497	14.40	14.16
P	219	33	81.53	9.90	71.63	0.411	11.92	9.91
L	219	34	24.57	15.93	8.64	0.523	17.36	13.83
L	219	35	31.80	27.03	4.77	3.990	15.91	15.53
P	219	41	75.45	2.99	72.46	3.801	19.42	16.02
P	219	42	56.55	15.93	40.61	18.897	20.20	18.92
L	219	43	-	36.62	-	1.744	58.96	54.27
L	219	44	-	28.62	-	2.632	62.49	59.93
L	219	45	-	-	-	1.380	-	-
P	221	11	52.45	13.66	38.78	6.360	12.22	11.77
P	221	12	13.12	14.14		0.434	14.56	11.42
L	221	13	42.65	32.39	10.26	18.766	32.00	29.55
L	221	14	52.75	33.03	19.72	4.485	22.83	20.41
L	221	15	52.79	25.12	27.67	9.225	18.40	17.48
L	221	21	20.69	13.33	7.37	0.297	10.27	7.70
P	221	22	-	-	-	0.269	-	-
L	221	23	60.28	54.55	5.73	1.542	30.41	29.96
L	221	24	-	-	-	4.851	-	-
L	221	25	40.92	28.00	12.92	0.305	22.49	22.22
P	221	31	117.80	7.48	110.32	0.690	14.37	12.92
P	221	32	50.90	6.56	44.33	2.206	13.68	14.20
P	221	33	37.95	-	-	6.854	11.02	11.77

Sampler type*	Sampling Day	Sample Location	THg	DHg	pHg	MeHg	DOC	TOC
			—————pM—————			pmol g ⁻¹	—— mg L ⁻¹ ——	
L	221	34	20.48	19.13	1.35	5.877	18.72	15.30
L	221	35	27.21	18.11	9.11	6.458	19.85	18.58
P	221	41	32.89	7.23	25.67	20.697	17.41	15.43
P	221	42	-	16.98	-	63.871	20.90	19.97
L	221	43	20.03	13.52	6.52	6.894	60.28	59.09
L	221	44	22.33	16.11	6.22	6.752	66.75	67.52
L	221	45	-	-	-	3.646	-	-
P	223	11	57.38	20.06	37.32	6.392	12.23	12.14
P	223	12	39.10	10.73	28.36	3.591	13.38	11.75
L	223	13	22.12	40.60	-	3.111	32.43	29.29
L	223	14	69.86	35.65	34.21	8.253	23.77	22.04
L	223	15	51.15	28.30	22.85	6.940	20.87	22.65
L	223	21	24.69	10.36	14.34	0.280	6.85	5.94
P	223	22	-	-	-	0.261	-	-
L	223	23	68.68	42.79	25.89	0.230	30.83	28.12
L	223	24	42.17	30.78	11.39	1.552	30.40	27.38
L	223	25	30.69	21.29	9.40	1.794	23.47	22.76
P	223	31	237.73	11.90	225.83	3.515	13.04	12.71
P	223	32	42.68	5.59	37.08	0.390	15.41	11.80
P	223	33	65.26	10.47	54.79	0.445	11.20	9.41
L	223	34	-	-	-	16.176	20.30	15.20
L	223	35	28.18	16.87	11.31	5.897	19.58	1.21
P	223	41	24.25	5.22	19.03	4.608	18.51	17.35
P	223	42	61.92	11.21	50.71	3.696	21.60	20.20

Sampler type*	Sampling Day	Sample Location	THg	DHg	pHg	MeHg	DOC	TOC
			-----pM-----			pmol g ⁻¹	---- mg L ⁻¹ ----	
L	223	43	17.59	14.82	2.77	1.780	58.88	55.27
L	223	44	22.90	18.50	4.40	0.223	64.60	66.27
L	223	45	194.99	161.58	33.41	1.362	62.11	62.98
P	225	11	86.28	13.77	72.51	-	9.60	8.46
P	225	12	-	9.52	-	-	11.49	9.06
L	225	13	49.80	27.97	21.82	-	27.31	24.66
L	225	14	50.48	44.03	6.45	-	21.80	19.47
L	225	15	35.55	-	-	-	20.87	20.84
L	225	21	16.42	14.59	1.83	-	9.41	7.24
P	225	22	-	-	-	-	-	-
L	225	23	44.19	42.09	2.10	-	31.46	29.19
L	225	24	-	-	-	-	-	-
L	225	25	27.00	34.22	-	-	24.27	21.72
P	225	31	128.28	19.76	108.52	-	14.28	13.38
P	225	32	39.36	20.07	19.28	-	15.12	13.31
P	225	33	63.83	22.94	40.88	-	12.46	10.85
L	225	34	21.08	20.61	0.46	-	15.40	13.51
L	225	35	22.41	23.29	-	-	15.60	15.76
P	225	41	5.69	20.53	-	-	16.71	16.59
P	225	42	66.13	28.99	37.14	-	25.94	23.53
L	225	43	14.68	14.31	0.37	-	55.99	55.16
L	225	44	11.92	16.76	-	-	-	61.68
L	225	45	-	-	-	-	-	-

* Sampler types piezometer (P) and lysimeters (L)

Table A.3. Summary of results for cations and anions measured in soil pore water on Truelove Lowland, Devon Island, Canada.

Sampler type*	Sampling Day	Sample Location	Ca ⁺²	K ⁺	Mg ⁺²	Na ⁺	Cl ⁻	SO ₄ ⁻²	ΣS ⁻²	Fe ²⁺	Fe ³⁺
-----µM-----											
P	207	11	117	11.8	180	284	279	1.5	-	0	58
P	207	12	94	21.0	131	211	617	1.5	-	81	308
L	207	13	-	-	-	-	606	6.1	-	155	100
L	207	14	705	121.0	846	1853	477	10.3	-	138	-
L	207	15	480	104.1	499	2409	416	22.0	-	12	-
P	207	21	174	7.4	270	273	-	-	-	10	90
P	207	22	117	3.0	175	182	-	-	-	0	26
L	207	23	68	37.0	110	591	-	-	-	-	-
L	207	24	241	124.3	327	1555	-	-	-	49	18
L	207	25	224	81.4	290	1223	-	-	-	-	-
P	207	31	558	27.5	525	612	332	13.7	-	-	202
P	207	32	161	15.0	156	388	406	27.7	-	104	330
P	207	33	147	0.0	169	130	322	8.9	-	68	217
L	207	34	305	76.4	316	689	421	62.8	-	-	-
L	207	35	743	66.7	588	877	317	12.9	-	155	0
P	207	41	344	25.2	302	283	237	5.3	-	5	190
P	207	42	899	301.8	832	-	270	1.5	4.2	109	304
L	207	43	287	2.9	267	216	-	-	-	-	-
L	207	44	186	9.1	170	203	483	19.2	-	95	0
L	207	45	683	66.8	524	847	810	62.9	-	-	72
P	210	11	560	33.5	811	419	71	1.5	-	56	80

Sampler type*	Sampling Day	Sample Location	Ca ⁺²	K ⁺	Mg ⁺²	Na ⁺	Cl ⁻	SO ₄ ⁻²	ΣS ⁻²	Fe ²⁺	Fe ³⁺
-----μM-----											
P	210	12	826	17.3	1049	577	250	1.5	-	56	68
L	210	13	1312	76.4	1570	741	286	2.9	-	47	219
L	210	14	1206	87.3	1428	763	365	1.5	-	107	323
L	210	15	963	42.7	1011	763	207	6.7	-	10	160
P	210	21	581	31.3	829	509	294	1.5	-	29	51
P	210	22	-	-	-	-	-	-	-	-	-
L	210	23	297	81.0	449	508	281	2.0	-	9	90
L	210	24	372	52.5	572	714	572	4.8	-	42	109
L	210	25	411	41.6	592	783	618	7.1	-	29	131
P	210	31	1037	7.0	996	456	449	2.9	-	13	138
P	210	32	979	11.1	931	480	472	1.5	4.8	26	153
P	210	33	701	12.4	767	468	2705	1.5	-	212	338
L	210	34	920	28.6	1044	544	271	2.3	-	164	63
L	210	35	889	33.7	711	450	261	1.5	-	182	129
P	210	41	1092	19.5	974	420	277	4.8	3.6	21	61
P	210	42	758	25.9	696	305	211	1.5	-	25	160
L	210	43	1093	45.8	908	548	243	1.5	-	163	184
L	210	44	1123	76.8	964	486	304	1.5	-	196	89
L	210	45	-	-	-	-	-	-	-	-	-
P	213	11	1039	22.3	1444	611	197	1.5	-	128	152
P	213	12	610	34.2	756	414	164	1.5	8.1	56	115
L	213	13	1102	39.0	1327	501	268	1.5	5.4	26	485
L	213	14	1556	74.0	-	1302	322	1.5	-	105	386

Sampler type*	Sampling Day	Sample Location	Ca ⁺²	K ⁺	Mg ⁺²	Na ⁺	Cl ⁻	SO ₄ ⁻²	ΣS ⁻²	Fe ²⁺	Fe ³⁺
-----μM-----											
L	216	23	421	35.4	637	627	167	1.5	-	26	213
L	216	24	324	31.2	506	584	215	1.5	-	91	117
L	216	25	337	20.2	480	651	230	1.5	-	51	159
P	216	31	847	8.1	816	436	182	2.9	-	3	56
P	216	32	997	32.0	911	536	251	3.6	2.8	31	112
P	216	33	665	12.9	701	397	207	4.2	3.1	154	242
L	216	34	809	16.3	877	-	182	1.5	-	110	145
L	216	35	-	-	-	-	-	-	-	-	-
P	216	41	919	25.5	901	333	140	1.5	2.9	25	49
P	216	42	959	18.5	924	558	91	3.1	3.3	43	188
L	216	43	-	-	-	-	-	-	-	-	-
L	216	44	1210	15.1	1075	579	175	1.5	-	127	174
L	216	45	-	-	-	-	-	-	-	0	219
P	219	11	779	22.3	1175	649	453	1.5	-	7	24
P	219	12	823	29.7	1168	658	416	1.5	4.8	20	61
L	219	13	1175	38.4	1415	675	228	1.5	4.9	82	381
L	219	14	1148	43.1	1421	810	456	1.5		105	392
L	219	15	-	-	-	-	-	1.5	-	-	-
L	219	21	693	36.7	1029	601	315	16.7	-	0	197
P	219	22	-	-	-	-	-	-	-	-	-
L	219	23	504	18.0	707	721	321	1.5	-	0	354
L	219	24	358	23.8	558	571	316	1.5	-	69	175
L	219	25	408	20.5	606	782	409	1.5	-	40	122

Sampler type*	Sampling Day	Sample Location	Ca ⁺²	K ⁺	Mg ⁺²	Na ⁺	Cl ⁻	SO ₄ ⁻²	ΣS ⁻²	Fe ²⁺	Fe ³⁺
-----μM-----											
P	219	31	927	9.4	901	463	456	4.0	-	84	236
P	219	32	996	123.2	898	639	418	5.7	-	17	83
P	219	33	728	6.8	812	417	364	5.7	-	173	193
L	219	34	757	23.6	878	430	210	1.5	-	151	223
L	219	35	1108	28.3	868	464	353	1.5	-	177	151
P	219	41	-	-	-	-	253	9.5	4.0	35	58
P	219	42	1023	8.1	921	447	215	3.6	-	43	73
L	219	43	1139	56.6	960	552	119	1.5	-	84	201
L	219	44	1633	17.5	1400	706	275	1.5	-	151	201
L	219	45	-	-	-	-	-	-	2.9	-	-
P	221	11	768	9.1	1129	508	355	1.5	-	7	54
P	221	12	830	14.7	1087	548	394	1.5	6.0	50	54
L	221	13	1122	82.4	1337	617	236	1.5	5.0	115	242
L	221	14	773	23.5	929	484	349	1.5	-	111	208
L	221	15	698	43.4	691	381	76	1.5	-	5	232
L	221	21	566	20.4	812	569	231	1.5	7.1	4	94
P	221	22	-	-	-	-	-	1.5	-	-	-
L	221	23	492	19.3	691	642	78	1.5	-	48	250
L	221	24	-	-	-	-	-	-	-	-	-
L	221	25	364	9.8	535	601	288	1.5	-	60	180
P	221	31	1010	10.0	973	489	326	1.5	-	2	45
P	221	32	935	16.2	887	466	419	1.5	-	16	51
P	221	33	862	48.7	936	557	360	2.2	-	78	69

Sampler type*	Sampling Day	Sample Location	Ca ⁺²	K ⁺	Mg ⁺²	Na ⁺	Cl ⁻	SO ₄ ⁻²	ΣS ⁻²	Fe ²⁺	Fe ³⁺
-----μM-----											
L	221	34	732	18.5	831	379	156	1.5	-	150	343
L	221	35	1219	8.9	950	483	339	1.5	-	188	164
P	221	41	1042	19.3	967	390	250	3.9	3.9	28	38
P	221	42	955	10.9	870	371	248	4.6	-	38	55
L	221	43	1207	20.9	1015	545	158	1.5	-	163	221
L	221	44	1742	12.1	1511	645	195	1.5	-	129	217
L	221	45	-	-	-	-	-	-	-	-	-
P	223	11	847	8.7	1226	606	517	1.5		12	36
P	223	12	830	4.3	1059	525	519	1.5	5.1	92	59
L	223	13	1073	37.9	1251	595	180	1.5	5.2	112	248
L	223	14	795	22.8	962	561	516	1.5	-	122	156
L	223	15	840	16.1	826	417	221	1.5	-	105	265
L	223	21	780	16.6	1161	858	221	1.5	8.9	4	96
P	223	22	-	-	-	-	-	-	-	-	-
L	223	23	494	8.5	689	652	75	1.5	-	44	30
L	223	24	404	6.5	650	664	331	1.5	-	151	179
L	223	25	482	94.8	686	775	335	1.5	-	78	146
P	223	31	899	0.0	890	426	367	1.5	-	0	35
P	223	32	1201	0.0	1170	612	403	1.5	-	39	63
P	223	33	780	0.0	895	445	354	1.5	-	138	32
L	223	34	696	12.8	755	419	242	1.5	-	141	206
L	223	35	1182	6.3	941	494	383	1.5	-	162	179
P	223	41	527	3.8	512	198	251	1.5	2.8	21	25

Sampler type*	Sampling Day	Sample Location	Ca ⁺²	K ⁺	Mg ⁺²	Na ⁺	Cl ⁻	SO ₄ ⁻²	ΣS ⁻²	Fe ²⁺	Fe ³⁺
-----μM-----											
P	223	42	454	7.2	432	194	223	1.5	-	45	35
L	223	43	1280	64.9	1183	613	214	1.5	-	131	98
L	223	44	572	0.0	472	264	211	1.5	-	135	148
L	223	45	1384	14.1	1241	545	252	1.5	-	70	156
P	225	11	821	35.0	1171	560	539	10.9	-	0	26
P	225	12	863	13.6	1120	601	560	5.7	4.6	50	60
L	225	13	1144	36.2	1281	565	245	1.5	5.7	73	97
L	225	14	1244	99.5	1470	781	487	1.5	-	77	144
L	225	15	1062	143.2	1036	644	295	1.5	-	128	162
L	225	21	849	51.7	1179	902	474	1.5	11.6	9	74
P	225	22	-	-	-	-	-	-	-	-	-
L	225	23	312	91.7	397	419	269	12.5	-	40	273
L	225	24	283	29.6	394	393	-	-	-	59	178
L	225	25	496	24.2	689	734	356	1.5	3.1	83	141
P	225	31	1605	13.7	1511	616	715	108.6	-	0	41
P	225	32	917	12.2	849	371	793	120.4	-	2	34
P	225	33	676	12.7	689	364	397	6.4	-	50	121
L	225	34	727	38.2	755	404	137	1.5	-	117	104
L	225	35	1401	16.0	1042	523	345	1.5	-	153	304
P	225	41	1093	14.2	931	402	204	2.5	-	13	38
P	225	42	747	8.0	645	310	282	4.8	2.8	12	34
L	225	43	1378	21.1	1147	535	193	1.5	-	121	176
L	225	44	1509	64.4	1220	583	238	1.5	-	145	268

Sampler type*	Sampling Day	Sample Location	Ca ⁺²	K ⁺	Mg ⁺²	Na ⁺	Cl ⁻	SO ₄ ⁻²	ΣS ⁻²	Fe ²⁺	Fe ³⁺
			-----μM-----								
L	225	45	-	-	-	-	-	-	-	-	-
L	225	44	1509	64.4	1220	583	238	1.5	-	145	268
L	225	45	-	-	-	-	-	-	-	-	-

* Sampler types piezometer (P) and lysimeters (L)

APPENDIX B. QUALITY ASSURANCE/QUALITY CONTROL RESULTS FOR SELECTED ANALYSIS

Table B.1. Field blanks and MDL results for mercury analysis in porewater

Blank Type	Calendar Day	Concentration	Average Concentration
		-----pM-----	
Field	216	3.983	7.572
	219	6.018	
	219	6.053	
	219	5.394	
	221	4.684	
	223	10.725	
	223	13.675	
	225	10.045	
Field Lab*	216	3.265	4.791
	219	4.048	
	219	2.759	
	221	3.809	
	221	3.62	
	223	10.101	
	223	6.174	
	225	4.750	
	225	4.590	
Sample type	Measured Concentration	Stdev	MDL
		-----pM-----	
Spike 0.2 ppt	1.964	0.362	1.137
	1.406		
	1.170		
	1.488		
	1.509		
	2.242		
	1.676		

* Field lab refers to blanks that remained at base camp

Table B.2. Recovery and percent deviation of duplicate results for pore water mercury analysis.

Sample	Actual Concentration	Recovery	Deviation of Duplicates
	pM	—————%—————	
115 THg S1	87.817		7.7
115 THg S2	94.874		
215 THgNS	68.399	103.7	
215 THg S	120.099		
313 DHg NS	14.176	112.5	
313 DHg S	70.269		
411 DHg S1	78.605		1.1
411 DHg S2	77.758		
325 Dhg NS	22.284	115.3	
325 DHg S	79.756		
421 Hg S1	115.225		2.5
421 Hg S2	118.142		
424 DHg S1	90.166		3.4
424 DHg S2	87.122		
144 DHg S1	75.0676		8.1
144 DHg S2	81.383		
245 THg S1	78.412		1.1
245 THg S2	77.565		
342 THg NS	59.819	96.2	
342 THg S	107.770		
442 DHg NS	15.061	100.1	
442 DHg S	64.949		
164 THgNS	52.727	86.5	
164 THg S	95.853		
364 DHgNS	19.118	95.8	
364 DHg S	66.895		
462 THg S1	123.026		2.6
462 THgS2	119.847		
173 Hg NS	24.891	98.6	
173 Hg S	270.549		
182 THg S1	321.925		5.4
182 THg S2	339.736		
185 DHg S1	279.407		7.8
185 DHg S2	258.373		
275 DHg NS	24.059	98.0	
275 DHg S	268.235		

Sample	Actual Concentration	Recovery	Deviation of Duplicates
	pM	-----%	
374 THg S1	274.446		
374 THg S2	271.622		1.0
382 THgNS	42.118		
382 THg S	303.463	104.8	
484 DHg NS	19.537		
484 DHg S	255.594	94.7	
Average		100.6	4.1

* Deviation of duplicates calculated as $[200\% * (S1 - S2)] / (S1 + S2)$, S1 and S2 represent matrix spike duplicates

** NS represents unspiked samples, S represents spiked samples

*** Three digit number represents sample code

**** THg samples were not filtered, DHg samples were filtered

Table B.3. Quality assurance and control results from MeHg extractions and analyses.

Sample	Concentration wet weight	Recovery	Sample	Concentration wet weight	Deviation of Duplicates
	pmol g ⁻¹	%		pmol g ⁻¹	%
115	1241.9	41.7	215	90.4	8.0
115S	1372.1		215	83.5	
415	94.6		315	59.7	
415S	427.0	67.8	315	97.4	48.0
225	100.1		125	685.3	
225S	450.3		125	689.7	
421	115.5	98.2	135	137.9	36.3
421S	604.6		135	95.5	
235	156.9		335	178.6	
235S	572.3	84.0	335	240.8	29.6
435	Undetectable		145	220.8	
435S	318.7		145	302.6	
245	28.6	62.9	155	247.1	55.6
245S	340.7		155	437.2	
445	86.2		355	137.0	
445S	486.2	80.4	355	190.5	32.7
255	74.7		165	240.9	
255S	582.3		165	240.4	
455	59.0	56.5	365	173.0	5.2
455S	337.6		365	164.2	
265	Undetectable		175	181.2	
265S	353.8	70.8	175	112.2	47.0
475	66.3		375	49.8	
475S	393.3		375	45.6	
Average		74.8	Average		25.3

*Spike is equivalent to approximately 500 pg g⁻¹ wet weight

** Deviation of duplicates calculated as 200%* (S1 – S2)/(S1+S2)

Table B.4. Method detection limit based on a spike into mineral WSM soil

Sample type	Measured Concentration	MDL	Recovery
	-----pmol g ⁻¹ -----		%
	0.26		114.3
	0.30		128.2
	0.24		102.1
Spike 0.23 pmol	0.28		118.6
g ⁻¹ into mineral	0.31	0.09	131.9
wet sedge	0.23		97.6
meadow soil	0.22		95.4
	0.29		123.2
	0.27		118.2

*MeHg in mineral soil was undetectable

Table B.5. Precision of dissolved organic carbon analyzer

Sample Code	Sample Type	Concentration	Deviation of Duplicates
		mg L ⁻¹	%
322	DOC	13.06	9.91
322	DOC	14.43	
344	DOC	16.92	1.21
344	DOC	16.71	
352	DOC	14.29	1.49
352	DOC	14.51	
181	TOC	8.43	0.72
181	TOC	8.49	
385	DOC	15.51	1.15
385	DOC	15.69	
482	TOC	22.97	4.72
482	TOC	24.08	
164	TOC	20.40	0.12
164	TOC	20.42	
432	DOC	19.32	2.98
432	DOC	18.76	
235	DOC	19.02	1.66
235	DOC	18.70	
422	TOC	18.10	0.65
422	TOC	18.22	
441	TOC	15.27	3.36
441	TOC	15.79	
153	TOC	30.06	0.03
153	TOC	30.05	
251	TOC	6.75	8.95
251	TOC	7.38	
454	TOC	59.75	0.62
454	TOC	60.12	
285	TOC	21.95	2.10
285	TOC	21.50	
142	DOC	16.36	0.48
142	DOC	16.44	
274	TOC	27.72	2.53
274	TOC	27.03	
373	TOC	9.35	1.32
373	TOC	9.48	
461	TOC	14.53	11.60
461	TOC	16.32	

Table B.6. Precision of AA cation analysis

Sample ID	Analyte				Percent deviation of duplicates			
	Ca ⁺²	K ⁺	Mg ⁺²	Na ⁺	Ca ⁺²	K ⁺	Mg ⁺²	Na ⁺
	-----μM-----				-----%-----			
114	736	127	858	1969				
114	675	115	834	1737	8.72	9.36	2.76	12.52
115	504	109	519	2409				
115	456	99	478	-	9.89	9.58	8.13	
215	242	87	301	1298				
215	206	76	280	1149	15.88	13.07	7.14	12.13
315	862	71	675	968				
315	623	63	501	787	32.11	12.07	29.56	20.63
424	1115	77	964	485				
424	1131	76	964	487	1.38	0.76	0.01	0.40
235	181	19	257	336				
235	171	26	258	342	5.42	32.04	0.49	1.73
431	742	16	640	237				
431	684	9	597	221	8.24	63.16	6.90	6.91
431	773	22	686	271				
434	1121	30	943	427				
434	1112	29	945	426	0.76	0.69	0.16	0.12
154	1199	43	1411	808				
154	1098	43	1430	812	8.75	0.53	1.32	0.50
255	410	20	604	777				
255	407	21	608	787	0.72	1.21	0.63	1.26
355	1106	28	864	461				
355	1110	28	873	467	0.42	0.69	1.03	1.45
453	1155	58	973	560				
453	1122	56	946	543	2.91	3.48	2.85	3.22
265	363	10	535	602				
265	364	10	534	600	0.28	0.34	0.20	0.29
464	1771	12	1501	644				
464	1712	13	1521	647	3.38	7.60	1.32	0.48
175	833	16	824	416				
175	846	16	829	418	1.52	4.28	0.57	0.51
375	1204	6	949	499				
375	1160	6	933	490	3.76	3.76	1.65	1.82
285	496	25	692	736				
285	496	24	686	732	0.08	3.75	0.86	0.52
484	1471	64	1216	584				
484	1546	64	1225	581	4.94	0.11	0.72	0.51
Average					6.06	9.25	3.68	3.82

Table B.7. Precision of capillary electrophoresis for anion analysis

Sample ID	Analyte		Percent deviation of duplicates	
	Cl ⁻	SO ₄ ⁻²	Cl ⁻	SO ₄ ⁻²
	—μM—		———%———	
312	301	17	51.88	76.65
312	511	38		
225	614	8	1.30	32.88
225	622	6		
424	258		21.30	
424	319			
235	136		3.90	
235	142			
434	264		5.73	
434	250			
245	230		0.35	
245	229			
444	188		11.23	
444	168			
255	406		2.03	
255	414			
454	276		1.11	
454	273			
265	288		1.50	
265	284			
464	198		2.38	
464	193			
275	345		4.39	
275	330			
475	242		6.03	
475	257			
285	354		0.97	
285	357			
484	242		2.79	
484	236			
Average			7.79	54.76

Table B.8. Detection limit of capillary electrophoresis for detection of anions in water samples.

Parameter	Cl ⁻	SO ₄ ⁻²	NO ₃ ⁻
	-----μM-----		
	29.9	6.6	4.9
	35.2	6.1	8.5
Actual Concentration	36.5	4.8	12.0
	38.3	4.9	12.0
	40.6	6.1	11.3
	36.0	7.0	9.2
Std	3.6	0.9	2.7
MDL	12.1	3.0	9.2

APPENDIX C. EQUILIBRIUM CONSTANTS USED IN SPECIATION CALCULATIONS

Mass action equation	Log K	Source
$\text{HgS}_{(\text{s, cinn})} + \text{H}^+ = \text{Hg}^{2+} + \text{HS}^-$	-39.1 (I=0.0)	NIST (2003)
$\text{HgS}_{(\text{s, cinn})} + \text{HS}^- = \text{HgS}_2^{2-} + \text{H}^+$	-13.0 (I=0.3)	Jay et al. (2000)
$\text{HgS}_{(\text{s, cinn})} + \text{HS}^- = \text{HgS}_2\text{H}^-$	-4.5 (I=0.3)	Jay et al. (2000)
$\text{HgS}_{(\text{s, cinn})} + \text{HS}^- + \text{H}^+ = \text{Hg}(\text{SH})_2$	1.0 (I=0.3)	Jay et al. (2000)
$\text{HgS}_{(\text{s, cinn})} = \text{HgS}_{(\text{aq})}$	-9.3 (I=0.3)	Jay et al. (2000)
* Reproduced from Goulet et al. (2007)		

APPENDIX D. RESULTS FROM MICROCOSM EXPERIMENT

Table D.1 Gas sampling data from microcosm experiment corrected to room temperature

Treatment	Day Sampled	CH ₄	CO ₂	N ₂ O
nmol g ⁻¹				
Natural	10	0.243	237.307	0.057
Natural	10	0.190	269.761	0.057
Natural	10	0.094	301.326	0.053
Natural	10	0.272	199.156	0.055
Natural	40	0.721	316.450	0.183
Natural	40	0.287	320.243	0.136
Natural	40	0.366	302.781	0.132
Natural	40	0.314	242.504	0.119
Natural	45	0.463	1566.215	0.110
Natural	45	0.396	1558.889	0.067
Natural	45	0.236	1736.329	0.025
Natural	45	0.385	1605.584	0.071
Natural	50	0.384	2789.953	0.051
Natural	50	0.499	2952.804	0.046
Natural	50	0.325	3200.129	0.057
Natural	50	0.513	2842.500	0.061
Natural	70	0.381	6536.657	0.097
Natural	70	0.329	7373.556	0.058
Natural	70	2.236	6183.912	0.022
Natural	70	0.168	6428.892	0.063
Natural	99	2.965	11384.530	0.268
Natural	99	-	-	-
Natural	99	0.651	9884.531	0.116
Natural	99	3.984	8764.779	0.044
Natural	99	19.975	8969.786	0.031
Spike	10	0.035	184.747	0.282
Spike	10	0.088	145.653	0.335
Spike	10	0.205	178.869	0.201
Spike	10	0.299	170.010	0.348
Spike	40	0.247	205.168	0.258
Spike	40	0.116	224.393	1.063
Spike	40	0.171	286.982	0.709
Spike	40	0.126	233.714	0.385
Spike	45	0.233	1526.948	0.102
Spike	45	0.138	1704.051	0.278

Treatment	Day Sampled	CH ₄	CO ₂	N ₂ O
		-----nmol g ⁻¹ -----		
Spike	45	0.094	1771.837	0.532
Spike	45	0.242	1564.163	0.429
Spike	50	0.451	3109.476	0.083
Spike	50	0.637	3072.295	0.088
Spike	50	0.485	3032.321	0.167
Spike	50	0.596	3388.760	0.085
Spike	70	0.096	6779.193	0.145
Spike	70	1.356	6147.390	0.038
Spike	70	0.141	5179.583	0.079
Spike	70	0.200	6769.369	0.080
Spike	99	0.137	8567.738	0.735
Spike	99	1.584	6331.115	0.053
Spike	99	0.136	8340.976	0.907
Spike	99	0.250	7818.057	0.188
Sterile	10	1.011	3624.633	0.060
Sterile	10	1.379	1031.108	0.182
Sterile	10	1.162	683.195	0.144
Sterile	10	1.380	638.120	0.114
Sterile	40	1.160	1293.207	0.179
Sterile	40	1.638	1312.867	0.088
Sterile	40	0.976	1300.992	0.141
Sterile	40	1.060	604.991	0.104
Sterile	45	1.279	4028.870	0.108
Sterile	45	0.998	4056.229	0.175
Sterile	45	1.057	977.292	0.249
Sterile	45	1.429	934.234	0.255
Sterile	50	2.090	4855.099	0.171
Sterile	50	2.267	1988.647	0.180
Sterile	50	2.463	1626.517	0.254
Sterile	50	3.334	1581.367	0.129
Sterile	70	3.138	3756.102	0.205
Sterile	70	2.993	4273.062	0.150
Sterile	70	2.057	3321.989	0.227
Sterile	70	1.524	2331.846	0.127
Sterile	99	1.951	4210.816	0.165
Sterile	99	4.486	4082.479	0.057
Sterile	99	2.415	3633.433	0.325

* Gas samples corrected to room temperature using the combined gas law

** Gas samples corrected to molar concentrations using ideal gas law

Table D.2 MeHg concentration in soil and porewater data from microcosm experiment. Absorbance of filtered porewater is unitless.

Treatment	Day Sampled	MeHg pmol g ⁻¹	Cl ⁻ ——uM——	SO ₄ ⁻²	Absorbance 420 nmol
Natural	0	5.11	-	-	-
Natural	0	5.63	-	-	-
Natural	0	6.20	-	-	-
Natural	0	3.99	-	-	-
Natural	10	8.83	-	-	-
Natural	10	5.79	-	-	-
Natural	10	6.97	-	-	-
Natural	10	7.15	-	-	-
Natural	40	5.41	-	-	-
Natural	40	5.00	-	-	-
Natural	40	5.50	-	-	-
Natural	40	5.65	-	-	-
Natural	45	6.05	389.5	646.0	0.08
Natural	45	5.18	408.9	681.1	0.07
Natural	45	4.82	928.4	796.2	0.08
Natural	45	4.64	352.1	559.1	0.09
Natural	50	4.84	357.6	635.4	0.15
Natural	50	6.65	370.1	637.4	0.08
Natural	50	5.23	382.1	695.3	0.13
Natural	50	6.17	399.1	705.5	0.09
Natural	70	5.80	368.6	633.3	0.16
Natural	70	6.92	367.8	619.1	0.22
Natural	70	8.01	376.3	734.6	0.11
Natural	70	5.87	355.9	668.0	0.14
Natural	99	9.90	353.3	0	0.27
Natural	99	8.07	393.4	433.9	0.24
Natural	99	9.33	381.8	180.1	0.51
Natural	99	8.34	421.2	390.2	0.34
Natural	99	8.32	545.5	164.9	0.29
Spike	0	5.11	-	-	-
Spike	0	5.63	-	-	-
Spike	0	6.20	-	-	-
Spike	0	3.99	-	-	-
Spike	10	6.33	-	-	-
Spike	10	5.99	-	-	-

Treatment	Day Sampled	MeHg pmol g ⁻¹	Cl ⁻ ——uM——	SO ₄ ⁻²	Absorbance 420 nmol
Spike	10	6.80	-	-	-
Spike	10	4.75	-	-	-
Spike	40	4.92	-	-	-
Spike	40	4.49	-	-	-
Spike	40	4.48	-	-	-
Spike	40	6.80	-	-	-
Spike	45	5.18	663.1	723.1	0.04
Spike	45	9.75	801.7	693.9	0.05
Spike	45	6.09	361.5	591.4	0.05
Spike	45	8.68	700.2	742.6	0.05
Spike	50	10.42	391.3	750.1	0.09
Spike	50	10.19	389.9	700.3	0.07
Spike	50	13.63	378.7	725.5	0.09
Spike	50	9.72	377.9	697.6	0.1
Spike	70	34.59	378.6	725.3	0.16
Spike	70	32.03	435.7	904.4	0.09
Spike	70	17.99	446.5	955.6	0.12
Spike	70	15.14	393.1	731.2	0.09
Spike	99	44.68	425.9	730.9	0.18
Spike	99	45.39	383.0	876.8	0.27
Spike	99	52.09	449.4	848.6	0.1
Spike	99	51.66	419.2	768.4	0.19
Sterile	0	5.36	-	-	-
Sterile	0	5.01	-	-	-
Sterile	0	6.89	-	-	-
Sterile	0	6.03	-	-	-
Sterile	10	5.04	-	-	-
Sterile	10	5.24	-	-	-
Sterile	10	6.20	-	-	-
Sterile	10	5.38	-	-	-
Sterile	40	6.25	-	-	-
Sterile	40	6.39	-	-	-
Sterile	40	4.17	-	-	-
Sterile	40	6.46	-	-	-
Sterile	45	4.56	537.7	1492.2	0.42
Sterile	45	5.11	525.4	1268.8	0.59
Sterile	45	4.77	781.3	1287.8	0.41
Sterile	45	6.92	590.3	1430.1	0.42
Sterile	50	4.67	545.9	1528.6	0.38

Treatment	Day Sampled	MeHg pmol g ⁻¹	Cl ⁻ ——uM——	SO ₄ ⁻²	Absorbance 420 nmol
Sterile	50	6.00	515.7	1472.1	0.42
Sterile	50	6.13	534.7	1473.8	0.41
Sterile	50	6.49	555.1	1577.6	0.37
Sterile	70	4.40	515.0	1548.6	0.49
Sterile	70	8.36	573.2	1601.5	0.49
Sterile	70	5.15	594.8	1682.3	0.46
Sterile	70	4.70	500.0	1453.1	0.44
Sterile	99	5.35	541.2	1532.2	0.53
Sterile	99	5.34	668.9	1553.6	0.43
Sterile	99	6.85	511.0	1399.5	0.46

Table D.3. Soil water extractable mercury and oxalate extractable iron.

Treatment	Day Sampled	Oxalate	Water Extractable
		Extractable Iron	Mercury
		$\mu\text{mol g}^{-1}$	pmol g^{-1}
Natural	10	228	2.38
Natural	10	227	3.11
Natural	10	209	3.76
Natural	10	204	3.37
Natural	40	215	4.55
Natural	40	251	3.44
Natural	40	190	3.86
Natural	40	147	2.97
Natural	45	200	3.07
Natural	45	159	3.83
Natural	45	209	5.08
Natural	45	191	3.41
Natural	50	205	3.37
Natural	50	178	4.35
Natural	50	199	4.52
Natural	50	173	5.49
Natural	70	209	3.84
Natural	70	227	4.37
Natural	70	179	4.15
Natural	70	231	3.74
Natural	99	344	4.10
Natural	99	210	4.88
Natural	99	220	4.00
Natural	99	285	3.39
Natural	99	227	2.87

APPENDIX E. QAQC RESULTS MICROCOSM CHAPTER

Table E.1. Summary of QAQC for the microcosm chapter

Sample Type	Sample	Concentration	Deviation of Duplicates	Recovery
		pM	-----%-----	
Water Extractable Mercury	5	4.01	16.79	110.55
Water Extractable Mercury	5D	5.09		
Water Extractable Mercury	10	3.81	0.33	
Water Extractable Mercury	10D	3.83		
Water Extractable Mercury	15	43.59	117.19	
Water Extractable Mercury	15S	315.71		
Water Extractable Mercury	20	37.71		
Water Extractable Mercury	20S	329.16		
Average			8.56	113.87
		μmol g ⁻¹	-----%-----	
Oxalate Extractable Iron	6	250	1.16	22.33
Oxalate Extractable Iron	6D	253		
Oxalate Extractable Iron	9	201	1.85	
Oxalate Extractable Iron	9D	198		
Oxalate Extractable Iron	16	177	5.17	
Oxalate Extractable Iron	16D	168		
Oxalate Extractable Iron	21	306	22.33	
Oxalate Extractable Iron	21D	382		
Average			7.63	

Sample Type	Sample	Concentration	Deviation of Duplicates	Recovery
		pmol g ⁻¹	-----%-----	
MeHg Extraction	N4	5.86		
MeHg Extraction	N4S	40.27		72.58
MeHg Extraction	N5	4.85		
MeHg Extraction	N5D	4.02	18.72	
MeHg Extraction	S1	5.19		
MeHg Extraction	S1S	40.71		69.04
MeHg Extraction	S5	3.89		
MeHg Extraction	S5D	4.18	7.41	
MeHg Extraction	ST2.6	5.30		
MeHg Extraction	St2.6S	43.87		86.16
MeHg Extraction	N13	3.83		
MeHg Extraction	N13D	4.11	7.04	
MeHg Extraction	S9	4.25		
MeHg Extraction	S9S	46.01		92.42
MeHg Extraction	S14	8.51		
MeHg Extraction	S14D	8.20	3.74	
MeHg Extraction	ST1.7	3.83		
MeHg Extraction	ST1.7S	38.51		68.54
MeHg Extraction	S20	12.41		
MeHg Extraction	S20S	62.12		100.00
MeHg Extraction	S24	41.73		
MeHg Extraction	S24D	42.99	2.97	
MeHg Extraction	ST2.11	4.20		
MeHg Extraction	ST2.11D	3.50	17.97	
MeHg Extraction	ST1.15	5.61		
MeHg Extraction	ST1.15S	36.71		76.00
MeHg Extraction	N20	4.30		
MeHg Extraction	N20D	5.32	21.11	
MeHg Extraction	N25	6.82		
MeHg Extraction	N25S	55.80		94.07
Average			11.28	83.75
		uM	-----%-----	
Chloride	N17	363		
Chloride	N17D	374.2	3.05	
Chloride	S20	392.2		
Chloride	S20D	393.9	0.43	
Chloride	S9	659.8		
Chloride	S9D	666.4	1.00	
Chloride	ST1.5	573.7		
Chloride	ST1.5D	572.6	0.18	
Chloride	N14	368.6		
Chloride	N14D	371.5	0.80	

Sample Type	Sample	Concentration	Deviation of Duplicates	Recovery
		uM	-----%	
Chloride	N23	379.4	1.28	
Chloride	N23D	384.3		
Chloride	ST1.15	523.9	4.03	
Chloride	ST1.15D	545.4		
Average			1.28	
		uM	-----%	
Sulfate	N17	633.6	0.09	
Sulfate	N17D	633.1		
Sulfate	S20	716.8	3.94	
Sulfate	S20D	745.6		
Sulfate	S9	723.0	0.03	
Sulfate	S9D	723.2		
Sulfate	ST1.5	1595.7	0.72	
Sulfate	ST1.5D	1607.3		
Sulfate	N14	637.3	0.05	
Sulfate	N14d	637.6		
Sulfate	N23	180.9	0.84	
Sulfate	N23D	179.4		
Sulfate	ST1.15	1471.7	0.29	
Sulfate	ST1.15D	1475.9		
Average			0.85	

* The sample number corresponds to the treatment type (N=natural, S=spike and St=sterile) and a D (duplicate) or S (spike) denotes the type of QAQC (sequential extractions only)

** Spike recovery is based on a 249 pM inorganic mercury spike (water extracts) into the extractant solution or a ~ 46 pmol g⁻¹ MeHg spike (MeHg extractions)